TNO Defence Research

TD 92-1515 II

0

TNO-report
PML 1992-64

On the design of a gasgun accelerator for
dynamic warhead tests

October 1993

Copy no: -

AD-A285 335

S ELECTE OCT 01 1994 G D

TD 92-1515

TNO Prins Maurits Laboratory

TNO Defence Research

TD 92-515

2280 AA Rijswijk
The Netherlands

Fax · 31 15 84 39 91
Phone · 31 15 84 28 42

TNO-report
PML 1992-64

On the design of a gasgun accelerator for
dynamic warhead tests

October 1993

Copy no: -

Author(s):

M.P.I. Manders
J.B.M.M. Eggen

Total Number of Pages:
(ex. distr. list and RDP)
134

Number of Annexes:
2

TDCK RAPPORTENCENTRALE
Frederikkazerne, gebouw 140
v/d Burchlaan 31   **MPC 16A**
TEL. : 070-3166394/6395
FAX. : (31) 070-3166202
Postbus 90701
2509 LS Den Haag

Number of Figures:
78

Number of Tables:
11

DO assignment no.:
A91/K/429

Number of Copies:
25

Classification

Report:
ONGERUBRICEERD

Title:
ONGERUBRICEERD

Summary:
ONGERUBRICEERD

Annex(es):
ONGERUBRICEERD

94-31718

Summary

A study has been performed concerning the feasibility and general design of a gasgun accelerator for dynamic warhead tests in the Laboratory for Ballistic Research (LBO) of TNO-PML. The warhead accelerator system under consideration comprises the gasgun itself, a rail system to guide the warhead to the target, equipment to detonate the warhead, and a substantial backstop. The study included model calculations, scale experiments, design exercises, and cost evaluations.

The overall feasibility of the warhead accelerator system has been established and a number of design features formulated. Further design and construction of the system appear largely within the capability of the PML. Some questions remain, mainly related to the ability of anti-tank missile components to withstand acceleration. The attendant uncertainties may affect the present (December 1991) internal and external-cost estimates of 315 kf and 335 kf, respectively.

Samenvatting

Er is een studie uitgevoerd naar de haalbaarheid en het algemene ontwerp van een gasversneller voor dynamische warhead tests in het Laboratorium voor Ballistisch Onderzoek (LBO) van TNO-PML. Het beschouwde warheadversnellersysteem bestaat uit de eigenlijke gasversneller, een railsysteem om de warhead naar het doel te geleiden, een afvuurinstallatie om de warhead tot detonatie te brengen, en een stevige projectielopvang. De studie omvatte modelberekeningen, schaalexperimenten, ont-werpwerkzaamheden, en kostenramingen.

De algemene haalbaarheid van het warheadversneller-systeem is aangetoond en een aantal deelontwerpen opgesteld. Het nadere ontwerp en de constructie van het systeem lijken grotendeels binnen de mogelijkheden van het PML te vallen. Enkele vragen staan nog open, met name in verband met het vermogen van componenten van anti-tank missiles om versnellingen te doorstaan. Dit maakt de huidige ramingen voor de verdere interne en externe kosten, respectievelijk 315 kf en 335 kf (december 1991), nog enigszins onzeker.

CONTENTS

1 INTRODUCTION

1.1 The present PML test facility

In 1989, after nearly ten years of preparation, the TNO Prins Maurits Laboratory (PML) opened a unique, new facility for terminal ballistic research: the Laboratory for Ballistic Research (LBO) at Ypenburg Air Force Base.

The main features of the LBO are apparent from Figure 1.1 [1]. The laboratory consists of two firing tunnels separated by a large instrumentation area. The larger tunnel has a length of 60 m and allows firing HE (high explosive) shells of up to 76 mm calibre, and KE (kinetic energy) projectiles of up to 40 mm calibre. A second, 30 m firing tunnel permits testing with KE ammunition of up to 25 mm calibre. The massive target bunker at the end of the larger firing tunnel is capable of withstanding the force of a detonation of up to 25 kg of TNT, or its equivalent. In 1992 the flight length of the large firing tunnel will be extended to 200 m, for KE projectiles only.

Among the experiments currently performed in the target bunker are tests of large calibre shaped charge warheads. These are static tests, where the warhead is put in place near the target, and subsequently detonated. However, as is explained below, recent developments have given rise to a need for dynamic tests.
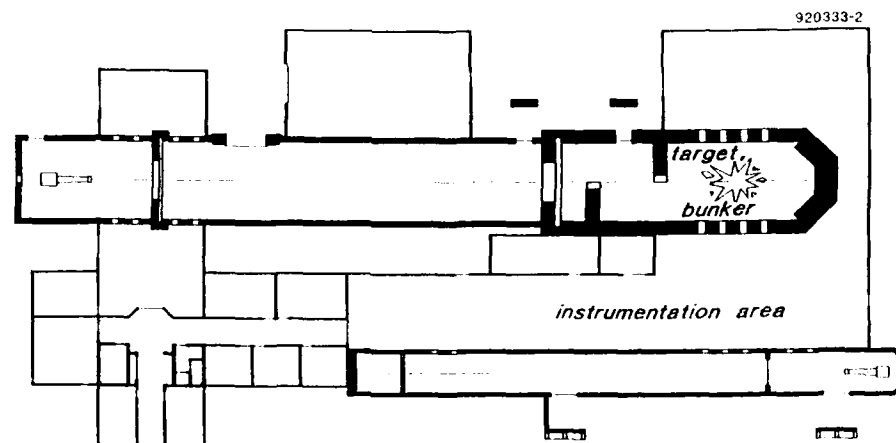
Figure 1 Layout of the PML Laboratory for Ballistic Research (LBO) at Ypenburg Air Base

1.2 Tandem and top attack charges

Ever since World War II, shaped charges have played a major role in the armour - anti-armour bat-
tle. In missile-type anti-tank weapons in particular, the shaped charge principle offers the only
means of combining superior penetration capability with a light weapon platform.

This is because the shaped charge penetrator, the jet, is formed through the action of an explosive
charge detonated near the target. Thus, the shaped charge is a CE (chemical energy) projectile
whose operation is essentially independent of the projectile velocity, as opposed to a KE projectile [2].

The vulnerability of tanks to anti-tank (AT) weapons based on shaped charge technology was
forcibly demonstrated by the Arab-Israeli war of 1973. This formed the prelude to the large scale in-
troduction of weapons of this type by NATO.

However, in the wake of Israel, the Soviet Union introduced a defence against shaped charge war-
heads in the form of explosive reactive armour (ERA) [3], consisting of a sandwich of two metal
plates flanking a sheet of explosive. This caused the early type of anti-tank weapons to lose much of
their effectiveness, infantry weapons in particular. The principles involved in the operation of ERA
are summarised in Figure 1.2.
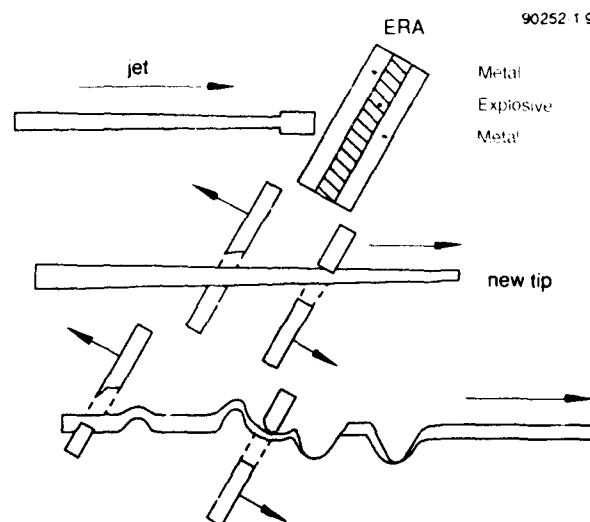
Figure 1.2   Schematic view of the ERA-jet interaction: 1) the impacting jet detonates the explosive
sandwiched between the two metal plates; 2) the plates are propelled across the jet's
path; 3) the jet is severely damaged by the plates

The threat posed by Warsaw Pact ERA instigated a determined search for countermeasures. These were found in the tandem warhead, and in the top attack warhead [3]. Some examples are shown in Figure 1.3.

Tandem warheads comprise two charges. Essentially, the front or precursor charge activates the ERA, thus clearing the way for the main charge which is detonated after a certain delay (Figure 1.4).

Top attack, which in the present context will mean overflying top attack (OTA) rather than dive-attack, circumvents the ERA-problem. It does this, preferably by hitting a spot not defended by ERA, but otherwise by profiting from lesser armour thicknesses in addition to more favourable angles of attack (Figure 1.5).
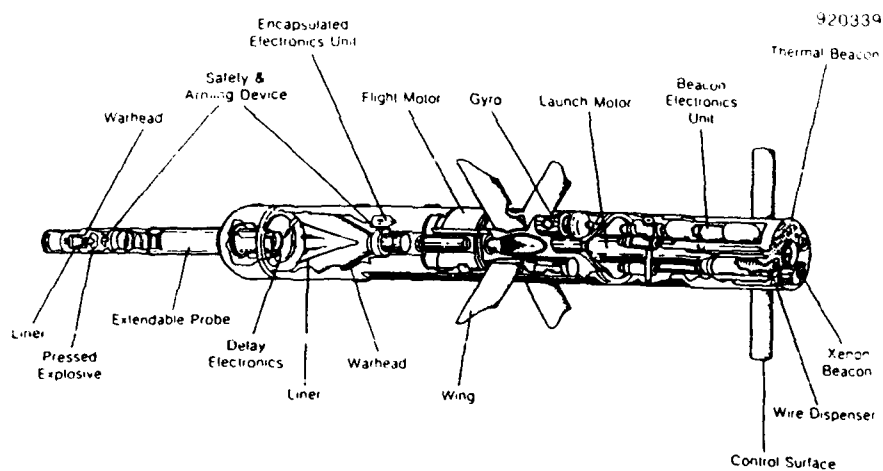
Figure 1.3   1) TOW 2A missile with probe-mounted precursor charge

920340

Dual Mode
Target Sensor
Explosively Formed
Penetrator
Warheads
Xenon
Source
Safe and Arm Device
Wing
Source
Modulator
Control
Surface
Over Rocket
Cover
Test
Connector

920341

Rear section
Missile battery
Rudder
Fin
Gyro
Impact fuze
Warhead
Wire reel
Sustainer motor
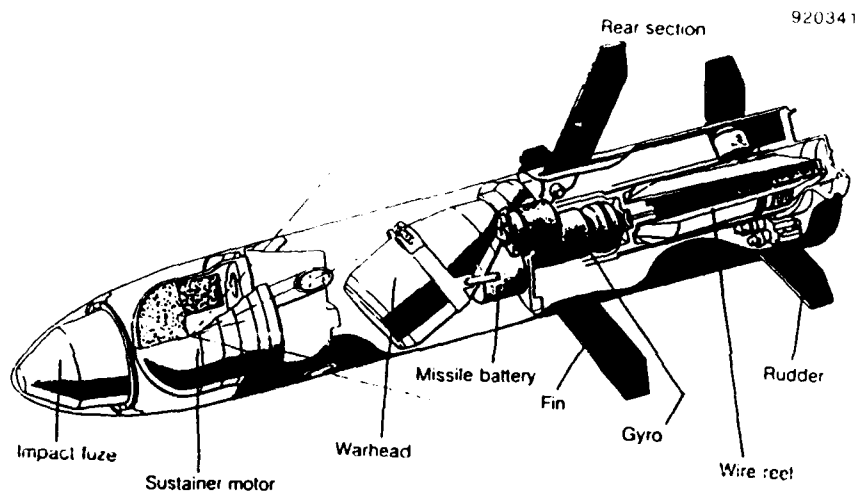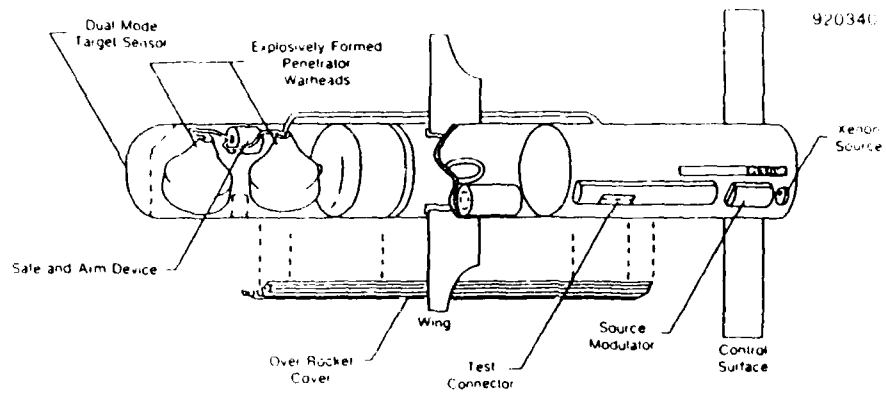
Figure 1.3   2) TOW 2B overflying top attack missile with dual EFP (explosively formed
               projectile) charges; 3) BILL overflying top attack missile with canted charge

#0252-7.3
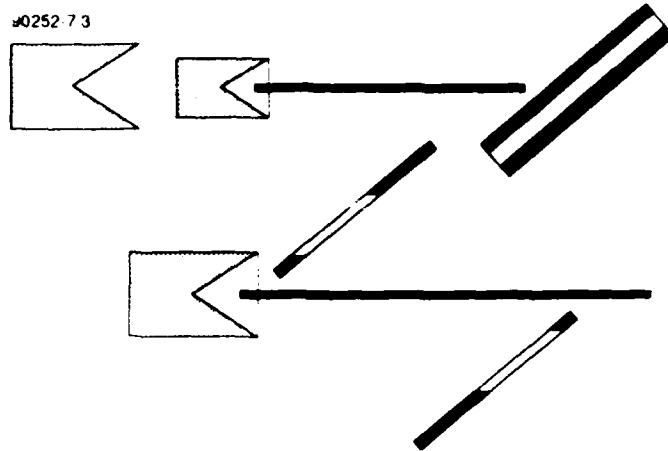
Figure 1.4   Operating principle of the tandem charge. The front charge activates the ERA. The second, main charge is detonated after the ERA plates have flown away

920336
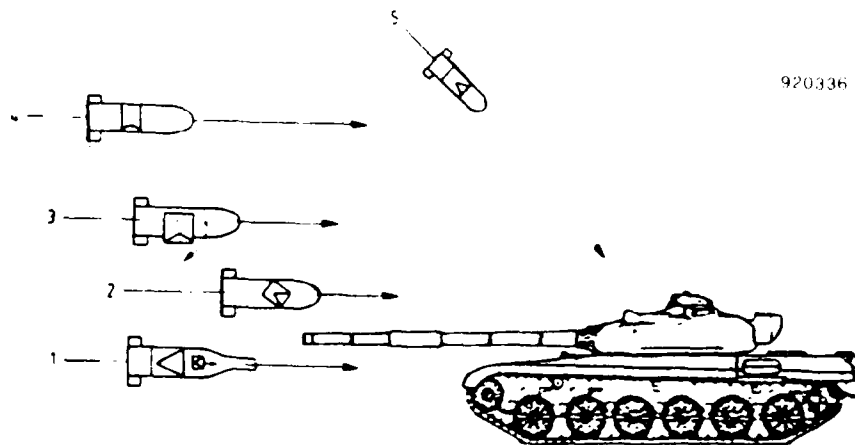
Figure 1.5   Warhead concepts and associated attack profiles. 1) Direct attack with a tandem charge; 2) overflying top attack with a canted shaped charge; 3) overflying top attack with a rotating larger diameter shaped charge; 4) overflying top attack with an EFP charge fired from a larger distance; 5) dive attack

1.3 Dynamic tests

Both tandem and top attack charges require dynamic rather than static tests for a detailed evaluation of their performance. For top attack charges, which are fired downward from a missile moving at several hundreds of m/s, this will be readily apparent. For tandem charges, static tests may offer an indication of the charge's effectiveness, but both the timing and the effect of the front charge on the second charge are influenced by missile motion.

Dynamic laboratory-type tests are not to be confused with dynamic field-trials, where missiles are fired from their launcher and experience a free-flight phase before impacting the target. This implies both increased material-expenditure (large target configurations) and diminished control over the experimental circumstances (impact point, impact angle).

In connection with dynamic warhead tests, it is worthwhile to consider two related types of dynamic tests. In *setback tests*, for instance, projectile components are subjected to controlled deceleration on impact [4]. Likewise, various applications require *impact tests* of large heavy projectiles against concrete structures. In view of this, a dynamic warhead test facility might conceivably be made to serve a dual or even triple use.

1.4 Warhead accelerators

Warhead accelerators for dynamic tests of advanced warhead configurations are known from literature. A number of establishments operate a rocket sled track. By way of example, the track at Los Alamos National Laboratory [5] is 305 m long. The sled can be launched from any position along the rail. In its present configuration, it has carried payloads of up to 35 kg to velocities of between 100 m/s and 330 m/s. Both direct and overflying top attack configurations can be tested. Missile dive and pitch angles can be simulated by adjustment of target obliquity and the mounting angle of the warhead package on the sled frame. A photograph of the sled and warhead assembly is shown in Figure 1.6.
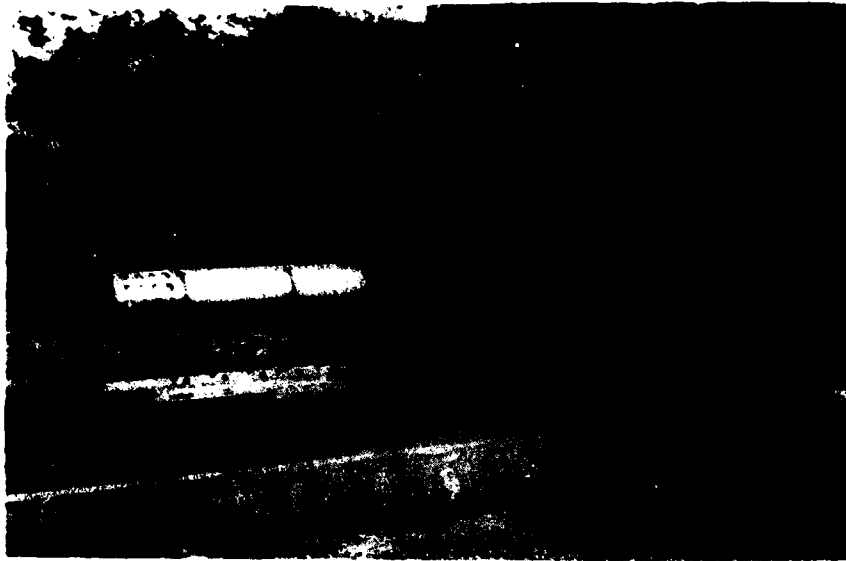
Figure 1.6   Sled and warhead package at Los Alamos National Laboratory ready for launch [5]

An alternative warhead accelerator has been constructed at the Franco-German institute ISL [6].
Here a large calibre gasgun is used to study top attack charges. The gasgun consists of a gas reser-
voir and a barrel of 19 cm diameter, separated by a diaphragm. Barrel length is 5 m. The reservoir
is filled with air at up to 150 bar pressure. After the diaphragm has ruptured, the carrier vehicle
and its payload are expelled from the barrel. The maximum velocity obtained so far is 440 m/s for
a 45 mm shaped charge embedded in a 2 kg carrier, giving a total weight of 2.3 kg. The attendant
acceleration loadings are on the order of 10000 g. The ISL gasgun is shown in Figure 1.7.

Figure 1.7   The 19 cm gasgun at ISL [6]

A rocket sled track after the Los Alamos pattern is basically an open-air installation. Both the length of the track, the use of rocket-propulsion, and the weight of the required launch vehicle make it appear ill-suited for indoor application.

From the LBO point of view, the ISL gasgun approach appears much more promising. It should be kept in mind, however, that the projectile packages accelerated at ISL have been relatively light and of simple construction. Problems are bound to arise for more realistic warheads.

1.5   The gasgun accelerator project

Based on the need perceived by the Netherlands MoD and the PML for dynamic tests of warheads, both in a national and in an international framework, the MoD has launched a project for preliminary research into the gasgun accelerator concept.

This project, carried out by the PML as a short-termed National Technology Project (NTP), comprised both a feasibility study and a cost estimate, as well as related (pre)design work and scale experiments.

In the project, a number of groups within the PML have co-operated. These include the Ballistics section, the Gas & Dust Explosions section, the Electromagnetic Launch Research section, the Accidental Explosions section, the Detonation section, and the Land Systems section, in addition to the PML Construction department. The Ballistics section provided the overall co-ordination.

1.6   This report

The layout of this report follows the general course of action adopted for the project. After setting the general performance requirements for the warhead accelerator, there followed a literature study and modelling effort to obtain insight into the workings of gasguns. Subsequently, the various components of a gasgun system for the dynamic testing of warheads were examined in detail. Where necessary, scale experiments were performed, either to provide input in the design phase or to test various modelling assumptions. A chapter by chapter description is given below.

After the introductory remarks provided by the present Chapter 1, Chapter 2 lists the various design considerations governing the construction of a gasgun, both from a performance point of view and regarding the conditions imposed by the present experimental facility. At the same time, the various components of a complete warhead accelerator system are introduced.

This is followed in Chapter 3 by the description of a simple, zero-order gasgun model. This provides a first indication that a gasgun accelerator is indeed feasible.

A much more elaborate gasgun model is introduced in Chapter 4, in order to impart a feel for the variables that enter into the design of a gasgun. A computer code based on this model is described, and its output compared with data from literature and scale experiments.

Chapter 5 presents the results of a parameter study on the optimum dimensions of the gasgun under consideration. Both air and helium are examined as driver gases.

In the subsequent Chapters 6 to 10, the design of the various subsystems of the warhead accelerator is discussed in some detail. Apart from the gasgun proper (Chapter 6), these include the projectile carrier vehicle (Chapter 7), a guidance section for directing the warhead to the target (Chapter 8), equipment for detonating the charges (Chapter 9), and lastly a backstop for the warhead (Chapter 10).

A cost estimate is given in Chapter 11. This deals, specifically, with the cost of designing, building, and operating a gasgun type warhead accelerator in the LBO.

Of the concluding chapters, Chapter 12 attempts to give an overall evaluation of the technical feasibility and the effectiveness of the warhead accelerator scheme. This gives rise in Chapter 13 to a number of recommendations for the continuance of the project. Lastly, some acknowledgements are made in Chapter 14.

The nature of this report is such, that it attempts to provide a fairly complete (and thus somewhat lengthy) picture of the knowledge and experience gained in the course of the project. This, in order to preserve this knowledge for a possible future follow-up. On the other hand, in spite of the great variety of subjects covered, the report concentrates on the "What" and "Why" rather than on the "How", which in conjunction with the manifold figures should improve the general readability of the text.

In line with the above, several pieces of information obtained after the conclusion of the project (in the first quarter of 1992) have been added to the first, draft version of the report. For the most part, this information may be readily identified by the date of the corresponding references.

2   WARHEAD ACCELERATOR DESIGN CONSIDERATIONS

2.1   Operational requirements

When looking into the feasibility of dynamic tests of advanced warhead configurations, the starting point must be the missiles and targets to be tested. This gives rise to a number of requirements, which are formulated below, and have been summarised in Table 2.1 in section 2.3.

Missiles

As set out in the introductory chapter, the missiles under consideration are of the tandem or top attack configuration [7]. Figure 2.1 shows three generic missile types (see Fig. 1.3 as well).

Several variations on the tandem charge theme are possible. Consider, e.g., the ejectable precursor of the HOT 2T missile, or the proximity fuzed operation of the AT6W-3MR.
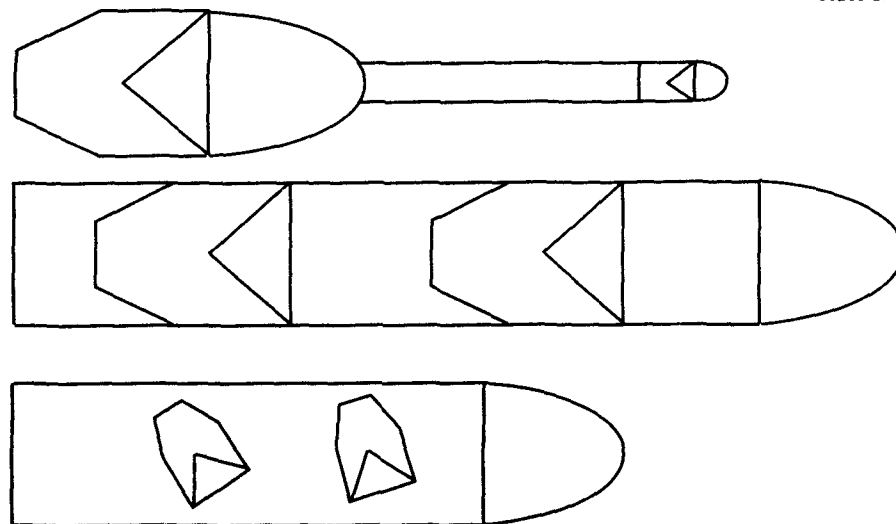
93269-2.1

Figure 2.1   Three generic missile types considered for dynamic testing

Of primary interest are the missile's dimensions and weight. It is the shaped charge which determines the missile *diameter*. Current AT-weapons have a maximum charge diameter of about 15 cm (TOW 2 : 15.2 cm, Milan 2: 11.5 cm, HOT 2: 15 cm); the 17.5 cm Hellfire is an exception.

Because of handling considerations, the maximum diameter for any future AT-weapon is estimated at 20 cm, irrespective of its configuration.

As a general rule, the warhead section would be tested separately, saving both length and weight. *Length* is not in itself a critical parameter. It is assumed, that accelerator payloads will be no longer than 1 to 1.5 m.

However, length has a direct bearing on the pitch angle under which any missile can be mounted inside a given launch tube. For a cylindrical missile of 17.5 cm diameter and 1 m length, the maximum theoretical pitch angle inside a 30 cm tube is slightly over 7°. Whether this is sufficient, remains to be seen [8]. Obviously, a rocket sled offers much more latitude in this respect.

Various considerations, cost among them, will ultimately determine the maximum practical barrel diameter of the gasgun. Of course, for general design purposes the diameter is merely a scaling factor. For this project, we have settled on 30 cm.

With respect to *weight* future missile designers may want to use the rocket motor as a substantial element of the blast shield system between the two charges of a tandem charge, in order to minimise parasitic weight. The missile safe-and-arm device, and the gyro, batteries, and circuit boards could also be used to aid in blast shielding [3,5]. Total weight for some of today's large-calibre missiles is 6.65 kg for the Milan 2, 10.1 kg for the tandem Dragon III (now cancelled), 16 kg for the top attack BILL, and 28 kg for the tandem TOW 2A [9]. It would appear that 20-25 kg represents practical upper limit for the warhead section. Somewhat arbitrarily, the maximum total weight to be accelerated (carrier vehicle plus payload) has been set at 30 kg.

From the point of view of a warhead accelerator, missile *velocity* is perhaps even more important than missile weight. For current Western missiles, the maximum velocity ranges from 100 m/s for the Dragon II to over 280 m/s for the TOW 2A, and 315 m/s for the Israeli Mapats [9]. This depends on the distance; for instance, at the end of its range the TOW-velocity is down to little more than 100 m/s.

For the foreseeable future, there are no clear indications of a significant rise in velocity. For man-in-the-loop systems, where the missile is directed to the target by a human operator, reaction time is a limiting factor. It is noted, however, that even now some Soviet missiles operate at considerably higher velocities of up to 500 m/s (AT-6 Spiral) or even 800 (?) m/s (AT-11 Songster) [10]. Disregarding these, 400 m/s would appear to be a comfortable upper limit for the accelerator, with operation in the 300 m/s regime being more likely. For a minimum velocity, 70 m/s seems appropriate. Lastly, of course, the velocity must be reproducible from one shot to the next, within fairly narrow limits.

There are additional limits set on the launch cycle of any warhead accelerator. These are the *peak acceleration levels* that may be applied to the payload and the peak rates of acceleration onset (*jerk level*). Basically, the jerk level of a launch cycle (the third derivative of space with respect to time) determines the amount of shock energy transmitted to the payload during launch [11].

The problem of maximum allowable acceleration and jerk levels for present and future missiles is not a matter of the forces acting on a missile in field-use, but of the missile's structural limitations (or in the present case those of its warhead section).

An important distinction in this respect is that between missiles attaining their final velocity in the launcher, and missiles having a flight motor. The first variety is subjected to very substantial g-loadings (e.g., 4200 g's on average for the AT4, and 3300 g's for the APILAS [9]. The TOW-2A, on the other hand, is subjected to a maximum of 300 g during launch and no more than rough-ly 25 g in flight [12]. Of course this may actually be far below the structural acceleration limit.

Opinion on the latter subject varies. It has been stated that acceleration levels near 500 g should accommodate virtually all launch needs [13]. On several occasions 1000 g has been mentioned [14, 15]. The TOW 2A, in any case, should accommodate 1000 g or possibly even 1500 g [12]. However, acceleration limits are not a subject of general interest, and there is a widespread wariness of making statements concerning "generic" missiles.

Two more facts may be worth mentioning. Some antitank missiles are designed to be launched from a gun barrel; the AT-10 Bastion missile for the 100 mm gun of the T-55 or BMP-3 is a case in point [10,16]. It is interesting to speculate about acceleration figures. At the extreme end of the acceleration scale is the steerable 155 mm Copperhead artillery anti-armour shell, which is sub-jected to 9000 g on firing [17]. However, this projectile has had to be especially hardened against ac-celeration damage. A similar statement applies to, e.g., the Merlin anti-tank mortar projectile.

While data on allowable acceleration levels are very scarce, no information at all has been un-earthed on jerk levels. Obviously, it is essential that reliable data on both quantities be obtained, be-fore any gasgun accelerator design is finalised.

As a rule, however, in any dynamic test it will be advisable to verify that the warhead has sustained no damage during the launch. If either the integrity or the relative position of the various compo-nent parts have been compromised, warhead effectiveness might suffer. For this purpose, orthogonal flash radiography will be indispensible.

Targets

Generally speaking, for tandem warheads the target of interest will be multiple reactive armours. To the extent that these are already routinely tested in the LBO, this represents no problem. It is imperative, however, that the warhead accelerator itself remains undamaged by either the combined explosive force of the warhead and the explosive armour, or by fragments or even ERA plates.

Secondly, the target will often be at an oblique angle. For the tandem charge in particular, this represents a complicating factor when a misfire occurs and the dud charge must be stopped.

Depending on the type of threat the tandem charge has been designed to counter, the delay between its charges will may vary. Typical delays will be on the order of 0.250 to 3.000 ms [5]. This calls for considerable flexibility in firing the charges.

It is noted, that in testing the performance of tandem warheads against multiple ERA an extensive diagnostic X-ray capability is once again indispensable. Any number of components may fail to function properly, and the evidence is often destroyed in the course of the experiment. This should be taken into account in determining the target set-up.

Top attack charges may be tested against both inert and explosive armour. Here it becomes of vital importance that the proper rotational orientation of the warhead be assured. Even a small rotation would affect the validity of the test, and large displacements could result in a missed target, with unfortunate consequences.

2.2   LBO-related requirements

Any warhead accelerator system must operate within the confines of the LBO. This has a number of consequences. It has already been explained that a rocket sled track is hardly feasible. Even in a gasgun approach, though, both the LBO's firing tunnel and target bunker impose a number of limitations.
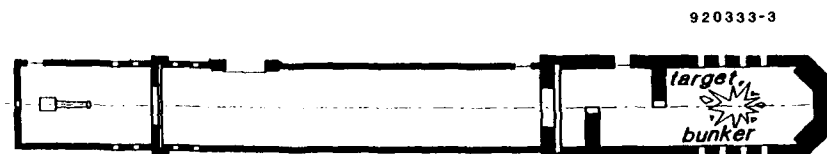
Firing tunnel

920333-3

Figure 2.2   The large firing range at the PML Laboratory for Ballistic Research (LBO)

Referring to Figure 2.2, the length of the firing tunnel implies an upper limit on the length of the gasgun. Depending on whether the gun room at the end of the firing tunnel is included, a total length of roughly 30 or 40 m is available. The shorter length is much to be preferred, since it allows the gun in the gun room to remain in place during dynamic warhead tests.

Conversely, the gasgun must lend itself to being removed once the warhead tests have been concluded. There is only a single shotline into the target bunker, through strategically placed openings in its doors and interior labyrinth walls. This also fixes the centerline of the gasgun at a height of 1.2 m.

Lastly, the gasgun may not completely obstruct the access from the firing tunnel to the target bunker, while in place. Perhaps, this means that (part of) it must be movable.

The firing tunnel is limited in the amount of explosive it can withstand in the case of a premature explosion. It has been established that 10 kg of TNT would present no danger to the surroundings, though the tunnel itself might sustain damage.

In any case, the use of sensitive detonators or on-board electrical energy would seem to be inadvisable (consider for example the situation where a projectile becomes stuck in the bore). A method must be devised that allows withholding electrical energy from the detonators until the last moment. This of course implies circumventing the missile's built-in safe-and-arm, initiation and timing functions. In some cases, as e.g. for the proximity-fuzed future ATGW 3 MR [18], this may entail some practical difficulties.

Target bunker

Safety considerations require that the projectile is guided to a point very near the target. Conversely, it is unwise to have the launching tube too close to the site of the explosion(s). This assumes a separate, expendable guidance section bridging the gap between the tube's muzzle and the target. Thus it can also be also guaranteed that the projectile is positioned properly for external initiation of the charges. While it has been argued that a projectile moving at 300 m/s would find it hard to deviate significantly from its trajectory over a distance of only a few meters, this would not apply to a slower, or failed, launch.

The fixed firing height of 1.2m will in most cases preclude firing top attack charges towards the floor of the target bunker. Since the floor consists of concrete plates resting on a sand bed almost 2m above the bottom of the target bunker, there is some room for increasing the effective firing height. However, it would probably be simpler to fire top attack charges in a sideward direction.

Under no circumstance may a charge hit the walls of the target bunker. A shaped charge jet with a penetration capacity of over 1m of RHA (rolled homogeneous armour) would be quite capable of completely penetrating the 1 m thick concrete bunker wall, with disastrous consequences. Similarly, if a warhead were to malfunction, the heavy, high-velocity projectile might do considerable damage in its own right. Therefore, a fail-safe backstop system must be devised. The available room space amounts to 4 m.

A dud charge would represent an additional problem. On impact it would be liable to scatter the explosive charges all over the target bunker, unless a spontaneous detonation occurred. It must be possible to clean up any explosive debris in a safe and thorough manner.

There are some additional requirements. Remote operation is a must for safety reasons. The time required for setting up the system for a test of maximum complexity should be limited to, say, 4 - 6 hours. And lastly, the whole installation should be as user-friendly as possible.

2.3   Overview of a possible warhead accelerator system

Based on the previous requirements (as summarised in Table 2.1), it is now possible to give an overview of a possible warhead accelerator system for the purpose of performing dynamic tests in the LBO. The overall picture provided here will be filled in and expanded in the rest of the report. (Although the device will be called a gun for convenience, it is of course not implied that it is designed to be a weapon.)

The various components making up the system, and their placement within the large shooting range of the LBO, are shown schematically in Figure 2.3. The gasgun is confined to the firing tunnel, while keeping clear of the range's gun room. The payload is ultimately delivered to the target in the target bunker, through the holes in the bunker's doors and labyrinth walls.
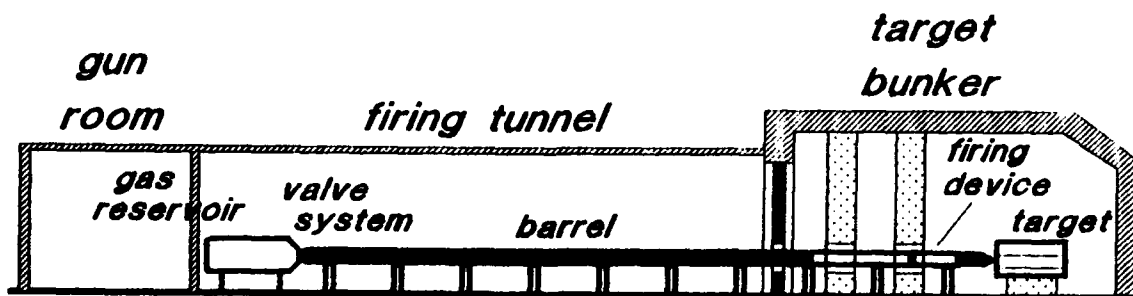
Figure 2.3   Schematic view of the contemplated warhead accelerator

At the rear end of the gasgun is a large gas storage tank. Connected to the tank by means of a gas valving mechanism is a launch tube or barrel. The launch tube consists of multiple segments, each having a separate support. This allows easy removal and storage after use.

Inside the barrel the projectile is mounted on a carrier or launch vehicle, which has the dual task of sealing the barrel and supporting the projectile during acceleration.

In order to keep some distance between the launch tube and the explosion site in the target bunker, an expendable guidance section steers the projectile over its last few meters of flight.

If an absolute guarantee was required against the gasgun being damaged by fragments produced in the target bunker, a fast closing velve in front of the gun muzzle would provide it.

Immediately before impact on the target, the warhead passes a contact section where electrical contact is established between the projectile and the firing equipment. The latter must be integrated with timing and diagnostic equipment.

After the charges are fired, the jets or EFP's (explosively formed penetrators) impact on the target. In case of a detonating failure, the dud charge must be stopped by a backstop construction, without damage to the target bunker.

The above overview leaves a number of questions to be answered, and any number of details to be filled in. Provisions for filling the gas tank, loading the projectile package, keeping it from rotating, suppressing the gun's recoil, etc., all remain to be considered. This will be done in Chapters 6-10. First, though, we must address the matter of the gasgun's dimensions, such as chamber volume and barrel length, as well as its performance. Chapters 3-5 are devoted to this subject.

Table 2.1   Upper-limit requirements for a warhead accelerator system in the LBO

Warhead section	
diameter	20 cm
length	150 cm
weight incl. launch vehicle	30 kg
velocity	70 - 400 m/s
acceleration	500 - 1500 g ?
jerk	?
Gasgun	
diameter	30 cm
height	120 cm
set-up	movable
warhead orientation	fixed
Firing device	
no. of charges	2
triggering distance	variable
delay times	0.250 - 3.000 ms
contact velocity	70 - 400 m/s
Backstop	
penetration capacity	150 cm
projectile weight	30 kg
attack mode	direct + top attack
braking distance	4 m

3   ESTIMATING GASGUN PERFORMANCE

3.1   Introduction

The performance requirements of a gasgun consist usually of specified parameters for the projectile to be launched and operational constraints on the gasgun itself. Relevant parameters for the projectile are its mass and geometry, the required muzzle velocity and the maximum acceleration level it can withstand without being deformed or even destroyed. Operational constraints for the gasgun are e.g. the maximum pressures the system can withstand, its maximum size, and the gas (or gases) that will be used as driver gas.

When designing a gasgun, a method for obtaining a first, crude estimate of whether it is possible to meet the requirements or not would be valuable. Fortunately such a method exists. It is based on two main assumptions:
-   the gas expands isentropically,
-   the available internal energy of the gas is fully transformed into kinetic energy of the projectile.
Furthermore, throughout this report,
-   the gases in use are considered to be ideal gases.
These assumptions are used to derive two equations to determine the barrel length and chamber volume needed to accelerate a projectile of given diameter and mass to a prescribed muzzle velocity at a maximum acceleration level for a choosen driver gas.

In the present chapter, the above method will be described and its limitations discussed. Additional information may be found in the next chapter, which is devoted to a much more realistic gasgun model.

3.2   Equations to determine barrel length and chamber volume

The energy stored in a driver gas of specific heat ratio γ at pressure P_c in volume V_c is:

$$E_c = \frac{1}{\gamma-1} P_c V_c \qquad (3.1)$$

If this driver gas expands isentropically to fill a volume $V_e = V_c + V_b$ (with V_b the barrel volume behind the projectile), its pressure in the new state is given by:

$$P_e = P_c V_c^{\gamma} (V_c + V_b)^{-\gamma} \tag{3.2}$$

and the energy in this new state is:

$$E_e = \frac{P_e V_e}{\gamma - 1} = \frac{P_c V_c}{\gamma - 1} (1 + \frac{V_b}{V_c})^{(1-\gamma)} \tag{3.3}$$

Now assume, that an energy equal to the energy difference between the initial state and the new state is fully transformed into kinetic energy of the projectile, so that:

$$\frac{1}{2} M_p U_p^2 = E_e - E_c \tag{3.4}$$

with M_p the mass of the projectile and U_p its velocity.

If it is required that for a given pressure P_c the projectile has a velocity U_p at the end of a barrel of length L_b and cross-sectional area A_b, Eqs.(3.1) - (3.4) yield the following relation between L_b and V_c:

$$V_c (1 - (1 + \frac{L_b A_b}{V_c})^{1-\gamma}) = \frac{(\gamma-1)M_p U_p^2}{2P_c} \tag{3.5}$$

This is the first of two equations used in the present simple method to estimate gasgun performance.

The second equation is derived as follows. The equation of motion for the projectile is:

$$M \frac{dU_p}{dt} = P(t)A_b \tag{3.6}$$

For an isentropically expanding gas the propelling pressure can be written as a function of the projectile velocity (see section 4.6):

$$P\left(U_p\right) = P_c\left(1 - \frac{(\gamma-1)U_p}{2a_0}\right)^{\frac{2\gamma}{\gamma-1}}$$ (3.7)

with a_0 the initial velocity of sound in the driver gas as given by:

$$a_0 = \sqrt{\frac{\gamma RT}{W_m}}$$ (3.8)

(Here R is the universal gas constant, W_m the molecular weight of the driver gas and T the gas temperature).

If only the expanding gas exerts a force $P(U_p)$ on the projectile (i.e. in the absence of friction, etc.), Eq.(3.6) can be rewritten as:

$$MU_p \frac{dU_p}{dx} = P(U_p)A_b$$ (3.9)

Solving this equation by substituting the expression for the driving pressure yields the following expression for the distance travelled by the projectile when it has obtained a velocity U_p:

$$L_b = \frac{M_p a_0^2}{P_c A_b} \frac{2}{\gamma+1} \left(\frac{\frac{2}{\gamma-1} - \frac{\gamma+1}{\gamma-1}(1- \frac{(\gamma-1)U_p}{2a_0})}{(1-\frac{(\gamma-1)U_p}{2a_0})^{\frac{\gamma+1}{\gamma-1}}} + 1 \right)$$ (3.10)

This is the second equation to determine the needed barrel length and chamber volume.

3.3 Acceleration restraints

This paragraph describes how to use Eqs. (3.5) and (3.10) to determine the barrel length L_b and chamber volume V_c needed to realise a certain projectile velocity U_p, under the additional constraint of a maximum allowable projectile acceleration a_{max}.

A projectile of mass M_p in a barrel of diameter D_b (and area A_b) experiences its maximum acceleration at the start of the launch. This yields the following relation between M_p, a_{max}, and the chamber pressure P_c:

$$P_c = \frac{4 M_p\, a_{max}}{\pi D_b^2} = \frac{M_p\, a_{max}}{A_b} \qquad (3.11)$$

With this substitution for P_c, Eqs. (3.5) and (3.10) can be rewritten and used to determine the barrel length and chamber volume needed to accelerate the projectile to the velocity U_p, while not exceeding the maximum acceleration a_{max}:

$$V_c\left(1 - \left(1 + \frac{L_b A_b}{V_c}\right)^{1-\gamma}\right) = \frac{(\gamma - 1) A_b U_p^2}{2 a_{max}} \qquad (3.12)$$

$$L_b = \frac{a_0^2}{a_{max}}\, \frac{2}{\gamma+1}\left(\frac{\dfrac{2}{\gamma-1} - \dfrac{\gamma+1}{\gamma-1}\,(1 - \dfrac{(\gamma-1)U_p}{2a_0})}{(1 - \dfrac{(\gamma-1)U_p}{2a_0})^{\frac{\gamma+1}{\gamma-1}}} + 1\right) \qquad (3.13)$$

3.4 Calculations

Section 3.3 has yielded two expressions (Eqs. (3.12) and (3.13) for barrel length L_b and chamber volume V_c. Equation (3.13) for the barrel length is plotted in Figures 3.1 and 3.2 as a function of the required muzzle velocity Up, for several values of the maximum acceleration a_{max}. Two ideal driver gases have been considered, air and helium, as characterised by Table 3.1.

Table 3.1   Characteristic parameters for air and helium

Gas	Specific heat ratio	Sound velocity (m/s)[+]
Air	1.4	343
Helium	1.667	1008

[+]   At temperature 293K
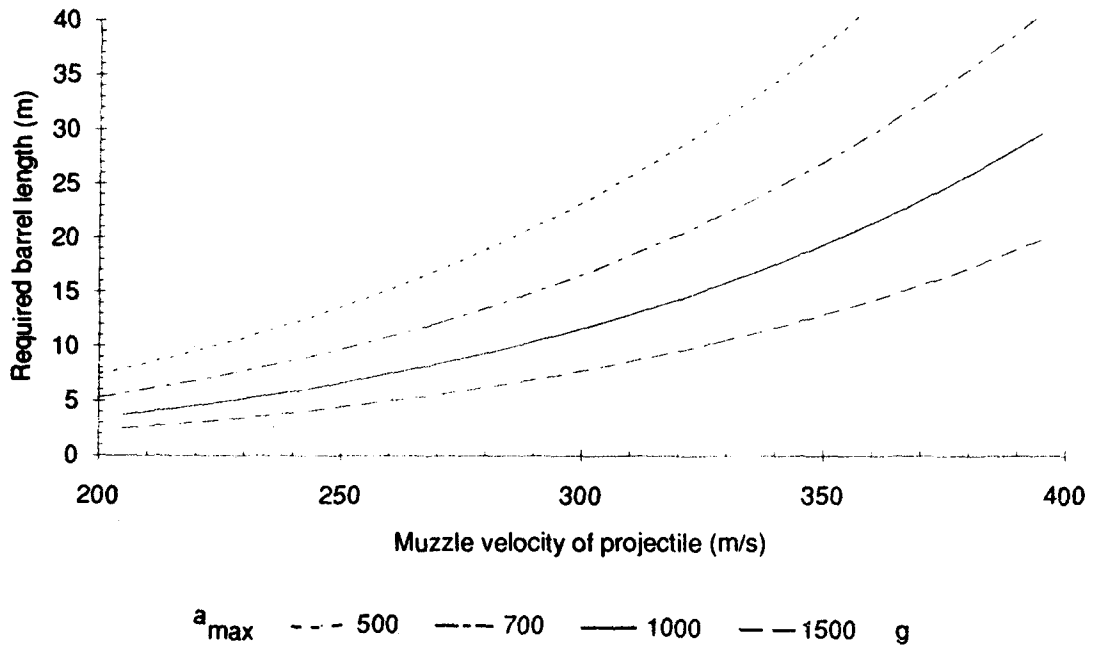
Figure 3.1   Barrel length as a function of muzzle velocity for several values of the maximum acceleration a_{max} (in g) with air as driver gas
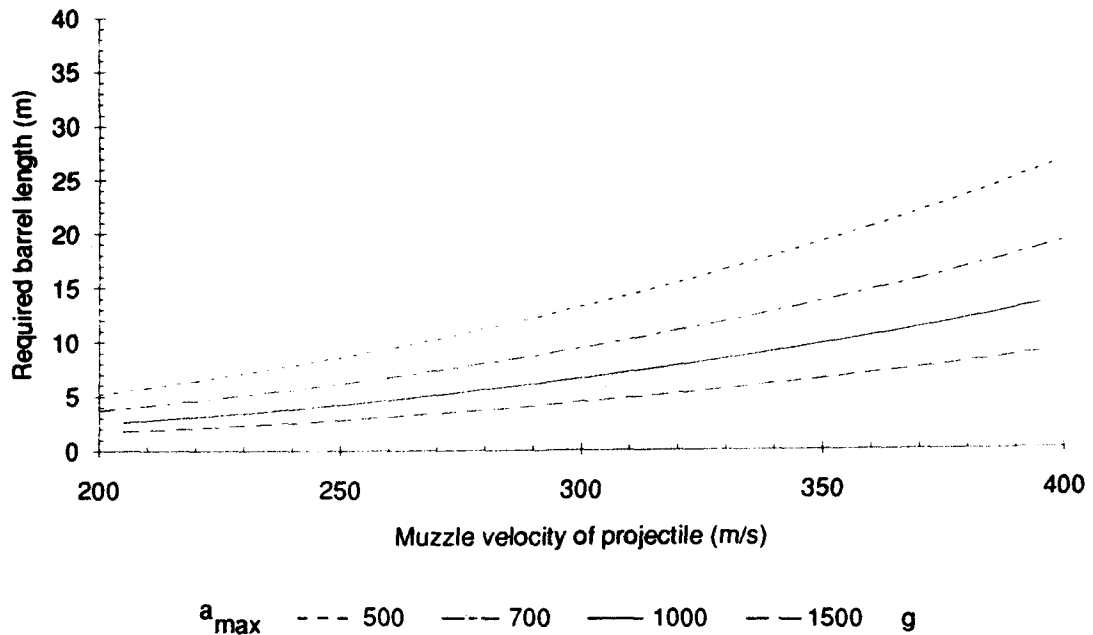
Figure 3.2   Barrel length as a function of muzzle velocity for several values of the maximum acceleration a_{max} (in g) with helium as driver gas

From Figure 3.1 and 3.2 it is evident that helium is a more efficient driver gas. This is further illustrated by Figure 3.3 where Eq.(3.7), used in the derivation of eq.(3.13), is plotted for both air and helium. For helium the driving pressure at the projectile base drops more slowly as a function of projectile velocity, resulting in a continuously higher acceleration force on the projectile.

The initial pressure of the gas in the chamber is proportional to the maximum acceleration a_{max} and to the ratio M_p/A_b of projectile mass to projectile area, as expressed in Eq.(3.11). Figure 3.4 plots the initial chamber pressure as a function of the maximum acceleration level for several values of M_p/A_b. Table 3.2 relates the values of M_p/A_b used in the figure to some relevant combinations of projectile mass and diameter.

Table 3.2   Projectile mass / barrel diameter combinations according to Figure 3.4

mass (kg)	diameter (m)	M_n/A_h
20	0.2	637
20	0.3	283
30	0.2	955
30	0.3	424
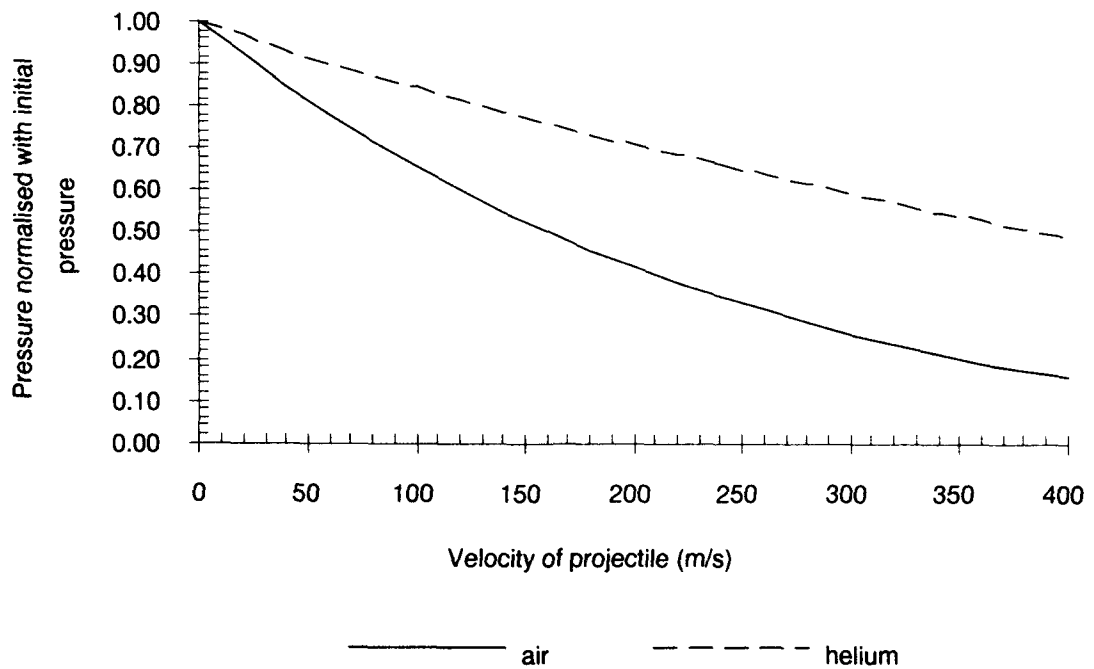
Figure 3.3   Driving pressure at projectile base as a function of projectile velocity for air and helium (at 20°C)
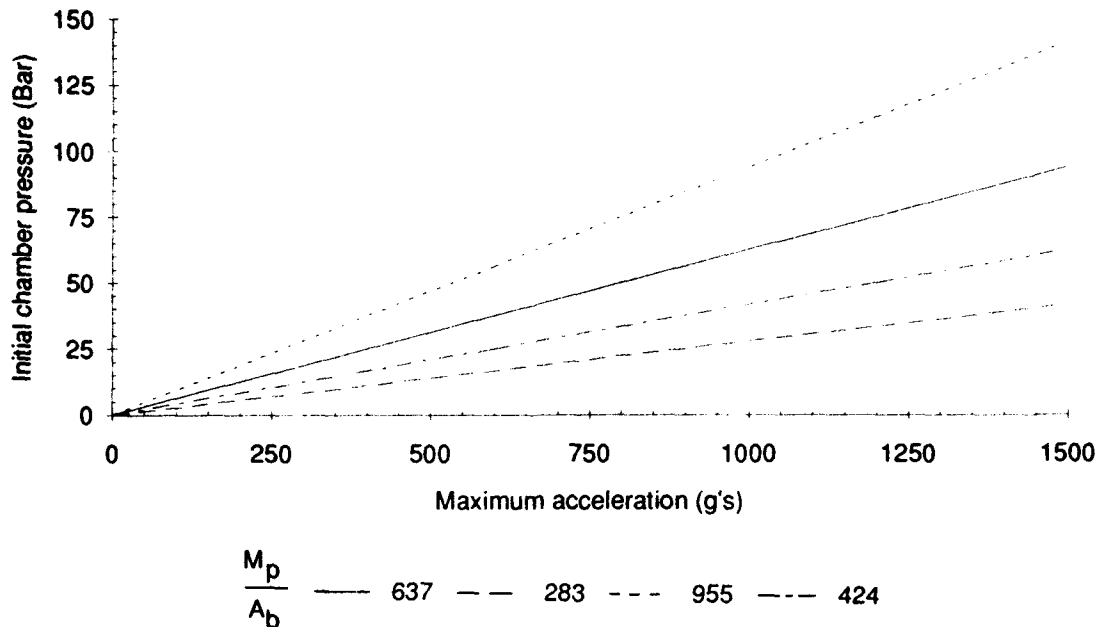
Figure 3.4   Initial chamber pressure as a function of maximum acceleration for several projectile
mass over area ratios

The first of the equations Eqs.(3.12) and (3.13) for determining barrel length and chamber volume
can be rewritten as:

$$L_b = \frac{V_c}{A_b} \left((1 - \frac{(\gamma-1)A_b U_p^2}{2a_{max}})^{\frac{1}{1-\gamma}} - 1 \right) \tag{3.14}$$

For a given maximum acceleration a_{max} and area A_b this equation can be used to calculate L_b as
a function of the particle velocity U_p for several chamber volumes V_c. The results of the calcula-
tions for three different values of a_{max} (500g, 1000g and 1500g) and a barrel diameter of 0.3 m
are plotted in Figures 3.5-3.6 for air and helium, respectively. In these figures, an extra curve for
every a_{max} represents Eq.(3.13). From Figure 3.5 it follows that for air as the driver gas, Eq.(3.13)
is more limiting than Eq.(3.12) for the parameter values investigated. That is to say, on the basis
of Eq.(3.13) a larger barrel length is indicated than required by Eq.(3.12). For helium as the driver
gas the situation is different, as can be seen in Figure 3.6. For high values of the maximum allow-
able acceleration Eq.(3.13) determines the minimally needed barrel length. However, for low accel-
eration values and small chamber volumes, Eq.(3.12) is more limiting than Eq.(3.13). This
means, that under the given conditions there is not enough energy stored in the helium in the
chamber volume, to realise the required projectile velocity at the barrel length calculated by

Eq.(3.13). In summary: for a given maximum acceleration value the minimum barrel length, needed to launch a projectile to a given muzzle velocity with a particular chamber volume, is the maximum value of the barrel lengths calculated using Eqs.(3.13) and (3.12) (or (3.14)), respectively.
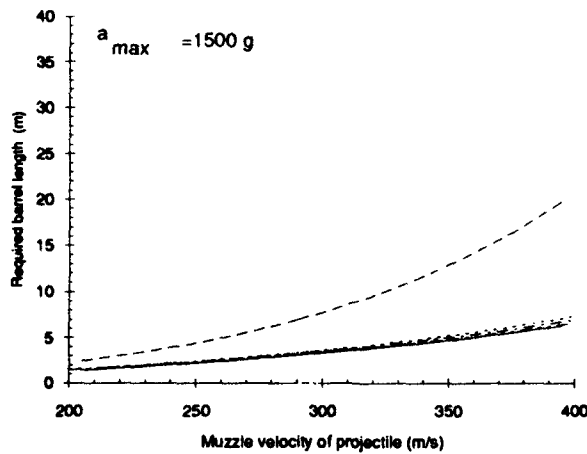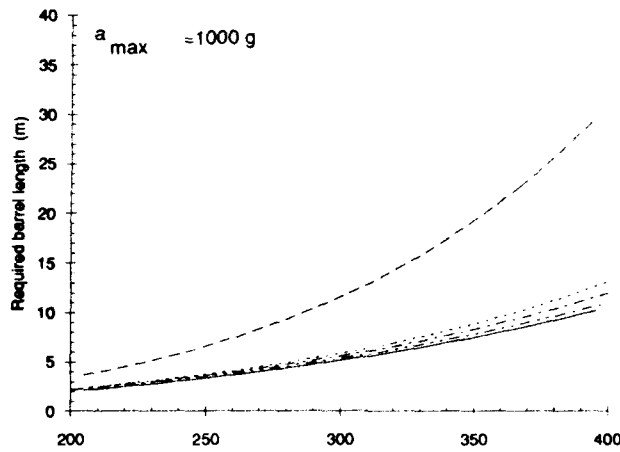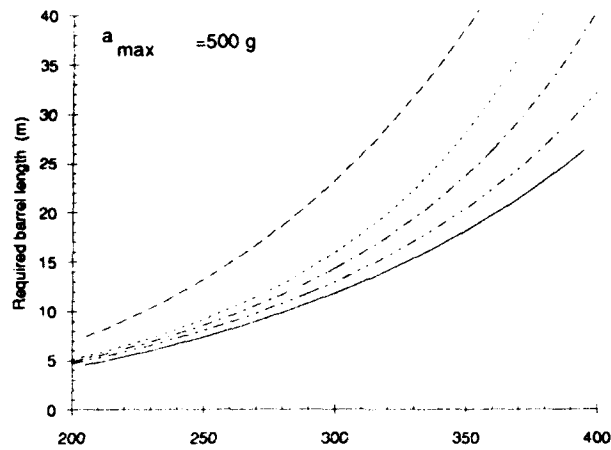
V_c – – –1 — - —1.2 — - - - 1.5 ——— 2m³ — — (Eq 3.12)

Figure 3.5   Barrel length as a function of projectile velocity for several chamber volumes with air
as driver gas; (top: 500g, mid: 1000g, bottom: 1500g)

Figure 3.6   Barrel length as a function of projectile velocity for several chamber volumes with helium as driver gas (top: 500g, mid: 1000g, bottom: 1500g)

3.5   Limitations

The two main assumptions underlying the procedure of the preceding sections have already been
mentioned:
   - the energy stored in the driver gas in the chamber of the gasgun can be fully transformed into
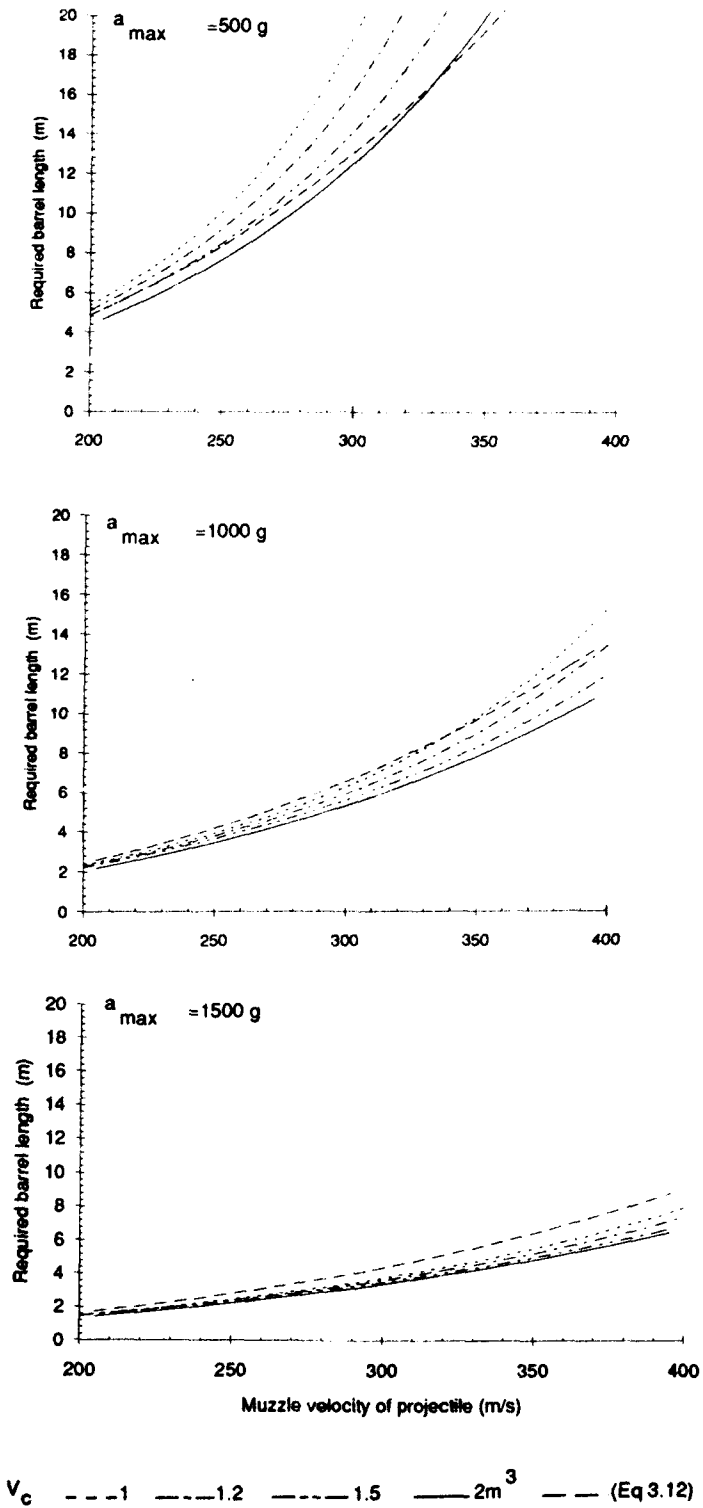   kinetic energy of the projectile;
   - the driver gas expands isentropically.

The limitations inherent to the first assumption become apparent if it is reformulated and split up
in three statements, in the following way:
   - the energy difference between the initial state and a current state is calculated as if the current
     state is a stationary state;
   - this energy difference is fully transformed into kinetic energy of both gas and projectile;
   - the total kinetic energy of the driver gas during expansion is negligible compared to the kinetic
     energy of the projectile.
Only if these three statements are correct, is the first assumption a valid one. By implication, if ei-
ther of the three is not met, then the barrel length L_b as calculated with Eq.(3.12) constitutes the
lower limit of the barrel length needed. Depending on how strong the violations are, a much larger
barrel length may be required in reality. As a result of this, the procedure outlined in this chapter
can really only be safely applied to prove that a certain configuration is incapable of meeting the
imposed requirements.

The second assumption states that the driver gas expands isentropically. As an isentropic process is
a reversible, adiabatic process, the effects of friction and heat transfer are absent. Isentropicity re-
quires that the process develops infinitesimally slowly, with infinitesimally small gradients. Every
real process is irreversible as a consequence of existing finite gradients, but it should be realised that
the irreversibility's associated with rapid gas expansion are inherently small compared to those asso-
ciated with rapid compression or retarded expansion. Therefore a proper reformulation of the as-
sumption is: the expansion process in a gasgun is negligibly non-isentropic. Determining the degree
of non-isentropicity of the expansion process requires both analytical and experimental considera-
tions outside the scope of this simple treatment.

In addition, we note that in the derivation of Eq.(3.13) it was implicitly assumed in Eq.(3.9), that
friction forces between projectile and barrel, and the resistance to projectile motion by the air in the
barrel are negligible. The influence of these forces is studied in the next chapter.

The validity of Eq.(3.9) is limited by yet another fundamental constraint. When disturbances in the gas, initiated by the acceleration of the projectile, are reflected (usually from the breech of the chamber) and reach the projectile again, the propelling pressure is no longer given by Eq.(3.7). This topic too is more fully discussed in the next chapter.

Again the main implication is that, if any of the explicit or implicit assumptions used in its derivation are not met, Eq.(3.13) predicts a minimally needed barrel length; actually, a larger length may be required.

3.6   Feasibility of the gasgun accelerator

We repeat the earlier conclusion, that the procedure outlined in this chapter can only be safely applied to prove that a given configuration can not meet the imposed requirements. It cannot guarantee that the predicted level of performance will in fact be realised.
On the other hand, within the limitations of the theory, it may be expected that the calculated results yield a fair indication of the general level of performance to be expected.

In this sense, the basic feasibility of fulfilling the requirements listed in Table 2.1 has been established. For a barrel diameter of 0.3 m and taking 20 m as the maximum barrel length, we find from Figure 3.5 that for air as the driver gas 1500 g gives the desired 400 m/s muzzle velocity. Likewise Fig. 3.6 shows that for helium roughly 800 g should yield 400 m/s.
Turning to Figure 3.4 and Table 3.2, for a projectile mass of 30 kg and a barrel diameter of 0.3 m, 1500 g is seen to translate to approximately 60 bar chamber pressure, and 1000 g and 500 g to proportionally less. This is well within the acceptable pressure range of the contemplated gasgun.

4   GASGUN MODELLING

4.1   Introduction

This chapter describes how the performance of a gasgun was modelled. First a simplified description of a gasgun is given to introduce the main components of such a gun and the important parameters for its performance. Then the basic requirements to obtain a high projectile velocity are stated. The performance of a gasgun is strongly dependent on the behaviour of gas disturbances and corresponding pressure disturbances initiated by the acceleration of the projectile. This topic is discussed at some length, after which the reader should have a feeling for the fundamentals of gasgun performance.

Before going into details, the following two paragraphs provide an overview of this chapter's subject matter. Two types of gasgun are treated: first the constant diameter gasgun and then the chambered gasgun, corresponding with an increase in order of complexity.

In a constant diameter gasgun (or any gasgun for that matter), an accelerating (or decelerating) projectile creates gas and pressure disturbances. If the first pressure disturbance that was initiated by the projectile starting to accelerate cannot, after having been reflected from the breech, reach the projectile before it leaves the barrel, the gasgun is called an (effectively) infinite chamber-length gasgun. In a constant diameter gasgun of this type, where in addition the barrel has been evacuated and projectile-barrel friction has been modelled in a special way, the velocity of the projectile can be expressed analytically as a function of its position in the barrel. If the reflected disturbances reach the projectile while it is still in the barrel, or when the other conditions are not met, then the projectile velocity must be calculated numerically, as will be outlined below.

As opposed to the constant diameter gasgun, the performance of a chambered gasgun can only be calculated numerically, through a quite elaborate procedure. This will be described in general terms, and the numerical implementation discussed as well. In addition, however, reasonably accurate estimates for chambered gasgun performance can be given with pseudo-analytical approaches based on some simplifying assumptions. As in the case of the constant diameter gasgun, an important subtype of the chambered variety is the effectively infinite chamber-length gasgun.

Our objective of modelling gasgun performance was to perform parameter studies to design a gas-gun capable of meeting specified requirements and constraints. These parameter studies are described in the next chapter.

Lastly, for a general overview of gasgun theory, we refer to Seigel [19].

4.2   Gasgun overview
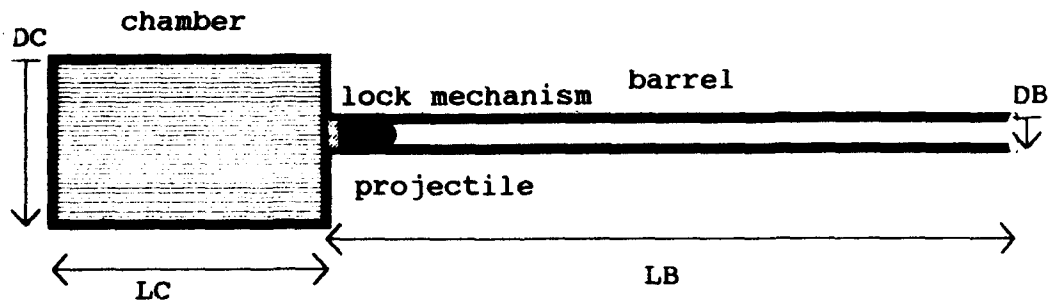
Figure 4.1   Schematic overview of a gasgun

A schematic overview of a gasgun is given in Figure 4.1. Such a gun consists of a reservoir, called the chamber, that contains a certain mass of a chosen gas at a predetermined (high) pressure. At the transition from the chamber to the barrel a locking mechanism prevents the gas from expanding into the barrel. The projectile to be launched is positioned almost directly behind this mechanism and has a certain mass. When the locking mechanism is unlocked, the gas will flow out of the chamber. As long as the propelling force on the projectile exerted by the expanding gas is larger than any opposing forces (e.g. projectile-barrel friction, and resistance of the compressed gas inside the barrel), the projectile will continue to accelerate.

The above is a simplified description of a gasgun. In the following more detailed study, it is assumed that both chamber and barrel are cylindrical in shape.

The main parameters characterising a gasgun are its dimensions and its physical state variables. These have to be specified for both chamber and barrel:

-   geometric parameters for the chamber: length L_c and diameter D_c;
-   state variables for the chamber: type of driver gas, with specific heat ratio γ, initial pressure P_c and temperature T_c (determining in turn the sound velocity);
-   geometric parameters for the barrel: length L_b and diameter D_b;
-   state variables for the barrel: type of gas and its specific heat ratio γ, initial pressure P_b and temperature T_b.

If the diameter of the chamber is the same as the diameter of the barrel, the gasgun is called a constant diameter gasgun, otherwise it is called a chambered gasgun.

The performance of a gasgun, that is the muzzle velocity attained by the projectile, is further dependent on:

-   the projectile mass M_p;
-   the friction between projectile and barrel;
-   the resistance due to compressed air in the barrel.

4.3   Basic requirements for a high velocity gasgun

The basic factors determining the velocity of a projectile propelled from a gasgun may be obtained by applying Newton's force equation to describe the trajectory of the projectile in the barrel at any moment in time:

$$M \frac{dU_p(t)}{dt} = A \, P_p(t) \tag{4.1}$$

where M_p denotes the projectile mass, $U_p(t)$ its instantaneous velocity, A the cross-sectional area of the barrel and $P_p(t)$ the propellant pressure acting on the rear end of the projectile. This equation can be transformed to:

$$M \, U_p(X_p) \frac{dU_p(X_p)}{dX_p} = A \, P_p(X_p) \tag{4.2}$$

with X_p the distance travelled by the projectile at time t.

Integrating this equation from the projectile's starting position (X=0) to the muzzle end of the barrel (X = L, L the barrel length) yields:

$$\frac{M\,U_p^2}{2} = \frac{A}{L}\int_0^L P_p(x)dx \qquad (4.3)$$

with U_p the muzzle velocity of the projectile.

If the spatial average of the propelling pressure is defined as:

$$\bar{P} = \frac{1}{L}\int_0^L P_p(x)dx \qquad (4.4)$$

the projectile muzzle velocity can be written as:

$$U_p = \sqrt{\frac{2\bar{P}AL}{M}} \qquad (4.5)$$

This result indicates the essential factors upon which the projectile velocity depends. To achieve a higher muzzle velocity, one must:
- increase the barrel cross-sectional area A;
- increase the barrel length L;
- decrease the projectile mass M;
- increase the average propelling pressure Pa.

However, practicality limits the changes in these parameters:
- usually a minimum M is prescribed;
- for too large an L the propelling pressure at the end of the barrel will become very low and friction effects may become dominant;
- too large an A will pose both cost and operational problems;
- the various components of a gun cannot withstand an arbitrarily high pressure.

Achieving a high projectile velocity can be realised by making first AL/M as large as possible and then generating a high average driving pressure behind the projectile, while at the same time limiting the pressure rise in all parts of the gun system so as not to cause unacceptable damage.

Ideally, the base pressure on the projectile would be constant and equal to the initial pressure, during the entire stay of the projectile in the barrel. A propellant capable of this is known as constant base pressure propellant. In this case the muzzle velocity of the projectile would be the maximum attainable velocity for the given gun system. This velocity is given by:

$$U_0 = \sqrt{\frac{2P_0AL}{M}} \qquad (4.6)$$

4.4 Pressure disturbances in a gasgun

Imagine the gas to be composed of thin layers of gas perpendicular to the axis of the gasgun. When the projectile in a gasgun (or pre-burned propellant gun) starts to move, it momentarily leaves a slightly evacuated or lower pressure space behind. The layer of gas that was initially in contact with the projectile, but is now infinitesimally behind it, quickly moves this infinitesimal amount toward the projectile into the evacuated space. Since this layer now has more space available, its pressure drops. The same happens to the layer next to the first layer, and so on. This progression of successive movement is a disturbance in the gas which proceeds at the local speed of sound in the gas. The disturbance decreases the pressure and density of the gas through which it passes and is thus called a rarefaction disturbance. During its entire motion in the barrel, the projectile continues to produce these rarefaction's.

However, when the first rarefaction reaches the breech of the chamber and the breech layer moves into the space evacuated by its neighbour, there is no neighbour behind it to fill up the space the breech layer is vacating and the breech layer is retarded in its motion; this retardation is felt by the layer ahead of the breech layer, so that layer is retarded as well, and so on until this so called reflected rarefaction reaches the projectile and lowers the propelling pressure. In fact, this means that the information that there is only a limited amount of gas available to fill the evacuated spaces, is transmitted back to the gas in the gasgun and to the projectile. So when this first and following reflected rarefaction's reach the projectile the acceleration of the projectile is less than had they not reached the projectile.

A more complex phenomenon occurs in a gasgun with chambrage.

When a rarefaction travelling in the barrel towards the breech reaches the transition section with its increasing area, the evacuated space is filled with gas flowing from a larger volume layer, so that the pressure is raised to a higher value than if the gas had moved from a layer of the same volume. This is the situation for all the layers in the transition section. In effect, rarefaction waves travelling to the transition section are partially reflected at the transition section as compression disturbances travelling towards the projectile, and partially transmitted as rarefaction's travelling towards the breech. Upon reaching the projectile the compression disturbances raise the pressure behind the projectile to a value above that of a constant diameter gasgun. The disturbances in a chambered gasgun are illustrated in Figure 4.2.

In summary, the main changes in the pressure of the gas propelling the projectile in a gasgun are:
- a drop in pressure from the projectile acceleration, present during the entire projectile motion in the barrel;
- a drop in propelling pressure caused by rarefaction's reflected from the breech reaching the projectile during the later stages of its motion;
- a rise in pressure from compression disturbances, i.e. rarefaction's reflected at the transition section, which are present during the entire projectile travel.
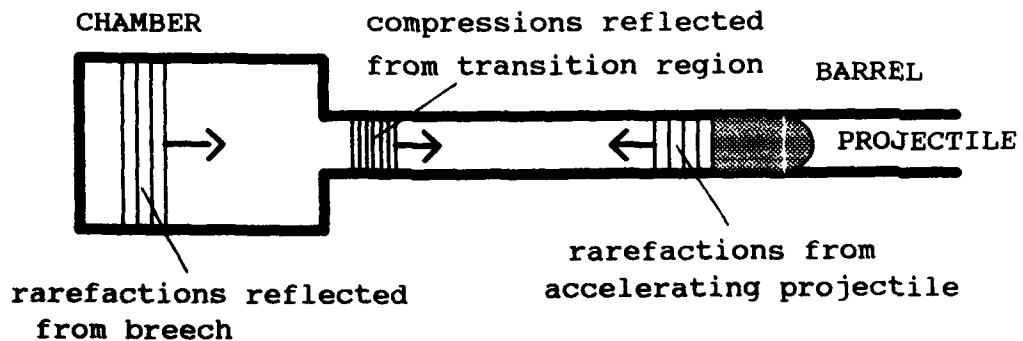

Figure 4.2   Rarefaction and compression disturbances in a gasgun.

4.5 Characteristic equations

The mathematical formulation for the infinitesimal pressure changes describes those changes in terms of changes that occur when travelling with or along a disturbance:

$$dp + a\rho\, du = 0 \tag{4.7}$$

$$dp - a\rho\, du = 0 \tag{4.8}$$

Here p is the pressure, a the local sound velocity, ρ the density and u the velocity of the layer of gas under consideration. In the derivation of these equations it is assumed that infinitesimal changes in the gas occur isentropically, so that:

$$p = P_c\, \rho^{\gamma} / \rho_c^{\gamma} \tag{4.9}$$

Eq.(4.7) applies to a so called upstream or "u+a" disturbance, that is travelling towards the projectile, while Eq.(4.8) applies to the downstream or "u-a" disturbance, that is either travelling towards the breech, if u-a<0, or towards the projectile, when u-a>0. These two equations are known as the characteristic equations and they permit a numerical solution to the interior ballistics problem of a gas flowing isentropically in a (constant diameter) gasgun. It is important to note that these equations apply only to the barrel section and the chamber section, not to the transition region! The transition region is described differently (see the paragraph on the chambered gasgun).

The characteristic equations, Eqs.(4.7) and (4.8), express that the acoustic inertia aρ of the gas is the fundamental gas property which determines the magnitude of the pressure changes required to produce given velocity changes. For small aρ the pressure change can be small to effect a given velocity change. This is easy to understand qualitatively: the more quickly each layer of gas moves into the space evacuated by its neighbour (meaning the gas has low inertia), the less is the pressure drop and the better able is the gas to push the projectile. Therefore, a good propellant gas would be a gas of low inertia; such a gas would yield a higher average pressure and thus a higher muzzle velocity than a gas of high inertia.

4.6 The constant diameter gasgun

4.6.1 *Governing equations*

In this paragraph and the next, the behaviour of a constant diameter (CD) gasgun is discussed. A sketch of such a gun just prior to the release of the projectile is given in Figure 4.3. The basic parameters have already been listed in section 4.2. The driver gas in the chamber is considered to be an ideal gas which expands isentropically.
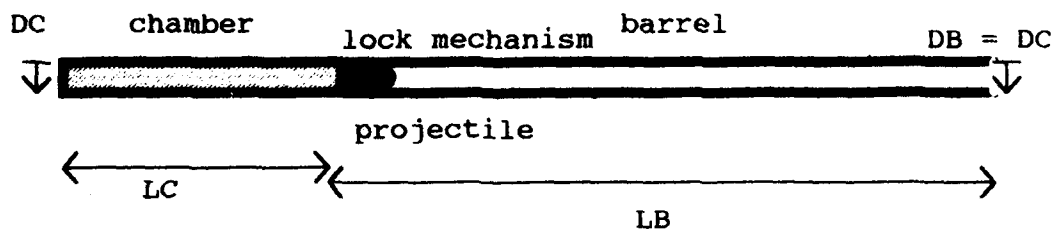
Figure 4.3   Schematic overview of a constant diameter gasgun.

The behaviour of a constant diameter gasgun is described by the *following set of equations*.
For the driver gas we have:

the characteristic equations:

$$dp + a\rho \, du = 0 \tag{4.10}$$

$$dp - a\rho \, du = 0 \tag{4.11}$$

together with the ideal gas law:

$$p = \rho k T \tag{4.12}$$

and the expression for an isentropic expansion:

$$p = P_c \, \rho^\gamma / \rho_c^\gamma \tag{4.13}$$

For the projectile we have:

the equation of motion:

$$M \frac{dU_p}{dt} = F(t) \tag{4.14}$$

together with an appropriate model for the resulting force $F(t)$:

$$F(t) = F_p(t) - F_f(t) - F_a(t) \tag{4.15}$$

where F_p is the driving force exerted on the projectile by the expanding driver gas, F_f is the friction force between the projectile and the barrel, and F_a is the decelerating force on the projectile caused by the air in the barrel.

For an isentropic gas Eq.(4.13) can be combined with Eq.(4.11) to yield the following relation between the pressure and the velocity along a characteristic:

$$P(U_p) = P_c (1 - \frac{(\gamma-1) \, U_p}{2a_0})^{\frac{2\gamma}{\gamma-1}} \tag{4.16}$$

The friction force between the projectile and the barrel will be modelled in the remainder of this report as either:

- a constant friction force, independent of projectile motion, described by a constant friction pressure factor times the barrel area:

$$F_f(t) = A C_f \tag{4.17}$$

- a force proportional to the net force, i.e. the difference between the propelling force of the driver gas and the resistance force due to the gas in the barrel, with a proportionality constant "a":

$$F_f(t) = a(F_p - F_a) \tag{4.18}$$

The performance of a CD gasgun can now be calculated by solving these equations, provided proper expressions are available for F_f and F_a in Eq.(4.15).

4.6.2 Analytic solution without reflections

A simple case allowing an analytical solution to the equations of section 4.6.1 is that where reflections can be neglected.

As long as pressure disturbances initiated by the acceleration of the projectile have not yet reached the projectile again, after having been reflected from the breech, Eq.(4.16) expresses the pressure exerted on the base of the projectile by the expanding driver gas. If we assume that there is no friction in the CD gasgun and that the barrel is evacuated, Eq.(4.14) can be rewritten as:

$$MU_p \frac{dU_p}{dx} = P(U_p)A_b \tag{4.19}$$

This equation can be integrated analytically to give the following relation between barrel length and projectile velocity:

$$L_b = \frac{M_p a_0^2}{P_c A_b} \frac{2}{\gamma+1} \left(\frac{\frac{2}{\gamma-1} - \frac{\gamma+1}{\gamma-1}(1 - \frac{(\gamma-1)U_p}{2a_0})}{(1 - \frac{(\gamma-1)U_p}{2a_0})^{\frac{\gamma+1}{\gamma-1}}} + 1 \right) \tag{4.20}$$

(This equation was used earlier in Chapter 3.) A graphic illustration of this result is given by Figure 4.4, where a dimensionless muzzle velocity has been plotted as a function of a normalised barrel length.

The dimensionless co-ordinates for velocity and positive (length) are respectively:

$$\bar{u} = \frac{u}{a_0} ; \bar{x} = \frac{A_b P_c}{M a_0^2} x \tag{4.20}$$
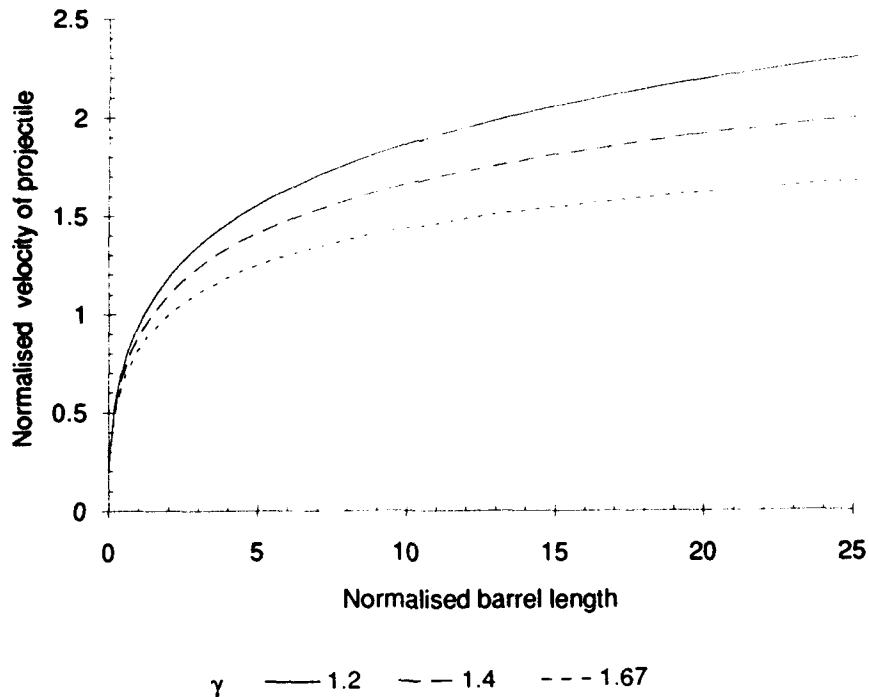
Figure 4.4   Normalised muzzle velocity as a function of normalised barrel length for several
              values of the specific heat ratio g of the driver gas, without reflections at the breech

Obtaining the chamber length L_c necessary so that the CD gasgun can be considered of effectively
infinite chamber length, requires the calculation of the path of the first returned, reflected distur-
bance. For a CD (ideal propellant) gasgun, Heybey [28] has obtained an analytic expression for the
chamber length L_c as a function of the velocity of the projectile U_p (at which the first reflected dis-
turbance reaches the projectile):

$$L_c = \frac{M_p a_0^2}{P_c A_b} \frac{2}{\gamma+1} \left(\frac{1}{(1-\frac{(\gamma-1)U_p}{2a_0})^{\frac{\gamma+1}{2(\gamma-1)}}} - 1 \right)$$

(4.21)

This equation can be regarded as a relation limiting the applicability of Eq.(4.20). In Figure 4.5
the Eqs.(4.20) and (4.21) are plotted together in dimensionless length (L_b and L_c) co-ordinates for
two values of γ, the specific heat ratio corresponding to air and helium.

The disturbances reflected by the breech of the chamber transmit the information that there is only
a finite amount of gas in the chamber. When these reflected disturbances reach the projectile, they

decrease the pressure behind the projectile to below the magnitude the pressure would have if there were no such returned reflections. The onset of this phenomenon (as indicated by Eq.(4.21)) is not incorporated in Eq.(4.20) and can only be calculated properly with a numerical solution of the governing differential equations. This is done in the next section.

For a desired normalised muzzle velocity $\bar{u}$, Figure 4.5 can be used to determine the normalised barrel length L_b and chamber length L_c. These values yield a ratio $\bar{l} = \frac{\overline{L}_b}{\overline{L}_c}$. If the ratio $\bar{l} = \frac{\overline{L}_b}{\overline{L}_c}$ .for an actual gasgun configuration is less then $\bar{l}$, the desired normalised muzzle velocity is realistic; if $l \rightarrow \bar{l}$, $\bar{u}$ over predicts the muzzle velocity realisable by the given configuration.
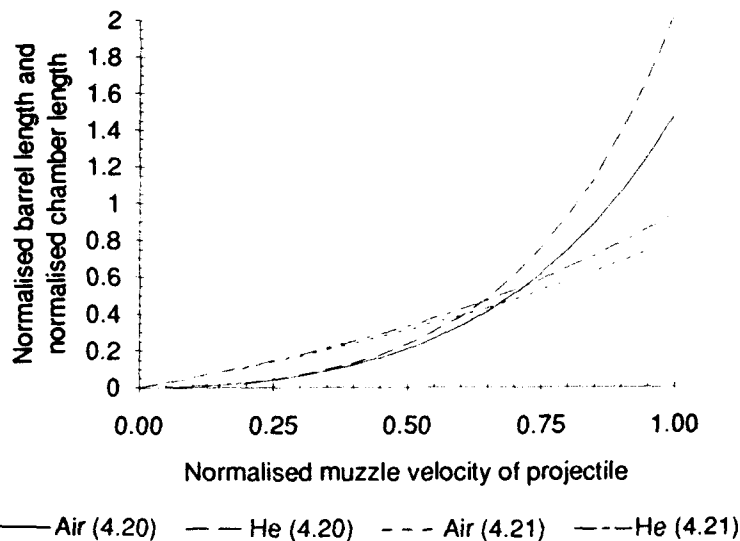
Figure 4.5   Normalised barrel length as a function of normalised muzzle velocity for helium and air, with curves indicating the limit (Eq.(4.21)) of the applicability of the reflection-less theory of Eq.(4.20)

4.6.3   Numeric solution with reflections

The procedure for numerically solving the equations of section 4.6.2 is not discussed here, since we want to focus mainly on the results and their implications. In this section, various cases are to be distinguished.

No friction, evacuated barrel

Assuming no friction and an evacuated barrel, Figure 4.6 plots the numerically calculated velocity of the projectile as a function of the position of the projectile in the barrel, for several values of the chamber length L_c. The initial chamber pressure was fixed at 40 bar, the driver gas is air at

ambient temperature (20°C), the barrel length was taken to be 20 m and the mass of the projectile is 30 kg.

The top-most curve in Figure 4.6 corresponding to L_c = 10m also represents the U-X relationship as expressed by Eq.(4.20). The figure clearly shows that, as the chamber length gets smaller, the calculated velocities differ more and more from the values as predicted by Eq.(4.20). This difference is caused by the earlier return at the projectile of reflections that cause a drop in the propelling pressure. This is more clearly seen in Figure 4.7 of the projectile acceleration.

It is easy to verify that for the smaller chamber lengths Eq.(4.21) gives a barrel length of less than 20m, meaning that reflections can indeed return at the projectile. It is also important to note that for this particular configuration increasing the chamber length over 10m does not increase the muzzle velocity of the projectile any further.

In Figure 4.8 and 4.9 the velocity and acceleration of the projectile are now plotted for several initial chamber pressures, assuming a fixed chamber length of 7.5 m while keeping the rest of the configuration unchanged. The same trends can be observed for the smaller chamber pressures at fixed chamber length, as earlier for the smaller chamber lengths at fixed initial chamber pressure.
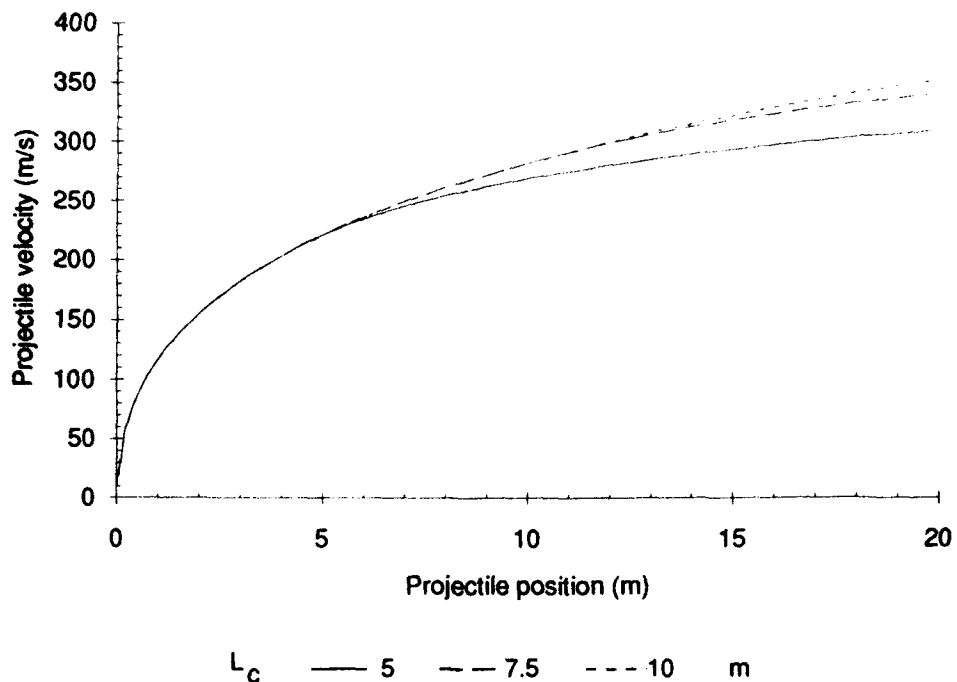
Figure 4.6   Projectile velocity as a function of position for several chamber lengths L_c for air, with a friction-less projectile and an evacuated barrel
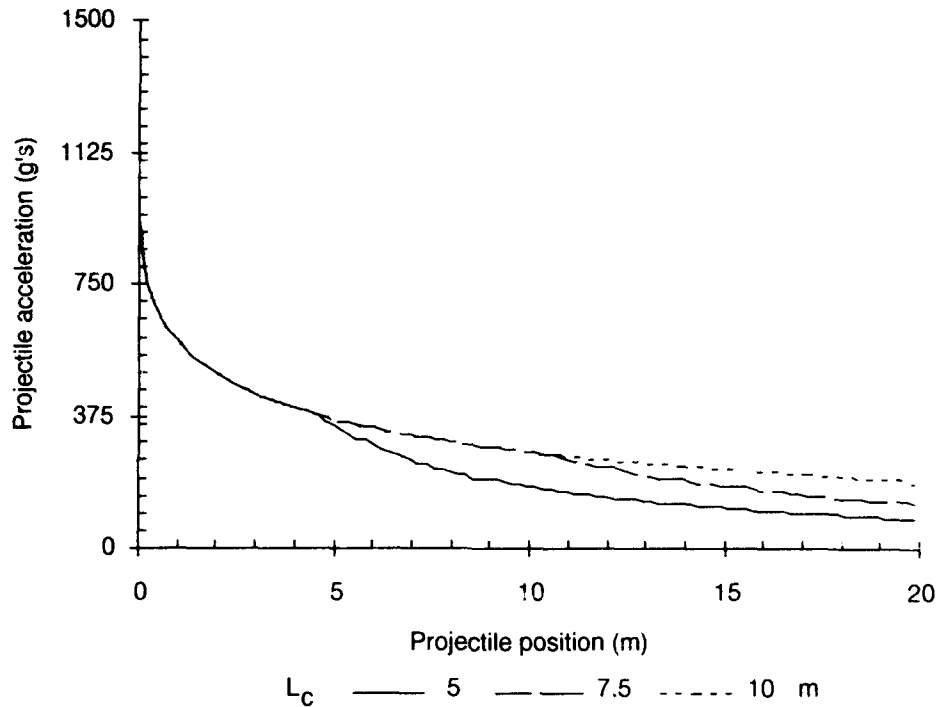
Figure 4.7   Projectile acceleration as a function of position for several chamber lengths L_c for air, with a friction-less projectile and an evacuated barrel
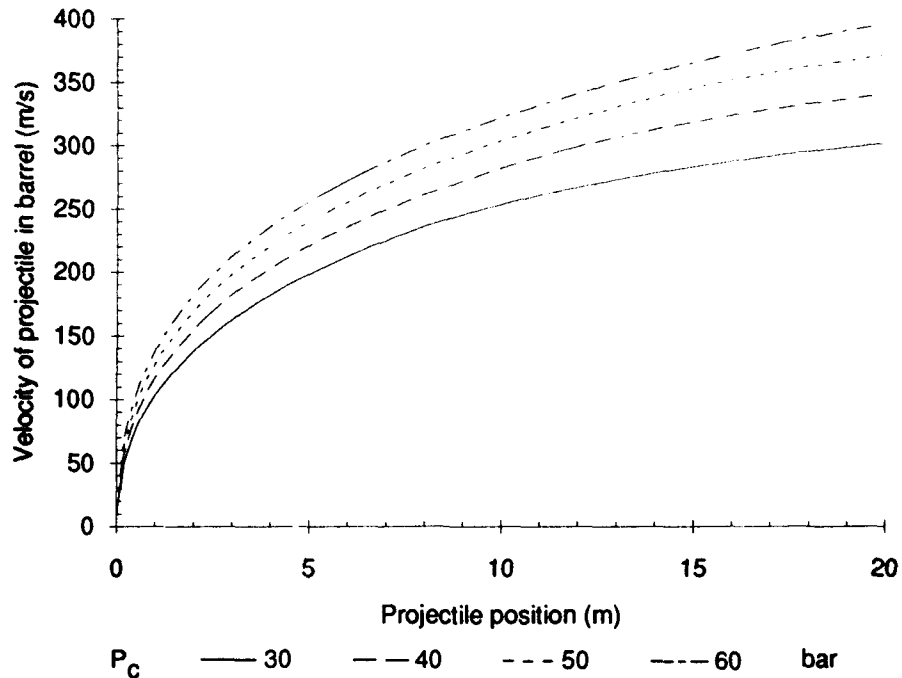
Figure 4.8   Projectile velocity as a function of position for several initial chamber pressures P_c, with a friction-less projectile and an evacuated barrel
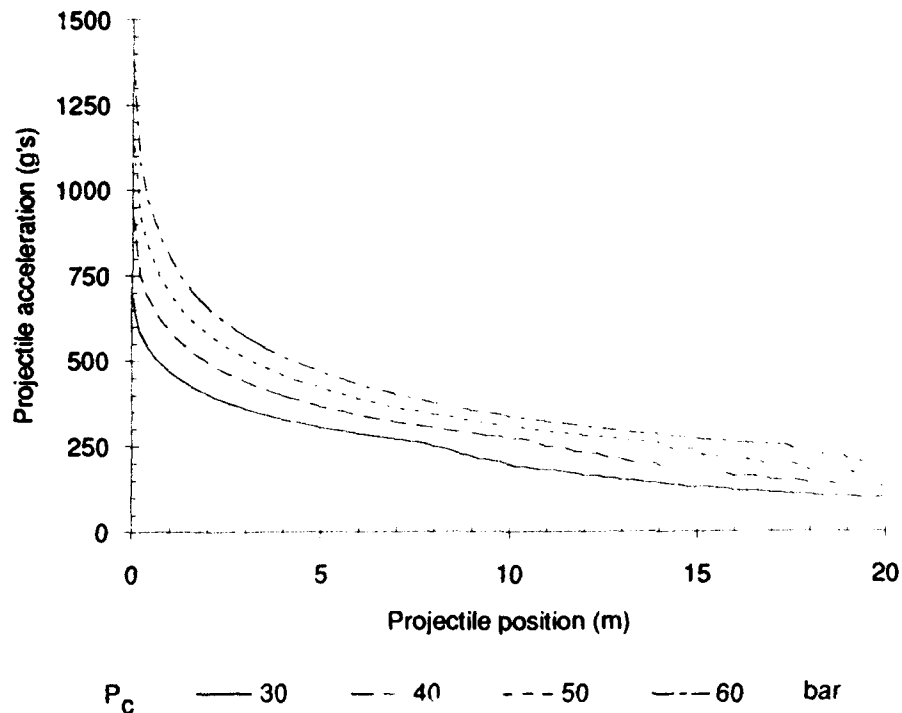
Figure 4.9   Projectile acceleration as a function of position for several initial chamber pressures P_c, with a friction-less projectile and an evacuated barrel

Effect of friction

The above results were all calculated for the case of no friction between the projectile and the barrel, and for an evacuated barrel. The effect of increasingly larger friction values on gasgun performance is illustrated in Figures 4.10 and 4.11. The configuration of the gasgun is defined by L_c = 10m, D_c = 0.3m, driver gas air, T_c = 293°C, L_b = 20m and M_p = 30kg. The barrel was still assumed to be evacuated.

Figure 4.10 uses several values of the friction proportionality constant a as introduced in Eq.(4.18). In Figure 4.11 the different curves correspond to different values of the constant friction pressure C_p of Eq.(4.17). As expected, the greater the friction is, the lower the muzzle velocity of the projectile.
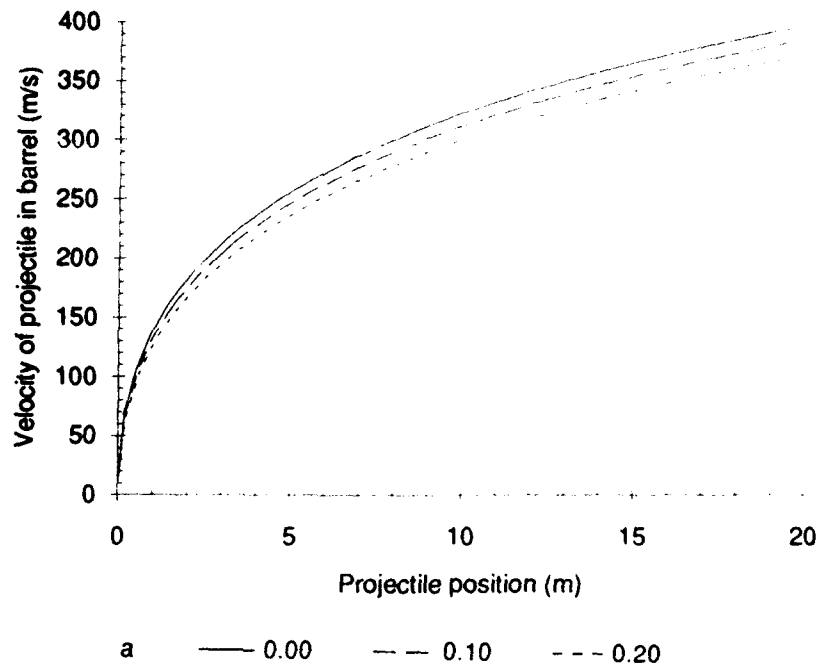
Figure 4.10   Projectile velocity as a function of position for several friction coefficients "a" (Eq.(4.18)) for air, with an evacuated barrel
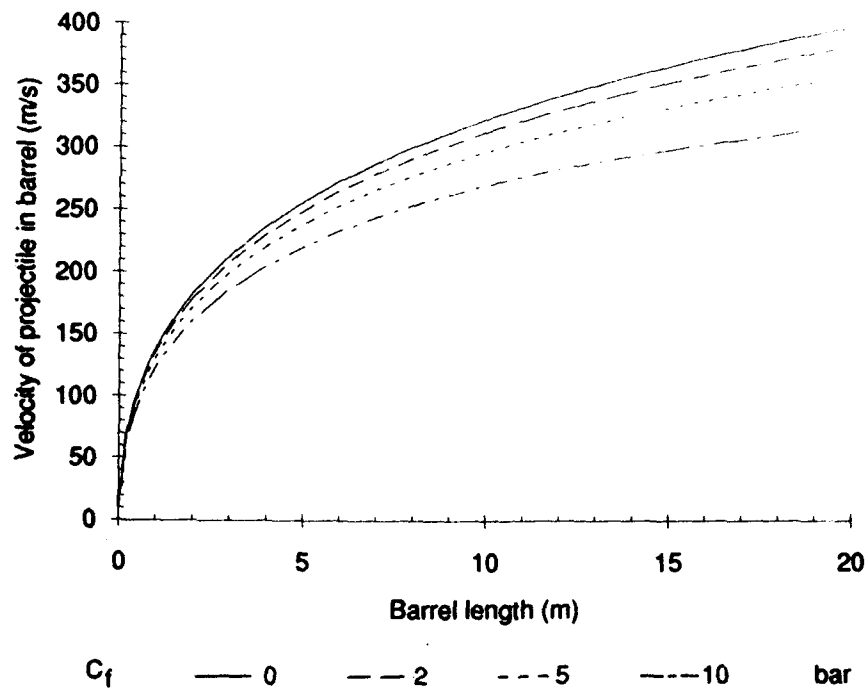
Figure 4.11   Projectile velocity as a function of position for several constant equivalent friction pressures C_f (Eq.(4.17)) (as in Figure 4.10)

It should be noted, that all these and the following figures lend themselves to a dual interpretation. They can be considered to express the muzzle velocity or acceleration of the projectile as a function of the barrel length, rather than as a function of the position of the projectile in a barrel of a given length.

Effect of barrel pressure

If the barrel of the gasgun is not evacuated, the air ahead of the accelerating projectile will be compressed and the projectile will experience a lower net accelerating force. For the calculations the opposing force as a result of the gas in the barrel is modelled as a function of the initial pressure P_i, type g and sound velocity a of the gas in the barrel, and the projectile velocity U_p, as expressed by:

$$\frac{P_f}{P_i} = 1 + \frac{\gamma(\gamma+1)}{4}\frac{U_p^2}{a^2} + \frac{\gamma U_p}{a}\sqrt{1 + \frac{(\gamma+1)^2}{16}\frac{U_p^2}{a^2}} \tag{4.22}$$

(For a derivation of this equation the reader is referred to an elementary text book on gas dynamics.)

Figure 4.12 illustrates the effect of increasing initial barrel pressure on the performance of the same gasgun as used before, assuming no friction. For this particular gasgun the minor effort of evacuating the barrel can result in a performance gain of maximally 10% for a completely evacuated barrel.
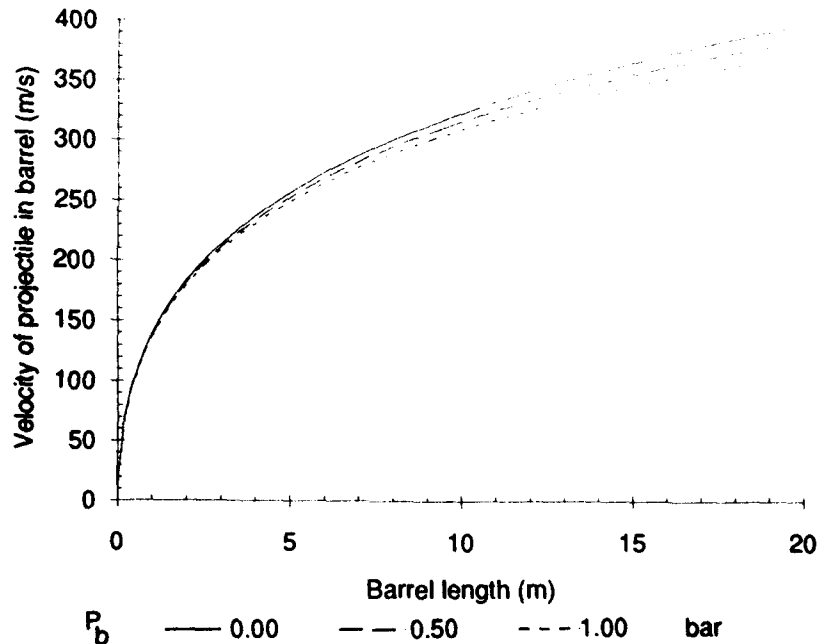
Figure 4.12 Projectile velocity as a function of position for several barrel pressures P_b, for air with a friction-less projectile

It is now possible to evaluate any combination of friction and barrel pressure. Some examples will be given in this and the next chapter.

Effect of driver gas choice

In all the previous examples air was the driver gas. For helium, the influence of chamber length, initial chamber pressure, projectile friction and barrel pressure is analogous. This is illustrated by Figures 4.13 and 4.14. These figures show projectile velocity and projectile acceleration, respectively, as a function of the projectile position for several values of the chamber length L_c. The gun was once again defined by $D_c = 0.3m$, $P_c = 60$ bar, driver gas helium, $T = 20°C$, $L_b = 20$ m, $P_b = 0$ bar, and $M_p = 30$ kg. Compare these figures with Figures 4.6 and 4.7 for a similar air gun.
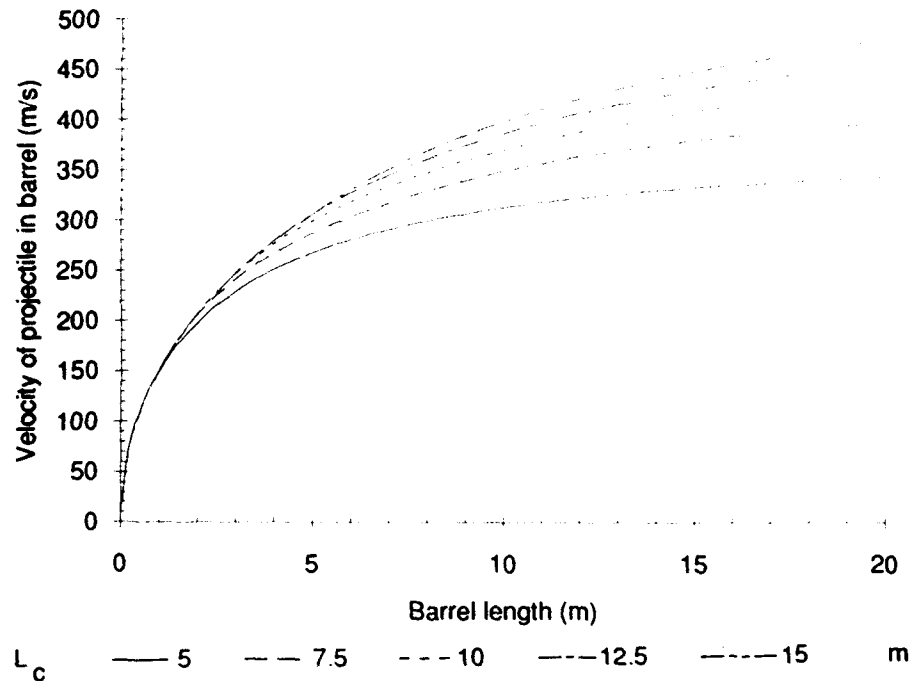
Figure 4.13   Projectile velocity as a function of position for several chamber lengths L_c for helium, with a friction-less projectile and an evacuated barrel. Compare Figure 4.6
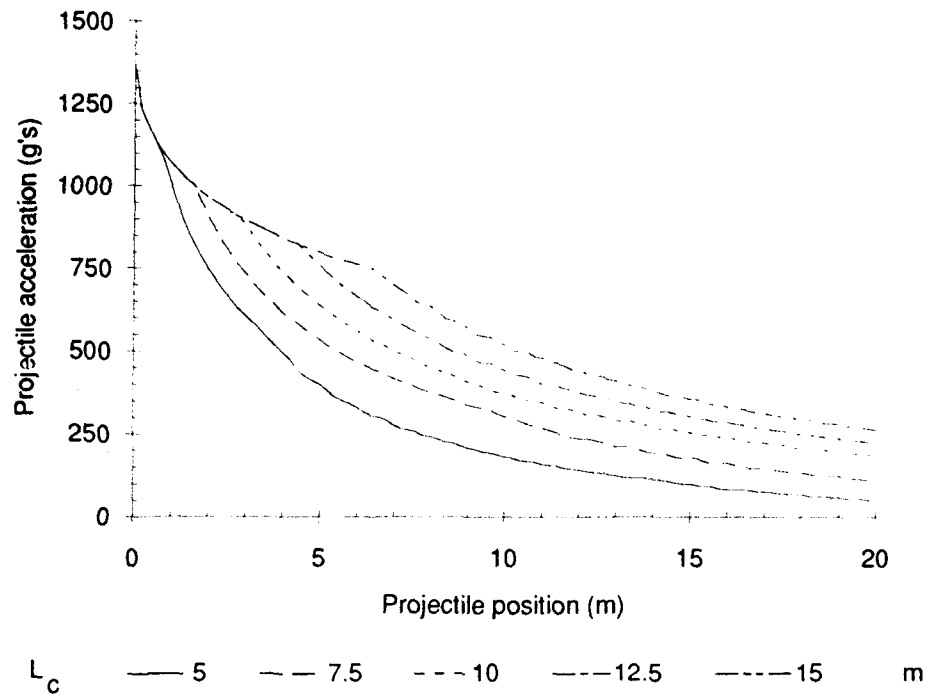
Figure 4.14 Projectile acceleration as a function of position for several chamber lengths L_c for helium (as in Figure 4.13). Compare Figure 4.7

This completes our treatment of the constant diameter gasgun. In the next section paragraph the chambered gasgun is discussed.

4.7 The chambered gasgun

If the driver gas reservoir of a gasgun is larger in diameter than the barrel, the gasgun is called a chambered gasgun. A schematic overview of a chambered gasgun was given in Figure 4.1. In this figure we have an abrupt transition from the chamber to the barrel; in reality this transition is usually more gradual. However in the model developed here only an abrupt transition is considered.

In this section we will first explain the advantages of chambrage. Then we will introduce a simple way to model a chambered gasgun, based on the method for the constant diameter gasgun. This will be referred to as the "pseudo-analytical approach". Lastly, a more rigorous and general numerical method to calculate chambered gasgun performance will be discussed.

4.7.1 Advantage of chambrage

Compared to a constant diameter gasgun containing an equal amount of driver gas, a chambered gasgun accelerates a projectile to a higher velocity in the initial stages of projectile motion (i.e. until a number of reflections have occurred). The larger the chambrage D_c/D_b, the higher the projectile velocity will be. The reason for this behaviour is that the rarefaction disturbances initiated by the accelerating projectile are partly reflected at the transition section as compression disturbances, as was already illustrated in Figure 4.2. (In the extreme case of an infinite D_c/D_b gasgun the rarefaction would be completely reflected as a compression at the transition section.) Upon returning at the projectile these compression's raise the driving pressure at the projectile base. This process continues as long as the rarefaction's that were partly transmitted at the transition section have not reached the transition region again after being reflected from the breech.

4.7.2 Governing equations for a pseudo-analytical approach

The calculations for a chambered gasgun in this report are based on the same equations as describe the constant diameter gasgun (see section 4.5), with one modification.

The characteristic equations Eqs.(4.10) and (4.11) describe the behaviour of the gas in the (constant diameter part of the) chamber and the barrel. The driver gas is considered an ideal gas (Eq.(4.12)), that isentropically expands as expressed by Eq.(4.13). Of course Newton's law in Eq.(4.14) is generally valid. For the chambered gasgun the decomposition of the force according to Eq.(4.15) together with the modelling of friction between projectile and barrel according to Eqs.(4.17) and (4.18) hold as well. The effect of the gas in the barrel in front of the projectile is once again expressed by Eq.(4.22).

As long as a gasgun is of effectively infinite chamber length, the propelling pressure as a function of projectile position for a constant diameter gasgun is given by Eq.(4.18). For a chambered gasgun this equation is replaced by the following expression, introducing the effect of chambrage:

$$P(U_p) = P_c(1 + (\sqrt{\tfrac{\gamma+1}{2}} - 1)(1 - \frac{A_c}{A_b})(\frac{\gamma U_p}{1.5a_0}) - \frac{(\gamma-1)U_p}{2a_0})^{\frac{2\gamma}{\gamma-1}} \quad \text{for } \gamma U_p <= 1.5a_0 \qquad (4.23)$$

$$P(U_p) = P_c(1 + (\sqrt{\tfrac{\gamma+1}{2}} - 1)(1 - \frac{A_c}{A_b}) - \frac{(\gamma-1)U_p}{2a_0})^{\frac{2\gamma}{\gamma-1}} \quad \text{for } \gamma U_p >= 1.5a_0 \qquad (4.24)$$

There is a lot of reasoning underlying and motivating this approach. Since it would require the introduction of some new concepts and equations relating to a more detailed description for the behaviour of the gas in the transition region, we dispense with an explanation here and refer the interested reader to Seigel [19].

With regard to the limitations of this pseudo-analytical approach we want to point out the following. Comparison of the performance predicted by this method with the results of a numerical solution to the full set of equations for a chambered gasgun, have revealed that the pseudo-analytical solution is quite accurate as long as the length of the chamber can be considered infinite. If the chamber is not effectively of infinite length, the more reflections of pressure disturbances between projectile and breech occur, the more the muzzle velocity predicted by this approach underestimates the actual muzzle velocity.

4.6.3 Governing equations for the general chambered gasgun approach

Compared to the description of a constant diameter gasgun, similar and additional equations govern the performance of a chambered gasgun.

Similar are:

- the description of the behaviour of the driver gas;
- Newton's equation for the projectile acceleration;
- the characteristic equations in the barrel.

In addition there are:

- the characteristic equations in (the constant diameter part of) the chamber;
- equations to describe the behaviour of the driver gas in the transition section of the chamber;
- equations to couple the constant chamber to one side of the transition region and the barrel to the other side.

In particular, so called quasi-static versions of the continuity and momentum equations are used to relate conditions at the chamber side of the transition region to those at the barrel side.

A full discussion of these equations requires a lengthy treatment. Such a discussion would not add much to the current understanding of the behaviour of gasguns and is therefore left out of this report. However, one fact should be emphasised here: both sides of the transition region form a discontinuity by which pressure disturbances are both partly reflected and partly transmitted.

4.6.4 Numerical solution to the equations

A computer program to calculate the performance of a chambered gasgun by numerically solving the governing equations is still under construction. Properly taking into account all the interactions

between partially reflected and transmitted pressure disturbances, requires a great deal of bookkeeping within the program. At present the program is able to predict the performance of gasguns with configurations that are of particular interest to this project, with respectable accuracy; however, it is not yet full proof for arbitrary configurations. The program's reliability will be discussed in the next paragraph on validation issues.

For several gasgun configurations the program was used to calculate the projectile velocity in the barrel and at the muzzle. This demonstrated the advantage of a chambered gasgun over a constant diameter gasgun as discussed in section 4.7.1. The numerical results for chambered gun performance with an ideal propellant gas indicate the following trends:

- for gasguns with an effectively infinite length chamber, the greater the chambrage, the greater the projectile velocity;

- for gasguns with equal amounts of driver gas, the larger the chambrage, the larger the projectile velocity in the initial stages of motion (i.e., before a number of reflections have occurred between the breech and the projectile); in the later stages (after a number of reflections) the projectile velocity will be approximately equal for all gasguns, irrespective of chambrage.

To illustrate these statements a few figures are presented; additional examples are found in the next chapter. Figures 4.15 and 4.16 for air and helium, respectively, show the effect of doubling the chamber diameter in a gasgun. The following parameters were common to all calculations: $P_c = 60$ bar, $M_p = 30$ kg, $D_b = 0.3$ m, $L_b = 20$ m. Chamber length and diameter were varied as follows: $L_c = 5$ m or 15 m, $D_c = 0.3$ m or 0.6 m, resulting in four curves for each figure. As before, in all cases projectile friction and air resistance in the barrel have been neglected.

Figure 4.15 for the air gun illustrates two aspects:

- as long as the chamber can be considered of infinite length (i.e. no reflections have returned at the projectile), the actual chamber length does not matter: the curves for different L_c (but the same diameter ratio) coincide; it is only after a rarefaction reflected from the breech has returned at the projectile for the $L_c = 5$ m chamber, that this curve starts to differ from the $L_c = 15$ m curve;

- the projectile velocity is clearly larger for the larger chamber diameter.

One remark should be made here: the point at which the curves for different chamber lengths L_c start to differ is the same regardless of the chamber diameter D_c. This is a result of the current modelling procedure. In reality (and when a more advanced chambered gasgun model is used) that particular point is also influenced by the diameter ratio.
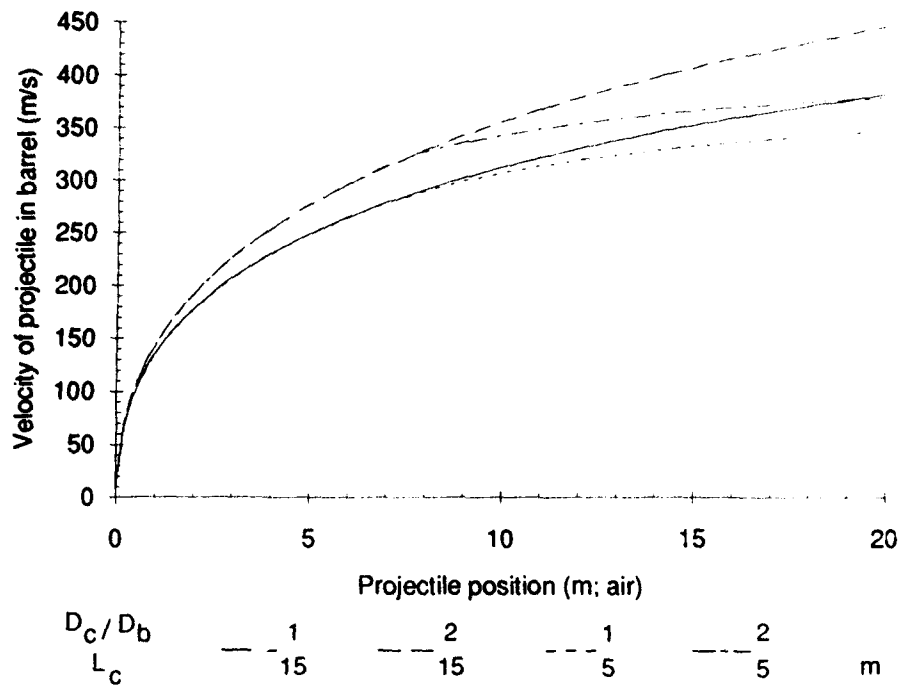
Figure 4.15   Projectile velocity as a function of position for several chamber diameters D_c and lengths L_c for air, demonstrating the effect of chambrage
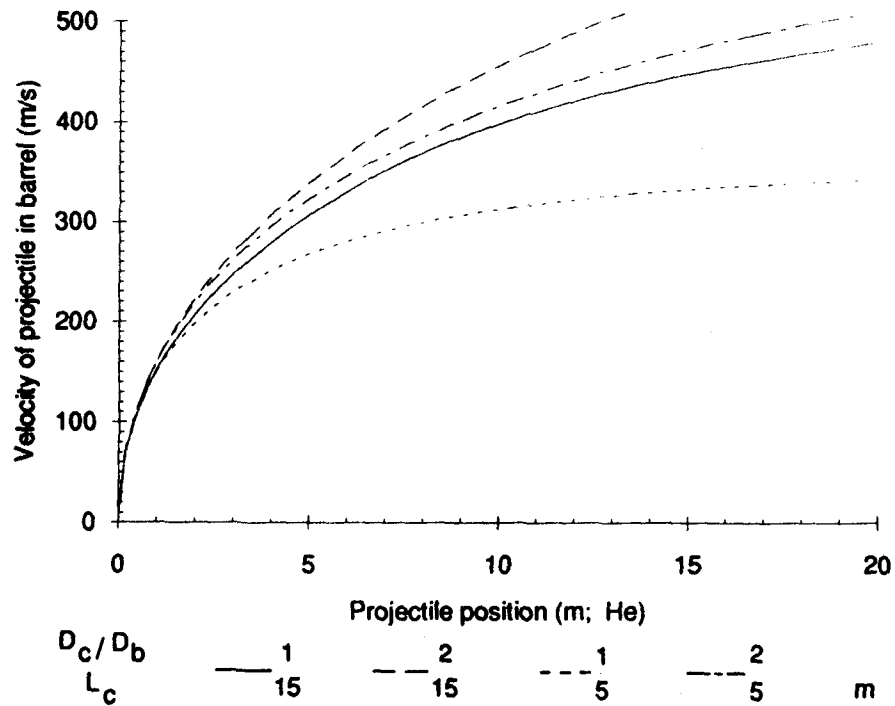
Figure 4.16   Projectile velocity as a function of position for several chamber diameters D_c and lengths L_c for helium. Compare Figure 4.15

Figure 4.16 for the helium gun differs from the previous figure, in that:

- the curves for the two different chamber lengths L_c start to differ at a much earlier position of the projectile in the barrel; this is because helium has a much higher sound velocity than air, so that the reflections return at the projectile much faster;
- for L_c = 15 m, the larger chambrage produces the higher velocities;

We note that, if a lower initial chamber pressure is used in the calculations, the effect of the returned reflections becomes noticeable for the larger chamber length L_c = 15 m as well.

This concludes the present discussion of the chambered gasgun. In the next chapter various other gasgun geometry's are studied; the results provide additional confirmation of the statements as discussed here.

4.8 Validation

The program developed to numerically solve the differential equations for either constant diameter or chambered gasguns has been tested extensively.

As a first test, for conditions allowing an analytical treatment, the program's results were compared with the analytical solution: agreement was excellent.

Then the program was used to reproduce calculations, performed by Seigel [19], for both constant diameter and chambered gasguns: again the agreement turned out to be very good. Details are given in Annex A.

Two other checks on the program were performed. For comparison purposes, ISL agreed to perform some gasgun calculations using their finite difference code. The gasgun parameters conformed to the standard set L_c = 7.5 m, D_c = 0.6 m, P_c = 60 bar, T = 20°C, L_b = 20 m, D_b = 0.3 m, P_b = 0 bar, and M_p = 30 kg, with both air and helium as driver gas. The ISL results agreed with ours within approximately 2%.

Lastly, the program was checked against experimental data from scale experiments performed at the LBO. For these a small-calibre chambered gasgun was used, firing 0.325 g and 1.1 g projectiles from a barrel of 3.6 mm and 5.4 mm diameter, respectively. Both air and helium were used to operate the gun. For several reasons a valid comparison proved difficult. Details are given in Annex A as well.

5   GASGUN PARAMETER STUDY

5.1   Introduction

In this chapter the results are presented of various calculations aimed at demonstrating that a gasgun can be used to accelerate a 30 kg projectile of 0.3 m diameter to velocities of up to 400 m/s. These calculations utilised the model introduced in the previous chapter. The calculations have the character of a parameter study, with some parameters being varied over a wide range of values. Typical parameter values used are (including those that were kept fixed throughout the calculations):

- chamber length L_c = 5, 7.5, 10, 12.5, 15 m;
- chamber diameter D_c = 0.30, 0.45 and 0.60 m;
- chamber pressure P_c = 30, 40, 50, 60 bar;
- driver gas = air, helium;
- projectile mass M_p = 20, 30 kg;
- barrel length L_b = 20 m;
- barrel pressure P_b = 0, 1 bar;
- temperature = 20°C;
- friction equivalent pressure C_f = 2 bar.

The friction pressure can be considered as an upper limit for friction losses, for most relevant cases; however it should be noted that this value is an assumed (chosen) value.

5.2   Results

5.2.1   Results for 30 Kg projectile

Tables 5.1 and 5.2 list, for air and helium as driver gas, the muzzle velocities obtained for a 30 kg projectile of 0.3 m diameter, as a function of chamber length, initial chamber pressure and barrel pressure, all with a barrel length of 20 m.

These results are also presented graphically in Figures 5.1 to 5.6. The first four figures plot the influence of the chamber diameter on the muzzle velocity of the projectile, for a gasgun with both an evacuated and a non-evacuated barrel for several initial chamber pressures and two different chamber lengths (L_c = 7.5, 15 m). Figures 5.1 and 5.2 are for air, Figures 5.3 and 5.4 for helium as driver gas.

Figures 5.5 and 5.6 illustrate, for air and helium respectively, the influence of chamber length and pressure on the muzzle velocity for various chamber diameters in a gasgun with an evacuated barrel.

Table 5.1   Muzzle velocity U_p as a function of chamber length L_c, chamber pressure P_c, chamber diameter D_c, and barrel pressure P_b, for a gasgun with air as driver gas and a 30 kg projectile (at 2 bar friction!)

L_c (m)	P_c (bar)	P_b (bar)	U_p (m/s)		
			Dc = 0.3m	Dc = 0.45m	Dc = 0.6m
5.0	30	0	239	297	325
5.0	30	1	201	266	296
5.0	40	0	281	339	365
5.0	40	1	245	308	338
5.0	50	0	316	373	399
5.0	50	1	282	343	371
5.0	60	0	346	402	427
5.0	60	1	313	373	400
7.5	30	0	273	319	339
7.5	30	1	238	289	311
7.5	40	0	317	362	381
7.5	40	1	285	334	355
7.5	50	0	351	395	413
7.5	50	1	321	369	388
7.5	60	0	378	420	437
7.5	60	1	350	396	413
10.0	30	0	293	332	347
10.0	30	1	262	304	321
10.0	40	0	333	369	384
10.0	40	1	305	344	360
10.0	50	0	360	397	413
10.0	50	1	335	373	389
10.0	60	0	381	420	437
10.0	60	1	357	396	413
12.5	30	0	301	333	347
12.5	30	1	274	308	322
12.5	40	0	334	368	384
12.5	40	1	309	344	360
12.5	50	0	360	397	413
12.5	50	1	335	372	389
12.5	60	0	381	420	437
12.5	60	1	357	396	413
15.0	30	0	301	333	347
15.0	30	1	276	308	322
15.0	40	0	334	368	384
15.0	40	1	309	344	360
15.0	50	0	360	397	413
15.0	50	1	335	372	389
15.0	60	0	381	420	437
15.0	60	1	357	396	413

Table 5.2   Muzzle velocity for a gasgun with helium as driver gas. See Table 5.1

L_c (m)	P_c (bar)	P_b (bar)	U_p (m/s)		
			Dc = 0.3m	Dc = 0.45m	Dc = 0.6m
5.0	30	0	224	309	360
5.0	30	1	180	272	326
5.0	40	0	270	363	418
5.0	40	1	229	327	385
5.0	50	0	309	408	468
5.0	50	1	269	373	435
5.0	60	0	343	449	511
5.0	60	1	304	413	478
7.5	30	0	268	346	389
7.5	30	1	227	311	356
7.5	40	0	317	403	450
7.5	40	1	280	369	418
7.5	50	0	359	451	501
7.5	50	1	322	418	468
7.5	60	0	397	493	545
7.5	60	1	360	460	513
10.0	30	0	297	369	405
10.0	30	1	259	335	374
10.0	40	0	350	428	467
10.0	40	1	313	395	436
10.0	50	0	395	478	519
10.0	50	1	359	445	488
10.0	60	0	434	521	564
10.0	60	1	399	489	533
12.5	30	0	319	384	416
12.5	30	1	282	351	385
12.5	40	0	373	445	479
12.5	40	1	338	413	448
12.5	50	0	418	494	530
12.5	50	1	384	463	500
12.5	60	0	459	537	574
12.5	60	1	424	505	543
15.0	30	0	335	396	424
15.0	30	1	300	364	393
15.0	40	0	390	455	485
15.0	40	1	356	424	456
15.0	50	0	437	505	537
15.0	50	1	403	474	507
15.0	60	0	480	550	583
15.0	60	1	446	518	552

Figure 5.1   Muzzle velocity as a function of chamber pressure P_c, for various combinations of chamber diameter D_c and barrel pressure P_b (E: 0 bar; N: 1 bar). Chamber length Lc = 7.5 m, driver gas is air. See text for further details
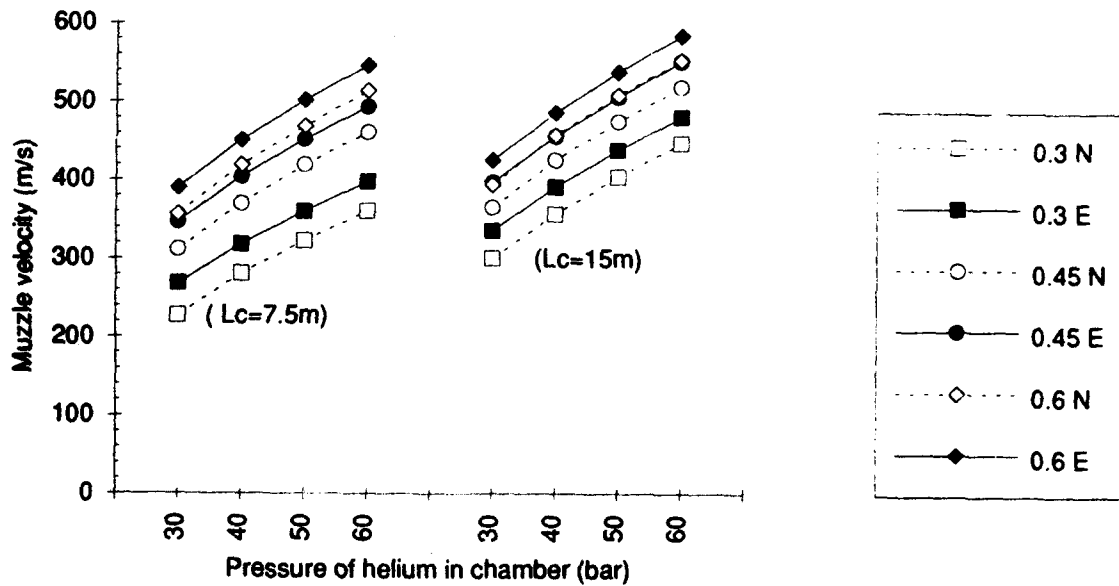
Figure 5.2   Muzzle velocity as a function of chamber pressure, for various combinations of chamber diameter and barrel pressure. Chamber length L_c = 15m, driver gas is air. See Figure 5.1
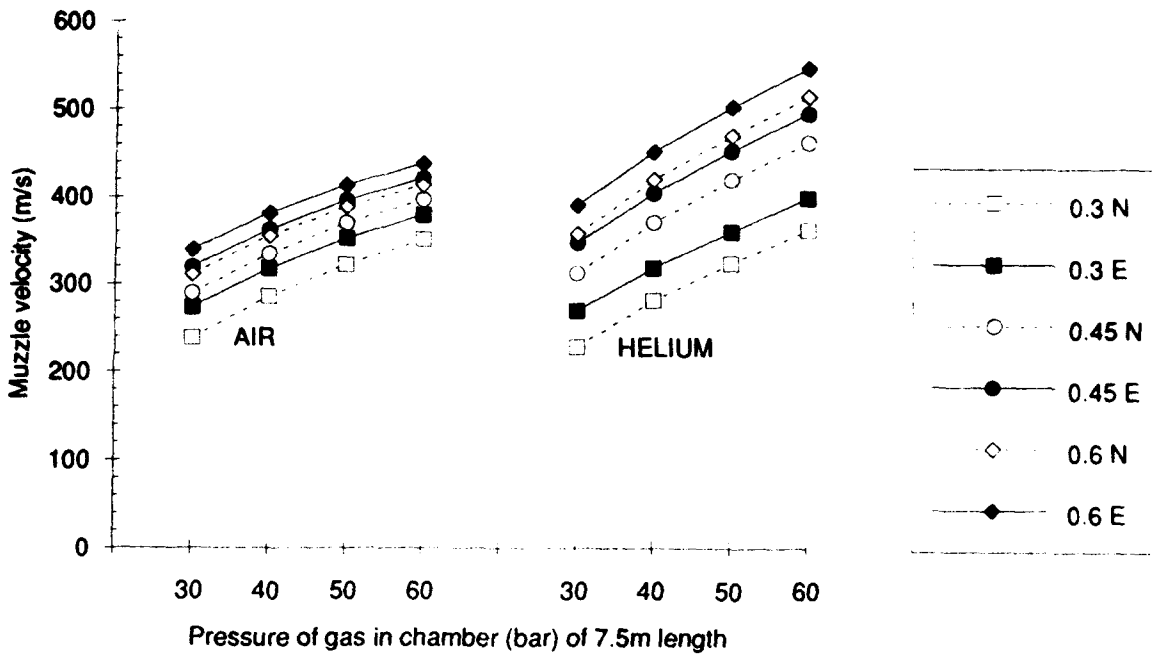
Figure 5.3   Muzzle velocity as a function of c' amber pressure, for various combinations of chamber diameter and barrel press..re. Chamber length $L_c \approx 7.5m$, driver gas is helium. *See Figure 5.1*
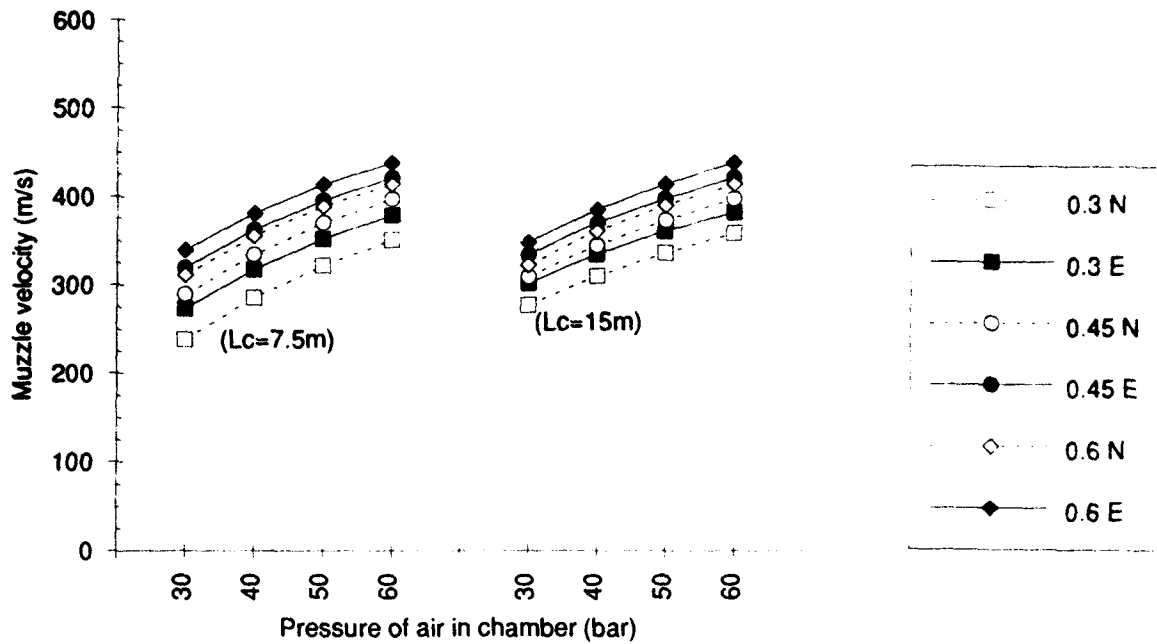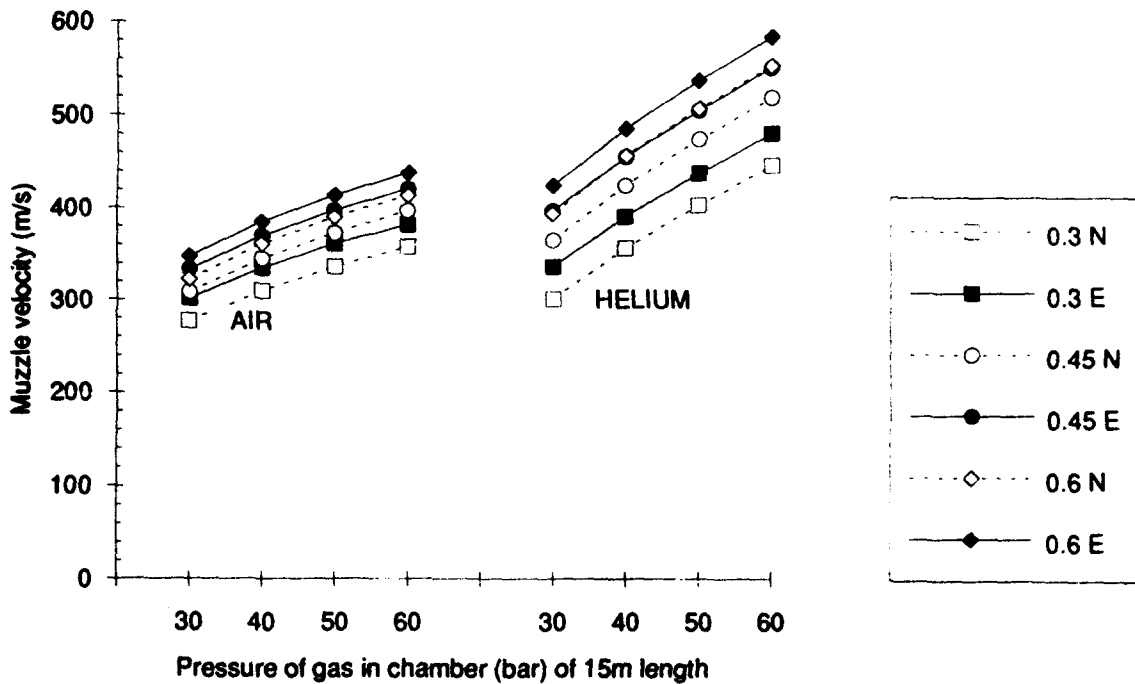

Figure 5.4   Muzzle velocity as a function of chamber pressure, for various combinations of chamber diameter and barrel pressure. Chamber length $L_c = 15m$, driver gas is helium. See Figure 5.1
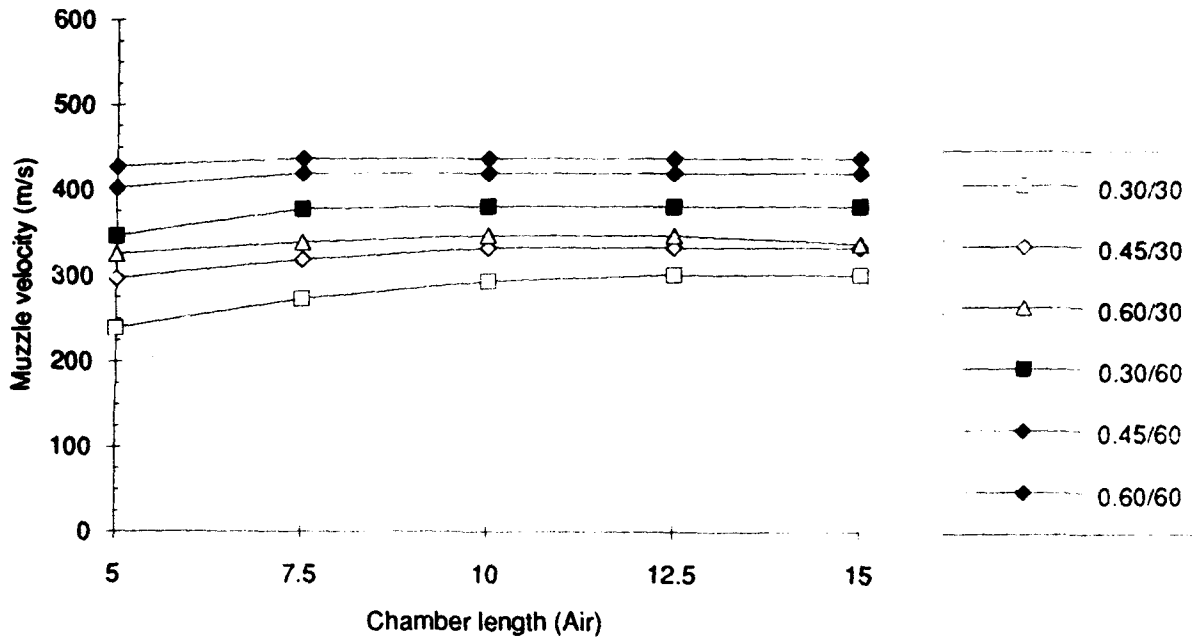
Figure 5.5   Muzzle velocity as a function of chamber length L_C, for various chamber diameters Dc and at two chamber pressures P_C, with an evacuated barrel. Driver gas is air. See text for details
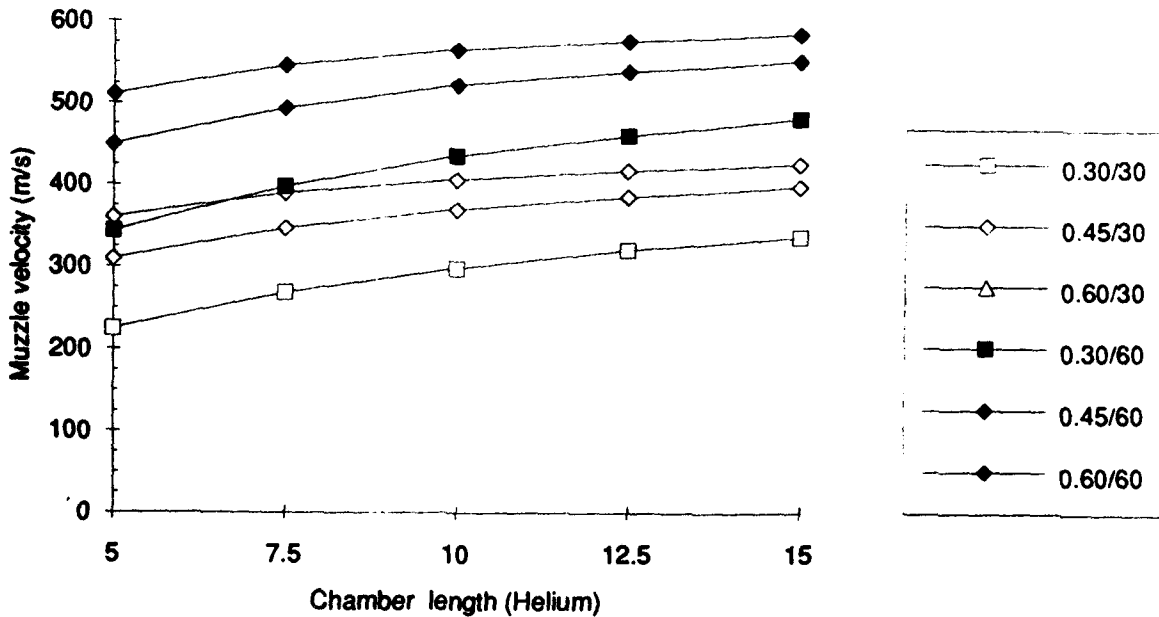
Figure 5.6   Muzzle velocity as a function of chamber length, for various chamber diameters and at two chamber pressures, with an evacuated barrel. Driver gas is helium. See Figure 5.5

5.2.2 Results for 20 Kg projectile

This section presents the results of calculations for a 20 kg projectile, as opposed to the 30 kg projectile of the previous section. Only the results for a constant diameter gasgun are considered here $(D_c = D_b = 0.3 \text{ m})$.

As in section 5.2.1, Table 5.3 lists the calculated muzzle velocities, while Figure 5.7 serves as a graphical illustration. In the figure, the influence of the chamber length on the muzzle velocity is plotted for several initial chamber pressures, for a gasgun with a fully evacuated barrel and for both air and helium as driver gas.

Figure 5.7   Muzzle velocity as a function of chamber length and chamber pressure with air and helium as driver gas in a gasgun with an evacuated barrel and a 20 kg projectile

This figure clearly shows that, when air is used as driver gas, the gasgun becomes effectively of infinite chamber length for $L_c \geq 10\text{m}$ if $P_c = 30\text{Bar}$ and $L_c \geq 7.5\text{m}$ if $P_c = 60\text{Bar}$.

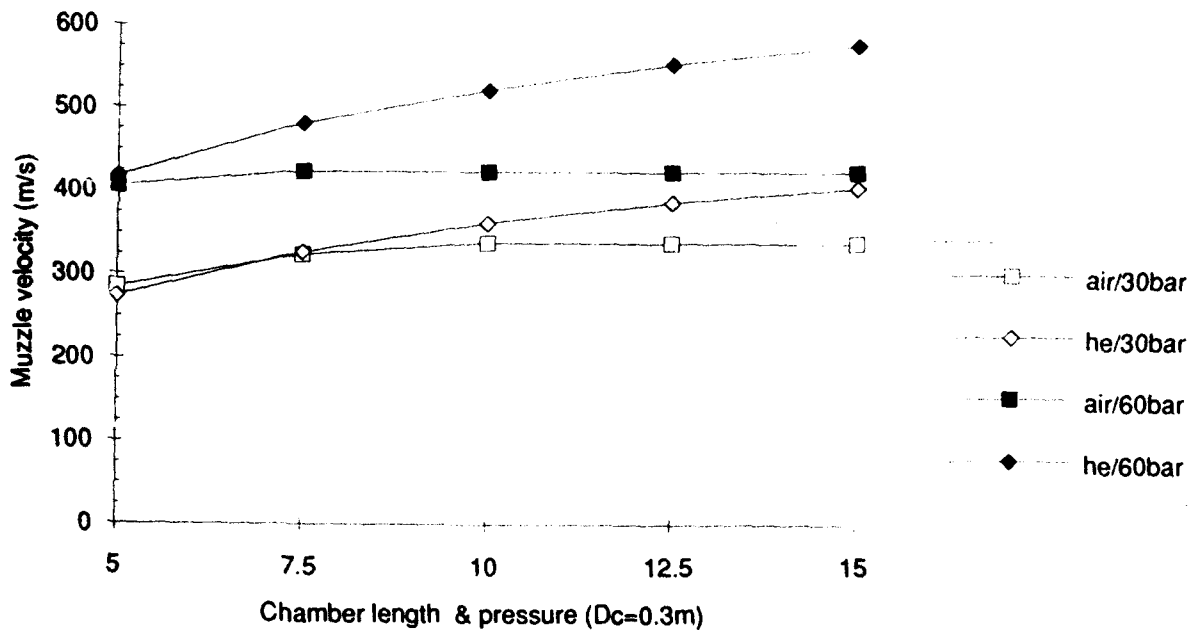Table 5.3   Muzzle velocity U_p as a function of chamber length L_c, chamber pressure P_c, and barrel pressure P_b, for a constant diameter (0.3 m) gasgun with both air and helium as driver gas and a 20 kg projectile (at 2 bar friction!)

L_c (m)	P_c (bar)	P_b (bar)	U_p (m/s) air	U_p (m/s) helium
5.0	30	0	285	274
5.0	30	1	232	211
5.0	40	0	335	330
5.0	40	1	285	270
5.0	50	0	374	376
5.0	50	1	327	318
5.0	60	0	406	417
5.0	60	1	361	359
7.5	30	0	323	326
7.5	30	1	277	269
7.5	40	0	369	386
7.5	40	1	327	330
7.5	50	0	401	437
7.5	50	1	363	382
7.5	60	0	423	481
7.5	60	1	388	427
10.0	30	0	338	361
10.0	30	1	299	306
10.0	40	0	373	424
10.0	40	1	338	371
10.0	50	0	401	475
10.0	50	1	365	423
10.0	60	0	423	512
10.0	60	1	388	468
12.5	30	0	326	386
12.5	30	1	294	334
12.5	40	0	360	449
12.5	40	1	328	398
12.5	50	0	387	504
12.5	50	1	355	453
12.5	60	0	409	553
12.5	60	1	378	501
15.0	30	0	312	404
15.0	30	1	284	353
15.0	40	0	345	471
15.0	40	1	317	420
15.0	50	0	371	528
15.0	50	1	344	477
15.0	60	0	393	577
15.0	60	1	366	527

A comparison with the earlier results for the 30 kg projectile is offered by Figures 5.8 and 5.9, which apply to air and helium, respectively. In both figures the muzzle velocity is plotted as a function of chamber length and chamber pressure for a constant diameter gun ($D_c = D_b = 0.3m$) with an evacuated barrel.
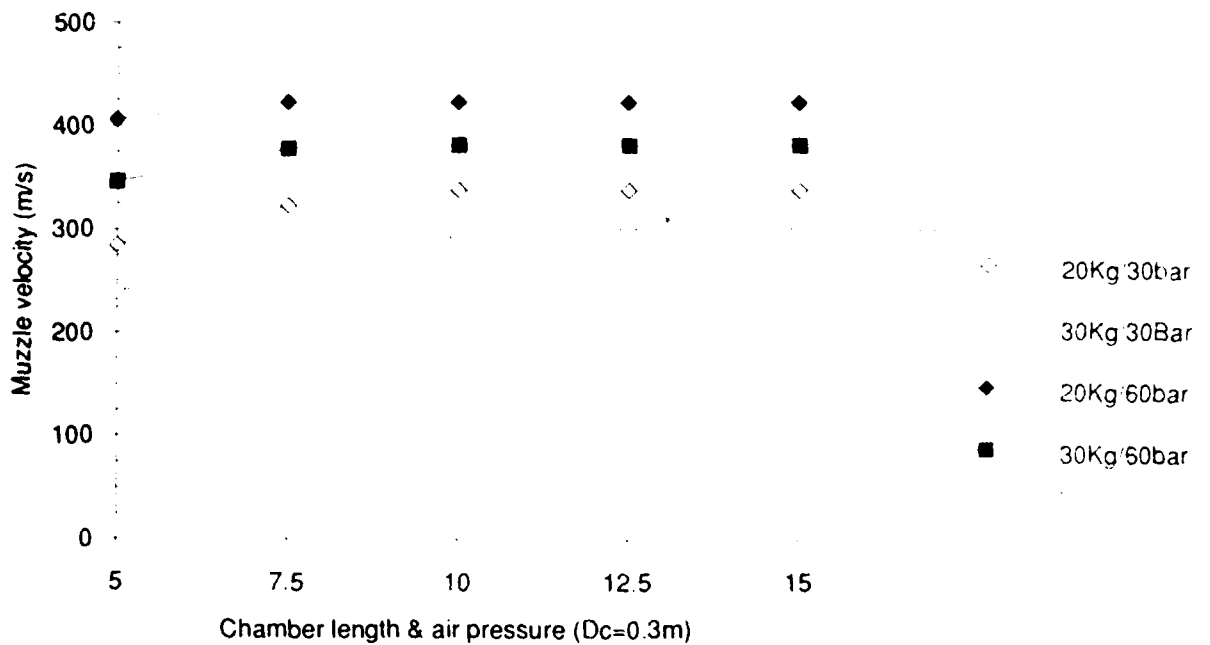

Figure 5.8   Muzzle velocity as a function of chamber length and chamber pressure for projectile mass M_p = 20 and 30 kg, with air as driver gas in a gasgun with an evacuated barrel
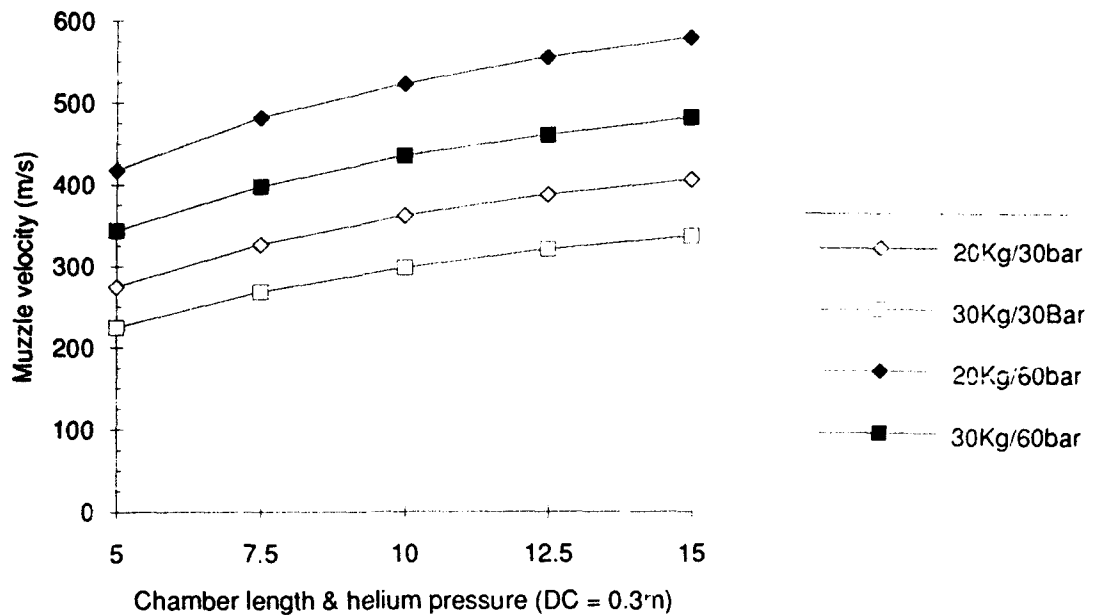
Figure 5.9   Muzzle velocity as a function of chamber length and chamber pressure for projectile mass M_p = 20 and 30 kg, with helium as driver gas in a gasgun with an evacuated barrel

5.3   Discussion

From the tables and figures in the previous sections the following conclusions may be drawn (with respect to the 30 kg projectile, in particular):

- increasing the chamber diameter results in a worthwhile increase in muzzle velocities;

- with air as driver gas a gasgun configuration becomes effectively of infinite chamber length at approximately L_c = 7.5 m for chamber pressure P_c = 60 bar and at 10.0 m for 30 bar, so that a further increase in chamber length is pointless; the larger the chambrage the earlier this is the case.

- only for the larger chamber diameters is helium significantly more effective than air; the advantage becomes more pronounced as the chamber length is increased;

- evacuating the barrel of the gasgun yields an easily obtained performance gain of approximately 10%.

At this point it must be emphasised again that the presented results were calculated with a constant friction pressure set to 2 bar; this is a conservative approach. For a low initial chamber pressure (P_c = 30 bar), negligible projectile-barrel friction would result in a 5% larger muzzle velocity.

5.4 Conclusions

The main conclusions of these investigations are:

- several configurations can be used to realise a velocity of 400 m/s for a 30 kg projectile of 0.3 m diameter. For example, the following configurations meet the performance requirements, if an evacuated barrel of 20 m length is used:
  - if the initial chamber pressure may be as high as 60 bar, a chamber length of approximately $L_C = 7.5$m or larger with $D_C = 0.3$m with helium as driver gas, or $D_C = 0.45$ m with air;
  - if the maximum chamber pressure is limited to 30 bar, none of the configurations with air as driver gas realises 400 m/s; for helium as driver gas a gasgun with $L_C = 7.5$ m and $D_C = 0.6$m suffices almost if the projectile friction is negligible; longer chamber lengths are better.
- a muzzle velocity of 300 m/s can be realised with almost all of the investigated configurations;
- the configuration of the actual gasgun will depend very strongly on the maximum acceleration level the projectile can withstand, since this also limits the initial chamber pressure.

6   GASGUN

Basically, a gasgun consists of a gas storage tank, a valve mechanism, and a launch tube or barrel. These and related subjects are discussed below.

6.1   Gas valving

One of the major questions in gasgun design concerns the way of switching the gas charge from the reservoir to the launch tube behind the projectile package. There are numerous valving methods in use, involving valves, diaphragms, pistons, etc.. Sometimes a single gun employs different, interchangeable valve mechanisms [19]. For an overview of appropriate gasgun valving techniques we quote verbatim from Swift in Reference 11.

Three basic techniques, sketched in Figures 6.1-6.3, are currently in use with modern gasgun accelerators.
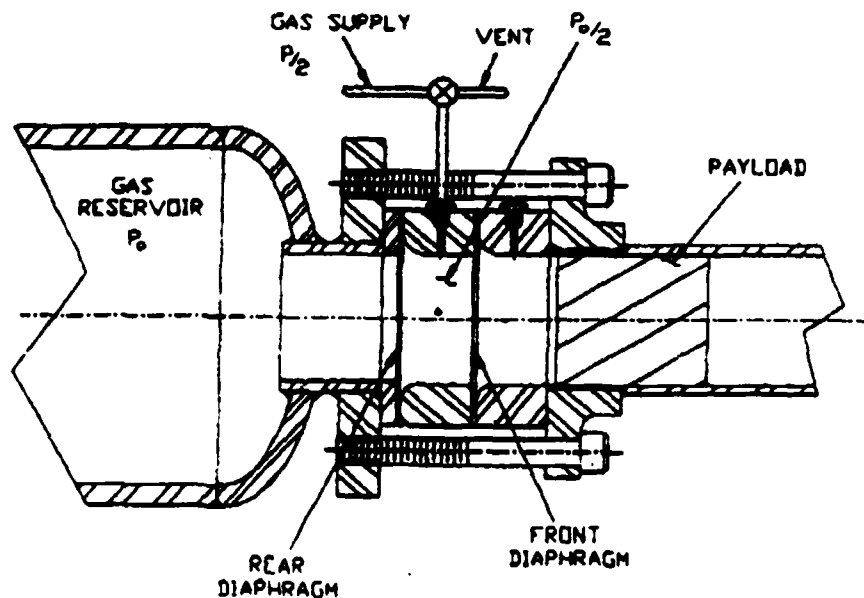
Dual diaphragm

Figure 6.1   Dual diaphragm valve system

The first technique (Figure 6.1) employs a pair of rupture diaphragms to produce the gas switching momentarily after a valve has opened. Basically, a reservoir charged to pressure P_0 is held closed by the rear diaphragm. The space ahead of this diaphragm is charged to a pressure of $P_0/2$ so that the rear diaphragm only "sees" a pressure differential of $P_0/2$. The inter diaphragm volume is closed by the front diaphragm which opens into an area of low gas pressure immediately behind the payload. Thus, the front diaphragm also "sees" a pressure differential of $P_0/2$. Each of the diaphragms is designed to tear open to form petals when exposed to a gas pressure differential of approximately 0.6 P_0. Thus, the situation is stable since both diaphragms see a pressure differential of 0.5 P_0.

The situation is destabilized by venting the volume between the diaphragms to atmosphere. The rear diaphragm experiences a rapidly rising pressure differential and bursts when the pressure across it exceeds 0.6 P_0. The action results in the entire reservoir pressure being applied to the front diaphragm which promptly bursts, thereby switching the reservoir gas directly into the launch tube behind the payload to begin the main launch cycle.

This dual diaphragm valving arrangement is preferred when maximum launch velocities are sought since the resulting channel between the reservoir and the launch tube is as free from obstructions as ever occurs. A distinct disadvantage of the dual-diaphragm system is that two precisely fabricated diaphragms must be sacrificed for each firing (but see section 6.2). Also, the structure holding the diaphragms in place must be disassembled between firings: the expended diaphragms must be removed; new diaphragms must be installed; and the assembly must be reinstalled before the next gun firing. Another problem with dual-diaphragm valving is that it subjects projectile payloads to nearly instantaneous application of maximum acceleration which is useful for obtaining maximum velocities with light projectiles but which produces launch cycles with very high jerk levels. Such cycles may be expected to inject significant shock energy into launched payloads.
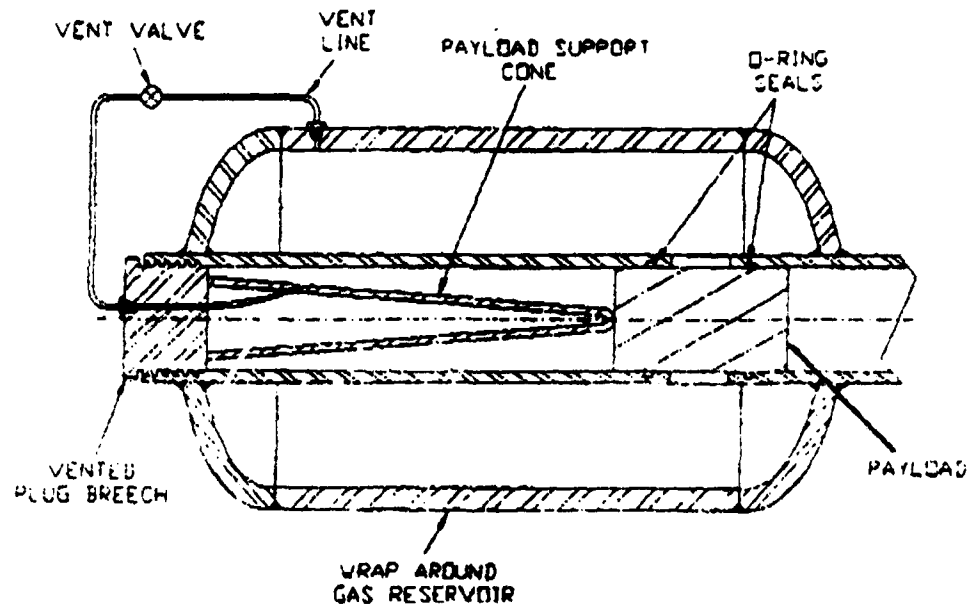
Basic regenerative valve

Figure 6.2   Basic regenerative valve system.

The second valving technique sketched in Figure 6.2 uses an entirely different switching concept that requires no expendable parts. The payload is mounted in the launch tube to cover four holes in the launch tube wall that connect the bore volume with a surrounding "wrap-around" reservoir. Each of the holes has a diameter of one launch tube radius so, together, they have a cross-sectional area equal to that of the launch tube. A substantial segment of launch tube behind the payload is closed with a screw breech which contains a conical fore-body that engages the rear surface of the payload when the breech is closed. Once the model is in its firing position and the breech is closed, the reservoir is filled with the high pressure gas charge.

The gun is fired by opening a small tube between the reservoir and the breech which allows gas to be admitted slowly into the launch tube volume behind the projectile. Gas pressure built up eases the projectile package forward until its rear edge begins to open the four large holes between the reservoir and the launch tube bore. Gas then flows rapidly into the launch tube behind the projectile: projectile acceleration increases; the projectile moves forward to open the holes completely; and the launch cycle is commenced.

This arrangement has several distinct advantages over the dual diaphragm valving. First, no parts are expended to trigger the launch which aids operational economy and simplifies between-shot preparations. Second, the launch tube bore space behind the model can be used effectively to mitigate the onset of peak launch package acceleration (reduces the jerk level of the launch profile). This space must be filled before peak acceleration is applied to the launch package. Shockwaves which might be produced in this space and transferred to the model base are attenuated or even eliminated by the central cone which disperses waves in the early behind-projectile volume. A disadvantage of the basic regenerative valve arrangement is that gas must pass through multiple holes between the reservoir and launch tube and turn 90° before being applied to the launch package base. Resulting turbulence tends to reduce launch efficiencies slightly. This tendency becomes progressively more severe as higher launch velocities are attempted which effectively eliminates regeneratively valved guns from attempts to reach very high muzzle velocities. Another problem with simple regeneration valving is that the projectile package must seal the access holes efficiently and must bear substantial compressive loads. Both of these factors can serve to limit flexibility of simple regeneratively valved gasguns.
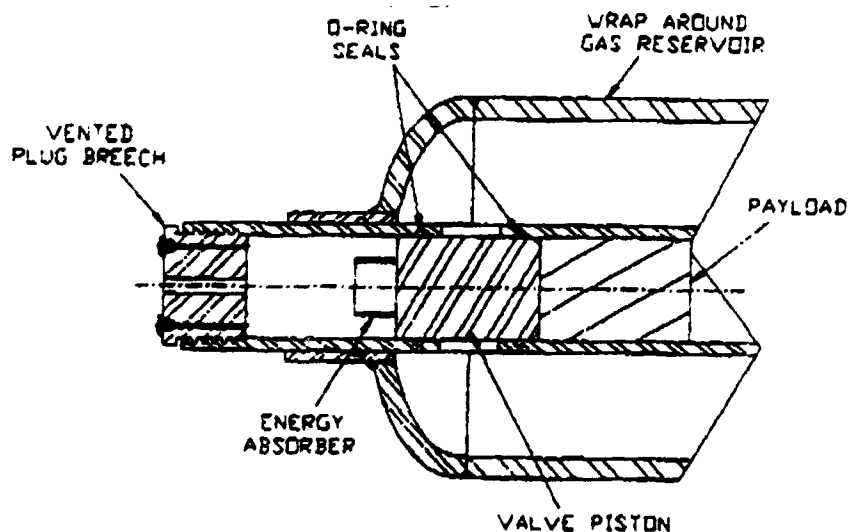
Separate piston regenerative valve

Figure 6.3   Separate piston regenerative valve system

The third technique, shown in Figure 6.3, is similar to the regenerative valve system depicted in 6.2 except that a separate valve piston is used t ᷉ control gas flow through the holes between the reservoir and the launch tube, rather than the payload itself. The piston engages O-ring seals just upstream and downstream from the holes. Occasionally, payload designs cannot be made to seal the reservoir/bore openings. Other payloads have walls too structurally weak to sustain radial compression by launch pressure without being crushed.

The valve system is triggered by drawing the valve piston rearward until its forward face starts to open the reservoir/bore holes. (No mechanism for producing this motion is shown in Figure 6.3.) The piston is then driven rearward violently as the valve opens completely and the launch cycle is begun by gas pressure being applied to the rear face of the payload. A payload support cone similar to the one shown in Figure 6.2 may be used between the valve piston and the payload to reduce jerk levels of the launch cycles. Meanwhile, the valve piston is driven violently enough into the vented plug breech to cause substantial damage if its stopping is not cushioned (a typical design might produce 16 KJ of impact energy). This energy may be absorbed by a length of tubing made from ductile metal (as shown in Figure 6.3). The metal is deformed by the impact so that the tube's inner diameter shrinks while its outer diameter enlarges. Typically, five to twenty firings can be conducted safely with a single energy absorber before it must be replaced. Replacement costs are generally nominal.

This valving arrangement shares at least most of the advantages of the basic regenerative valve described above, with the slight exception that an inexpensive semi-expendable item must be replaced periodically. The piston valve design has the distinct advantage that it puts fewer limitations upon the design of the projectile payload package than does the classic design. Of course, the piston valve design shares the disadvantage with the basic regenerative design that it is inapplicable for attempts to achieve ultimate projectile launch velocities. The jerk level of the resultant launch may be controlled both by adjusting the initial position of the projectile and by choosing one of various valve pistons with different masses. Also, the jerk level may be further reduced by fine tuning the shape of the holes in the launch tube wall.

About performance limitations caused by using regenerative valves, such limitations do, indeed, exist but they only manifest themselves when the guns are operated at or near their maximum velocity capability (somewhat over 1.0 km/sec for the case of guns operating with helium driver gas). At velocities of 400 m/sec and below, single-stage helium gasguns using regenerative valves may be

expected to operate at virtually identical efficiencies with similar ones using dual-diaphragm valve configurations.

(Here ends the quote from Reference 11.)

6.2 The dual rupture diaphragm

The PML has considerable experience with rupture diaphragms. They have been applied mostly in shock tubes, but have also been used in small gasguns. Valuable, additional information was obtained from ISL.

The 19 cm gasgun at ISL, described in section 1.4, is built around a dual rupture diaphragm construction. Construction drawings of the ISL diaphragm cassette were kindly made available to the PML [20], and are reproduced in Figure 6.4. While of course prone to generating the high jerk levels typical of a diaphragm arrangement, the low cost ISL design is both simple and flexible.

Rather than having two precision diaphragms tailored to the specific reservoir pressure, each of the diaphragms consists of a large number of cellulose-acetate foils. The required number of foils increases linearly with the desired operating pressure. This multiple-foil set-up has proven very reliable at pressures up to 150 bar, and reproducibility is reputed to be excellent (1 to 1.5 % in muzzle velocity) [14].
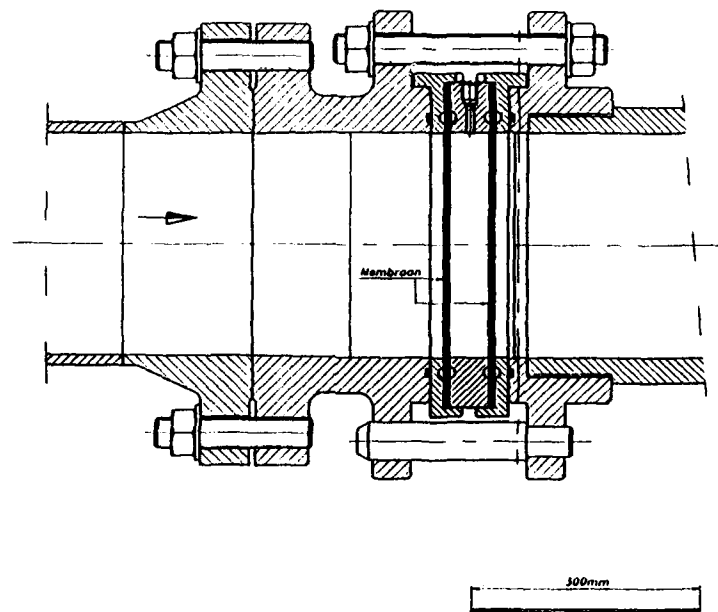
Figure 6.4   Dual diaphragm cassette (from ISL)

To verify this, the PML blast simulator has been used to test multiple 30 cm diameter mylar foils of varying thickness. These experiments are described in Appendix B. The results indeed testify to the linear behaviour of the foil packages, their larger diameter notwithstanding.

The experiments also demonstrated that some foil fragments tend to break off when the diaphragm ruptures (as opposed to pre-scored diaphragms). This is expected to present no particular problem. However, the improvised set-up proved incapable of holding the diaphragm foils reliably in place at 25 bar. While the ISL arrangement should do better, this phenomenon merits special attention.

6.3   Gas tank assembly

Given the tank volume and maximum driver gas pressure derived in Chapter 5, tank design in itself poses no problem. It is, however, dependent on the valve mechanism selected to release the driver gas. Additionally, some provision must be made for loading the projectile into the launch tube.

In-line tank

Dual-diaphragm guns, as in Figure 6.1, are awkward to load with large projectiles since the reservoir tank takes up the space immediately behind the launch tube. The tank has to be moved to the rear over the full length of the projectile, typically at least 1-1.5 m, thus opening the rear of the launch tube for loading. The tank support assembly in Figure 6.5 has been equipped with wheels, rolling on floormounted rails. This set-up is also able to take up all recoil motion.

Conversely, a much smaller lateral movement would suffice to clear the launch tube, but recoil motion, if any, would have to be taken up by another means.
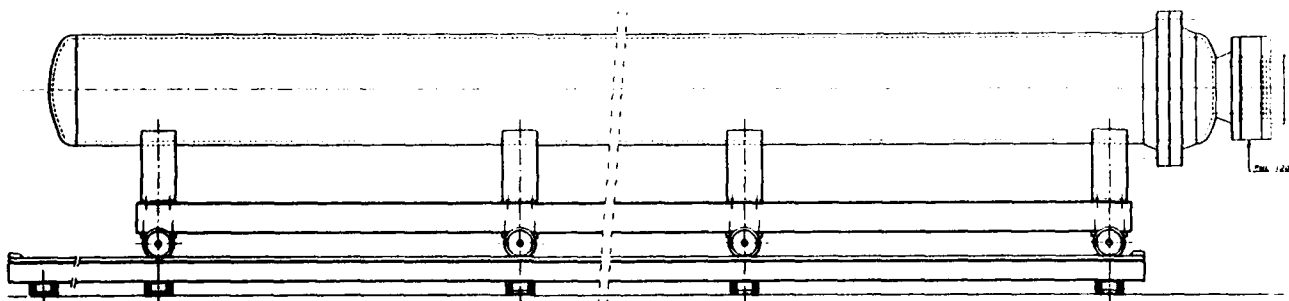

Figure 6.5   Gas tank support structure for dual-diaphragm gasgun, with provision for axial
movement to clear the launch tube for loading

Capped-breech tank

In the radial valve regenerative designs of Figures 6.2 and 6.3, the gas reservoir surrounds the launch tube, which has an opening at the rear. The gun is loaded by removing the valve plug from this opening and inserting a projectile package into the launch tube bore some distance downstream from the reservoir connection holes. A slight step in the bore diameter just downstream from the holes allows the projectile package to be moved past the holes and their seals without difficulty. The valve slug is then reinserted to block the openings between the bore and the gas reservoir. Next, a breech is screwed closed across the upstream end of the launch tube. A relatively simple tank support assembly incorporating rollers to accommodate the recoil motion, suffices in this case. Figure 6.6 illustrates this.

More complicated, and even leafier, versions of the regenerative valve mechanism are conceivable, as well. For these, disconnecting the task from the barrel, and moving it either rearward or to the side in its entirety, might be preferable to the set-up described earlier.
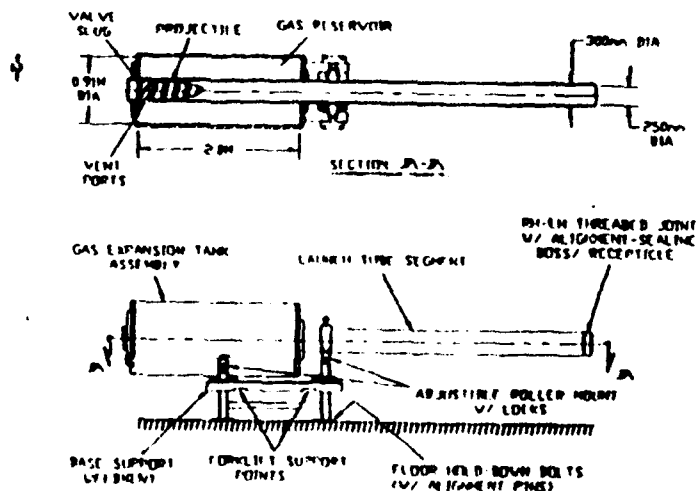

Figure 6.6   Gas tank support structure for capped-breech gasgun, with rollers allowing recoil motion [20]

6.4   Safety catch

When opting for a rupture diaphragm construction, it would seem that some sort of safety mechanism is in order. During the time required to fill the gas reservoir and prepare for the warhead test, the diaphragms are subject to a pressure some 20% beneath the rupture threshold. This pressure also acts against the clamping force holding the diaphragms in place. If the diaphragms were to let go, the projectile would be launched prematurely. While not necessarily constituting a safety hazard, this would entail the loss of warhead and target.

Such an incident may be prevented by locking the projectile package in place during the launch preparations. The construction in Figure 6.7 consists of four hydraulically operated arrester pins or catches, moving radially in O-ring sealed holes in the wall of the launch tube. The catches abut against the front face of the pusher plate during the critical preparation phase and are withdrawn prior to the launch. In the case of diaphragm failure the pusher plate is bound to sustain some damage, but the projectile package should remain in place. A gas release valve in the tank will be part of the safety system.
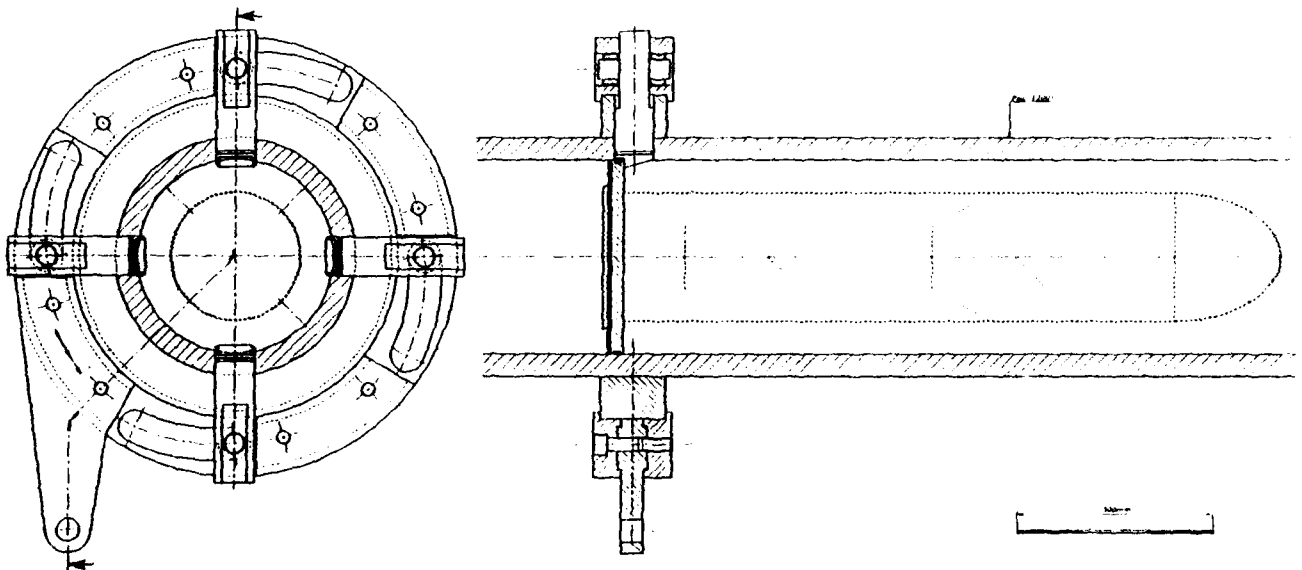

Figure 6.7   Hydraulically operated safety catch mechanism to secure the payload in case of premature diaphragm failure

6.5   Launch tube

Launch tube segments

The launch tube has a bore diameter of 30 cm. It consists of a number of separate segments, typi-
cally 5 m in length, with a carefully honed bore. The segments may be interconnected with
boss/receptacle joints held together by a flange/bolt arrangement (Figure 6.8) or by right-hand/left-
hand threaded collars. Dowel-pin/hole arrangements within each joint prevent misalignment, rota-
tional or otherwise.

Barrel grooves

As explained in Chapter 2, it is imperative to prevent the projectile from rotating during launch. In
smooth-bore guns, rotations are often caused by spiral micro-scratches in the bore wall, gas blow-by
along curved paths, etc. This can be prevented by straight grooves cut into the bore wall surface.

To inhibit gas blow-by around the projectile, which tends to produce variations in projectile veloci-
ties, the launch tube should be grooved very shallowly (0.1-0.2 mm deep by 3-4 mm wide) at, say,
four orthogonal angular locations. A smaller number of grooves might suffice as well, and present
less of a manufacturing problem. A soft plastic gas obturator at the rear of the projectile would de-
form sufficiently under gas pressure to engage the grooves. A small external flare at the rear of the
obturator assures that full groove engagement is produced by the projectile loading process.

The function of the obturator disk in engaging the grooves, could in principle also be filled by
several plastic plugs under spring pressure, incorporated into the rim of the launch vehicle [22].
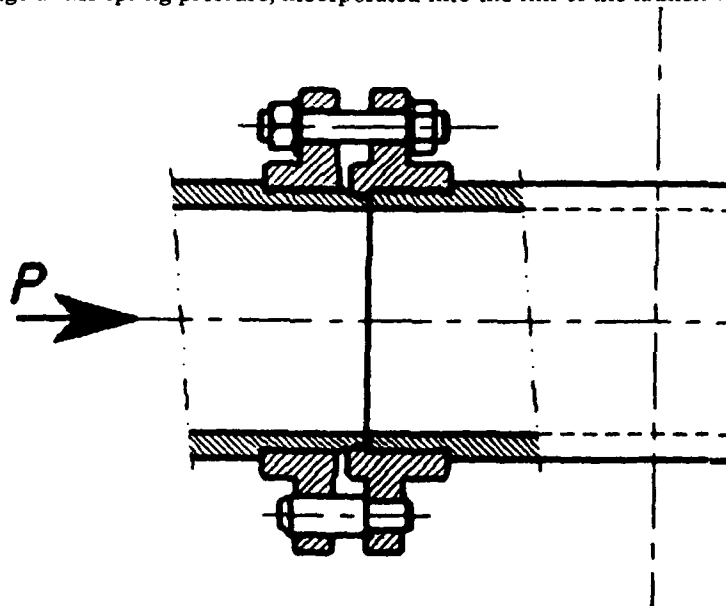

Figure 6.8   Flange/bolt connection between launch tube segments

By way of alternative a "wedge" could be screwed (or perhaps glued) in place along the bore wall of the launch tube. It must be held strongly enough to survive interaction with the projectile. Also, gas leakage will be hard to prevent.

This leads to a preference for a grooved launch tube. Since only very shallow grooves are required, it should prove possible to produce all grooves in one pass by pulling a honing device through the tube sections by brute force.

Gas release holes

Equipping the launch tube with a series of holes in the launch tube wall near its muzzle end will allow the driver gas to escape radially away, so that it does not interact with the projectile after launch. This should suppress any launch instability. In addition, it would lessen the blast associated with the gas emitted by the gasgun.

Barrel evaluation

In Chapter 5, evacuating the barrel in front of the projectile was seen to improve gasgun performance to a measurable degree. This should not be construed to mean that a high or even a perfect vacuum is required. A relatively simple sealing and pumping arrangement should suffice to reap most of the benefits of barrel evacuation.

A thin sealing diaphragm would not affect the projectile package. Any gas release holes in the launch tube would present a complicating factor however. In effect, it would be desirable to plug up these holes with one-directional valves.

6.6   Launch tube supports

In view of the gasgun's length, and also from the standpoint of disassembly and storage, the individual gun segments are each supported on their own steel support.

The supports are clamped to the range tie-down rail assembly and are held in more-or-less precise position with pairs of dowel pins which engage holes through the support and into the tie-down rails. Final alignment is by means of adjustable roller supports for the launch tube as shown in Figure 6.9.
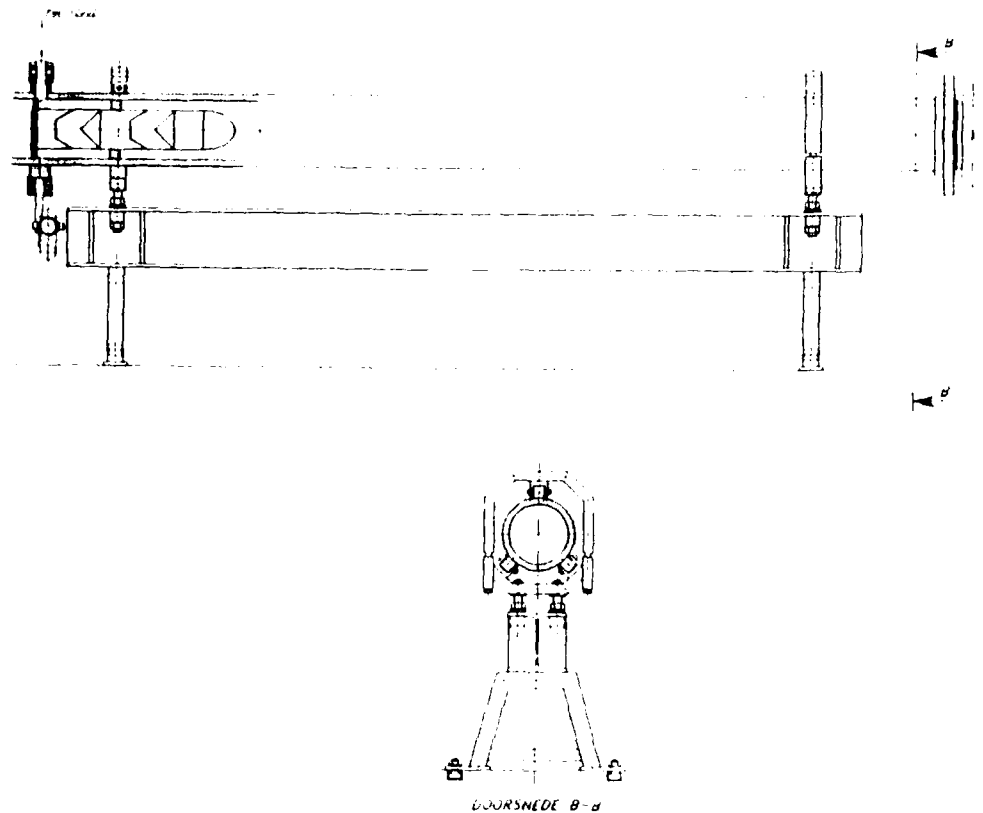
Figure 6.9   Launch tube support with adjustable rollers

6.7   Gun recoil unit

Gasgun recoil will be substantial. The impulse is effectively equal to the mass of the projectile package times its velocity. A small additional amount (below 2.0%) i produced by the gas movement. For a circularly symmetric gun, this recoil impulse is directed rearward precisely along the gun axis. The gun, moving rearward along its mount at a velocity near 1.0 m/sec, is stopped with hydraulic shock absorbers. The bodies of two shock absorbers are affixed to the gun structure so that their plungers point rearward on opposite sides of the launch tube with their ends accurately opposite one-another. Twisting impulses then cancel each other to produce nearly zero net transverse impulse. The shock absorbers come into play only when the projectile package has cleared the muzzle.

Thus, the impulsive forces accelerating and decelerating the gun both produce only axial forces. Tiny transverse impulses produced by non-ideality are effectively overcome by the gun weight which presses the gun down onto its roller mounts. Lightly-built hoops over the roller mount tube supports (as in Figure 6.9), while not strictly necessary, provide convenient means for restraining axial

tube motion when the gun mount is disassembled. In addition, it may be advisable to constrain the muzzle of the gun strongly against transverse motion because of its proximity to warhead blasts.

The recoil suppression unit of Figure 6.10 is mounted on the launch tube segment containing the launcher muzzle. The launch tube is stressed in tension, and not in compression which might cause it to buckle. The recoil suppresser currently in use on the PML 76 mm powder gun consists of a pair of hydraulic shock absorbers mounted on a disk clamped tightly around the launch tube. The rearward facing plungers engage vertical surfaces of a braced structure attached to range tie-down rails. In order to provide a safety margin in case of shock absorber failure, each shock absorber is rated sufficiently strong to safely stop the gun on its own.

In a different approach, a rigid mounting structure would transfer the recoil forces directly to the range floor. Since the launch tube as such experiences no recoil forces, the breech end of the gun recommends itself for the massive mounting structure.

While some preliminary design work has been performed in this area, a more detailed evaluation of both recoil forces and floor strength would be required, if this option were to be pursued further.
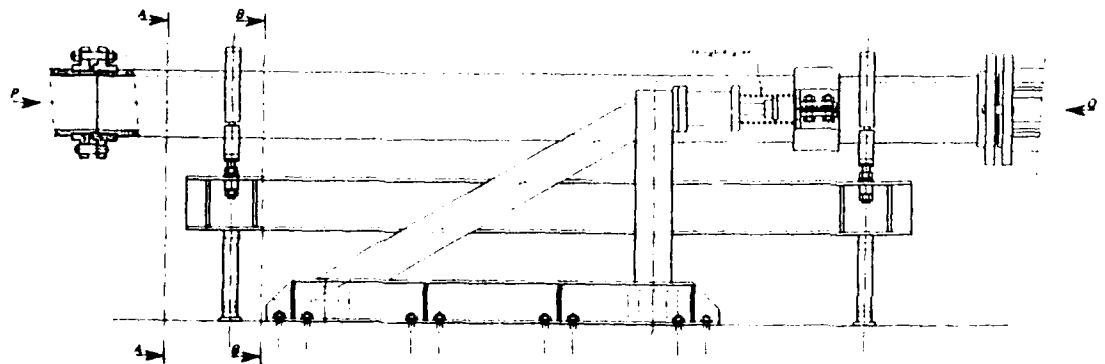
Figure 6.10   Recoil suppression unit, with dual shock absorbers

6.8 Gas delivery system

The gasgun needs a remotely operated gas delivery system to charge the driver gas reservoir to pre-scribed pressure levels. Commercial cylinders offer the most convenient (and for helium the only) source of supply. A compressor, while conceivable for air as the driver gas, would be both expensive and slow (perhaps even to the point of incompatibility with a diaphragm valving arrangement). It might be worthwhile, though, to employ a small compressor to fill any air cylinders. Cost, which is related to the number of firings over a given period, is the determining factor here.

One aspect of operating the gasgun on compressed air merits further consideration. Compressed air, in combination with oil, grease, or organic material, could give rise to an explosive mixture. The concentration levels which this would occur, as well as measured to prevent contamination in the first place, need to be investigated.

Remote location for the cylinders would protect the facility from damage if one of them were rup-tured during facility operation. Lastly, given the substantial amount of driver gas involved in each firing, the firing range should be ventilated thoroughly when using any other gas than air, before personnel are allowed to enter.

6.9 The complete gasgun

The various components discussed above have been combined into a complete system in Figu-re 6.11, which pictures the contemplated gasgun within the firing range of the LBO. It should be noted that the gasgun, as described in this chapter, stops just short of the entrance to the target bunker; there it connects to the guidance section of Chapter 8.
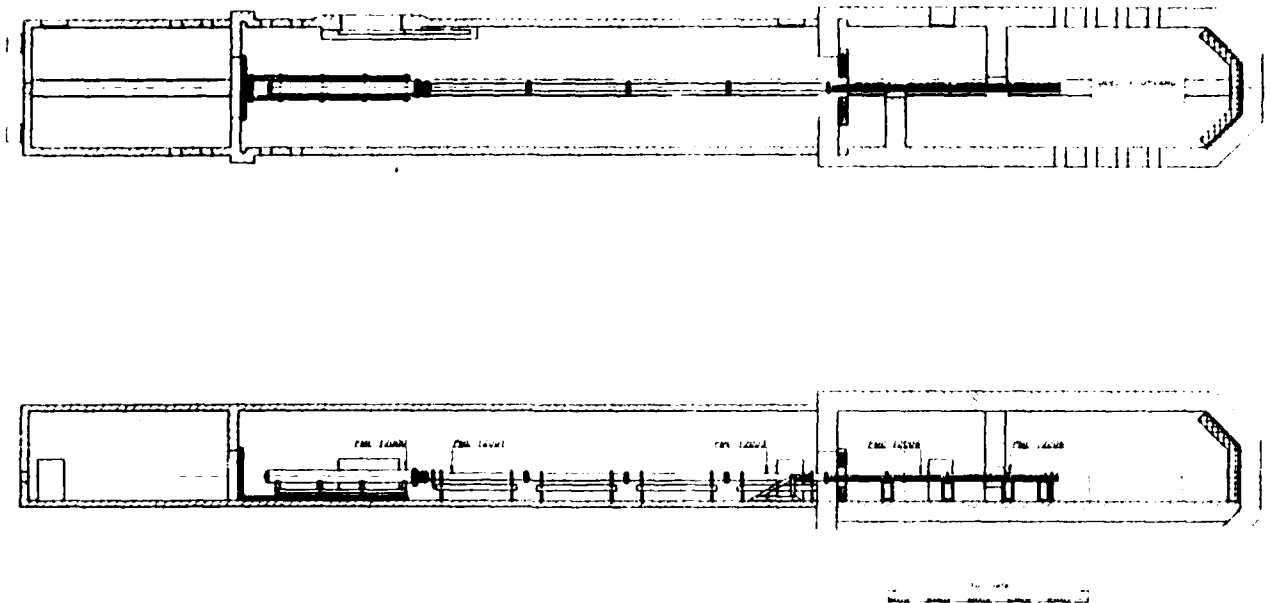
Figure 6.11   Gasgun system with gas reservoir, launch tube, and recoil suppresser within the firing range of the PML Laboratory for Ballistic Research

6.10   Design options

There is no doubt that a gasgun along the lines of Fig. 6.11 is capable of launching the required projectile mass at the required velocities. It is only when the presently intangible criterion of allowable acceleration limits is considered, that additional design decisions are in order.

Generally speaking, a launch tube of greater length will result in a reduction in the initial acceleration levels. This reduction is rather limited though, and certainly not proportional to the increase in tube length (and cost). The need of containing the gasgun in the present firing tunnel imposes a definite upper limit on tube length.

The use of helium rather than air offers a more effective way of reducing peak acceleration levels. Helium's high sound speed gives it a more efficient acceleration profile, thereby increasing the average acceleration level and allowing lower peak accelerations. However, this implies a larger gas reservoir as well as higher operating costs.

A reduction in jerk levels can be achieved by opting for regenerative valving techniques in preference to dual-diaphragm valves. According to Swift [23], the jerk levels associated with acceleration of a missile in its actual launcher can be matched during launches from the contemplated gasgun, provided the gun is designed carefully. More in particular, the captured-piston triggering system can be made to achieve sufficiently low jerk levels through a judicious choice of the piston mass and the shape of the holes connecting the launch tube and the surrounding gas reservoir.

It is important to note, that dual-diaphragm valve technology cannot in itself be used to adjust jerk levels over any reasonable range. Possibly, though, a honeycomb buffer could be employed to shield the warhead payload, as discussed in the next chapter. (A similar technique could of course be employed in conjunction with regenerative valving.) In addition, a small buffer space between the launch vehicle and the diaphragm closest to it, would have a jerk-reducing effect.

(Replacing the gas reservoir by a gas generator, loaded with a propellant grain dimensioned to maintain a constant driving pressure behind the projectile, might constitute the ultimate solution to any acceleration problems. Such a system would in theory be capable of keeping the maximum acceleration down to the level of the average acceleration. Likewise, it could provide for a very soft and controlled launch initiation phase, thereby obviating any jerk-related concerns. Unfortunately, both the design and operation of such a system would be rather more complicated and costly than for the gas-reservoir gun under consideration. Incidentally, the latter type of gun is also known as a "pre-burned propellant gun".)

7   LAUNCH VEHICLE

When propelling a payload through the gasgun's launch tube, a launch vehicle or payload carrier is required. In the context of dynamic warhead tests, the launch vehicle has to fulfil two primary functions, and several secondary ones. At the same time the launch vehicle represents a parasitic weight which should be kept to a minimum.

First of all a gas seal is required to keep the high pressure driver gas from blowing by the missile payload. Secondly, the payload must generally be prevented from coming into contact with the launch tube. Essentially, the launch vehicle has to play the role of both pusher plate and sabot.

In addition it or the missile itself must supply a platform for electrical contacts to connect the missile's detonators to the firing circuitry. For this reason and others that have been mentioned, the roll orientation of the missile needs to be fixed. Lastly, as will be explained below, the launch vehicle may even be configured so as to reduce jerk levels.

7.1   Launch vehicle design

The simplest form of launch vehicle supposes two bearing surfaces, or disks. Its design further depends on the length and weight of the payload in question. For a short payload, the launch vehicle could take the shape of a piston-like construction, consisting of two disks connected by a central tube as sketched in Figure 7.1. For strength, or more importantly, rigidity, additional braces might prove necessary.

For larger payloads, which would exert considerable torque on the above type of launch vehicle, a pusher plate/sabot combination, again with any interconnecting braces required, would be preferable. Again, refer to Figure 7.1 for details.
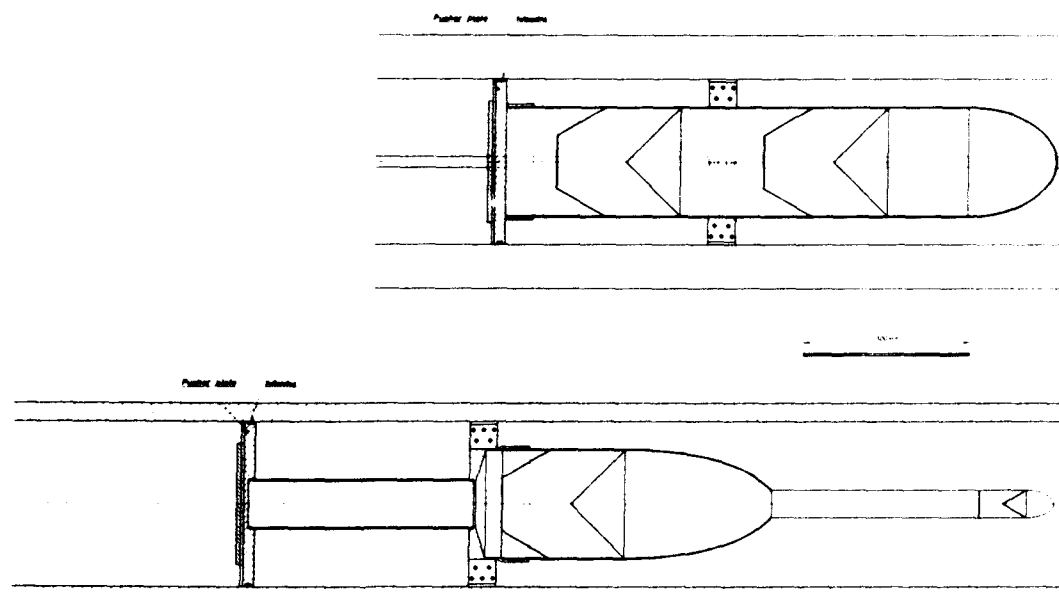
Figure 7.1

7.2 Pusher plate with obturator

A pusher plate that is made fairly strong will stand up to the gas pressure and provide a means for attaching the projectile, as well. Since metal-on-metal contact between the launch tube and the pusher plate is on general principle to be avoided, the pusher plate can either be fabricated from a plastic material or be equipped with a driving band (both thermohardening!). At ISL and also at the PML teflon has been used for driving bands. Teflon is a clear ablator, which turns to gas rather than leave a reside in the gun bore. Coating the pusher plate with teflon is also an option.

To form an effective obturation seal, any obturator material must be fairly soft. It can take the form of a separate disk attached to the rear of the pusher plate proper. A slight flare on the obturator engages the straight rifling lands of the launch tube. When the obturator material is forced into the corresponding straight grooves, this prohibits projectile packages from rotating during the launch cycles.

Alternatively, an obturator proper could be dispensed with. It constitutes a complication, the more so since its material properties conceivably might require tuning depending on the driving pressure. Also, any gas blow-by would to some extent be compensated by reduced bore friction.

A mount is needed to attach the missile to the pusher plate. Its configuration will depend on the missile in question. In its most simple form it could take the shape of a cylindrical receptacle, as used e.g. at MICOM for the TOW 2A warhead [24]. This feature and others have been sketched in Figure 7.2.
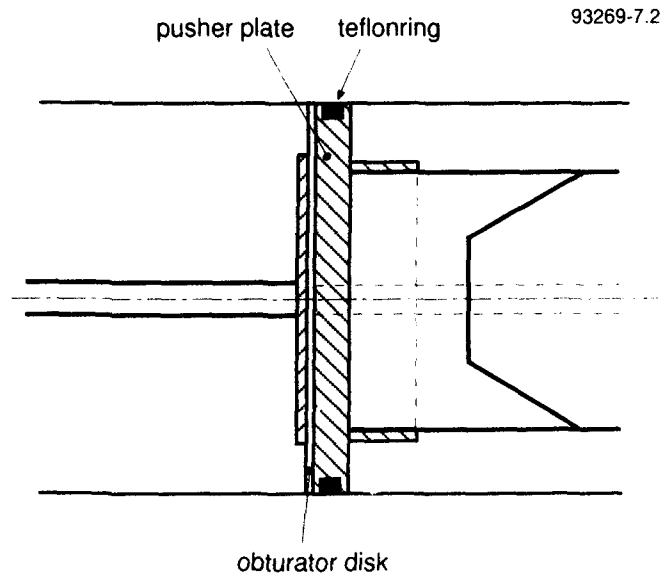

Figure 7.2   Detail of the pusher plate, with obturator disk, driving band, and missile mount

7.3   Jerk reduction

Depending on the structural limitations of the missile payload, it may be worthwhile to further reduce the applied jerk levels, in addition to any reductions achieved through the use of regenerative valving systems. This could be accomplished by interposing a honeycomb buffer between missile and pusher plate. Basically, honeycomb crushes at pressure levels that are independent of loading rate. Thus the rate at which acceleration is applied to the missile can be controlled, within limits. Honeycomb structures (though of far greater strength) are routinely applied in controlled impact tests [4, 25].

A buffer will cause a reduction in the maximum acceleration level as well. However, since no great length is available for the buffer, the room for improvement in this area is limited. On the other hand, the initial high acceleration levels are of relatively short duration. Preliminary simple calculations have yielded a reduction of 25% in the maximum acceleration level, for a buffer having a 10 cm crushing zone. For every further decrease in payload acceleration, a disproportionally larger buffer length would be required. Jerk reduction is bound to remain the main benefit of buffering.

7.4 Sabot

For any but short and relatively light projectiles, the projectile will have to be supported in the gun bore during launch. The most convenient way of doing this is by means of a sabot or slipper ring surrounding the missile at some point along its length. Referring to Figure 7.2 of possible missile configurations, the exact location of the sabot must depend on the missile's layout. Extreme care must be taken that the sabot does not affect the operation of any of the charges involved. This strongly militates against positioning the sabot directly next to a charge. In addition it seems desirable to minimise the sabot's effect, if any, on the properties (vibrational, and otherwise) of the missile structure.

The sabot should be as light as possible. Again there should be no metal-on-metal contact with the bore wall. We have been advised to consider cloth phenolic [26]. The sabot could be clamped, bolted, and/or glued to the outer skin of the missile. Also, some sort of support structure connecting the sabot to the pusher plate might be considered (compare Figure 9.5). In the latter configuration, the sabot could then serve to remedy a structural weakness of the missile in question.

7.5 Electrical contacts

The final requirement governing the design of the launch vehicle concerns the electrical contact which is to be established between missile and firing circuitry. This subject will be dealt with separately, in Chapter 9.

7.6 Warhead preparation

On the question of a missile-warhead being able to withstand the acceleration during launch, the answer is that some may need to be strengthened in some way. This strengthening can almost certainly be limited to the overall structure of the warhead, since individual components such as explosive charges should be robust enough to withstand peak gun-launch acceleration levels with ease. Relatively delicate electronic components will be rendered non-functional anyway.

The load-bearing interface between missile and pusher plate, in particular, merits close attention. The thin outer skin of a missile might well, by itself, prove incapable of sustaining the acceleration forces generated during a launch. Finite element calculations, e.g. with the Ballistics section's Autodyn code, could be expected to provide some information on this.

The installation of whatever sort of bracing calls for very careful consideration, at least where the warhead section proper is concerned. Anything that might influence the functioning of the charges must be avoided. The same applies to the removal of non-essential components.

8   GUIDANCE SECTION

In order to prevent the forward launch tube sections from being destroyed or damaged on a regular basis, an expendable guidance section is needed to guide the projectiles safely and reliably to the target. A rail system would seem most suitable for the purpose. (This, of course, presupposes the necessity of the guiding function, which has been examined in Chapter 2.)

8.1   Guiderails

The objectives in designing a guiderail system are threefold. First, the rails must guide the projectile package effectively but without damaging it. Second, the launch tube may not be damaged, either by impulse transmitted by the disintegrating guiding system or by the rails themselves. And last, since we are dealing with (semi-)expendable components, manufacturing costs must be kept as low as possible, but without sacrificing the necessary precision.

Before anything else, it must be decided where the rail system will take over from the launch tube. From the point of view of handling and dismantling the launch tube sections, there are numerous advantages in limiting the tube's overall length to the firing tunnel. Also, by keeping the launch tube out of the target bunker, it will be less likely to come to harm from blast and fragments. This implies a rail system of some 10m length, as was pictured in Figure 6.11.
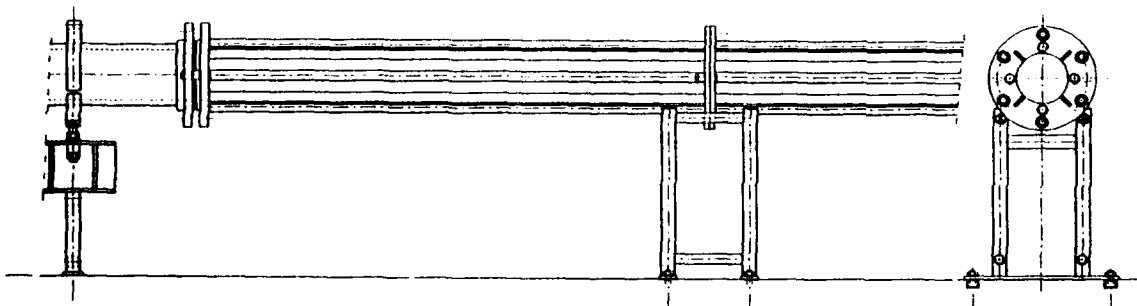

Figure 8.1   Rail system, guiding the projectile over the last few m to the target

Figure 8.1 shows a possible 4-rail guiding system. The forward sabot and the pusher plate constitute the bearing surfaces of the projectile package. The rails consist of several sections which are bolted

together. They are supported on weldments clamped to the target bunker tie-down rail assembly, as depicted in the figure.

A trough-like support structure could provide an alternative means of guiding the projectile. An additional hold-down rail would have to serve as a safeguard against any tipping or lifting tendencies of the projectile.

The length of the guidance section (10 m) suggests configuring it in two separate segments. An elastic connection or even an airspace between the two segments would probably allow the one farthest away from the explosions to have a semi-permanent character. The projectile should have no trouble jumping a small gap, if the rails, etc., are configured accordingly, i.e. slightly funnel-shaped.

Given the short time it will take regular projectiles to traverse the guidance section (some tens of ms), it seems superfluous to provide a positive inhibition against projectile rotation.

8.2   Rail materials

To protect the launch tube, it is advisable to have no fixed connection between it and the guiderails. That way, no impulse will be transmitted directly by the rails to the tube's muzzle. This also serves the purpose of decoupling the guiderails from the gasgun's recoil motion, if any. Again, jumping the gap should present no problem to the projectile, especially if the gas pressure behind it has been bled off through radial holes in the launch tube.

The guiderails should be made of a material presenting no risk to either the muzzle or the bore of the launch tube. In a nightmare scenario, a rail could conceivably be thrown into the launch tube, damaging the bore all the way upstream to the gas reservoir. This effectively rules out metal rails. Plastic rails would be more satisfactory, but could still transmit dangerously large impulses. A frangible material might be best of all. The use of carbon epoxy or polystyrene or even glass tubing has been suggested [27]. The latter material practically turns to dust when subjected to shock waves (perhaps constituting a health risk?). Filling the glass tubes with water or sand provides a means of increasing their mass.

A most promising candidate material for the guidance section appears to be wood. Wood is relatively inexpensive and easy to handle. Also, it may be expected to disintegrate into splinters, with little danger to the gasgun.

While dimensional stability is a possible area of concern, properly cured wood would probably prove sufficiently stable, especially if prepared not too long in advance.

Figure 8.2 shows the target bunker and part of the firing tunnel with the guiderail system in place, in more detail than Figure 6.11. We point out that the final section of the guiderail system must be integrated with the contact section which is to provide an interface to the firing circuit. This is discussed in the next chapter.
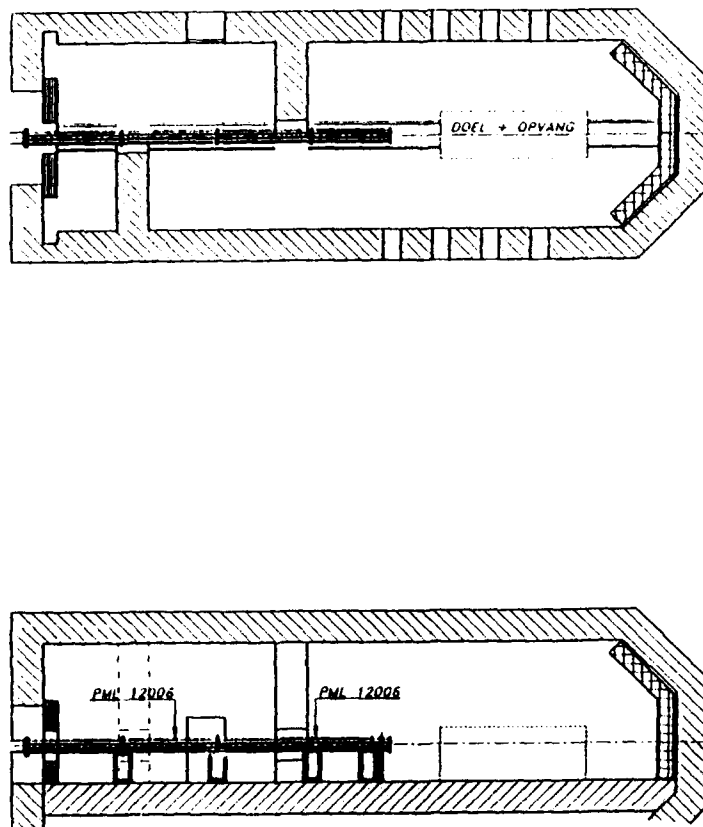

Figure 8.2   Rail system, guiding the projectile over the last few m to the target

9 FIRING CIRCUIT

In designing the firing equipment, the premise is that the electrical energy for detonating the charges is best provided by an external source, if only for safety reasons (Chapter 2). The firing circuit must allow detonating two charges: the first generally at a fixed distance from the target, the second a fixed time interval after the first. As explained earlier, warhead tests require extensive diagnostics, and the diagnostic functions must be closely co-ordinated with those of the firing equipment.

Establishing electrical contact between firing circuitry in the laboratory and detonators aboard launched projectiles, requires that two conducting surfaces be brought together at high velocity. In the present set-up, the problem is alleviated by two fortunate circumstances. First, the combination of a rifled gasgun barrel and a separate guidance section ensures that both the orientation and the position of the projectile are accurately fixed. And second, by using guiderails over the last part of the projectile's trajectory the side surfaces of projectile packages are exposed.

9.1 Possible means of firing warheads

In Reference 5 four knife blades are used for transferring power to a rocket sled, two for each warhead's circuit. See Figure 9.1 of the rocket sled assembly. (An additional knife blade is used to cut a foil make/break switch to provide a time fiducial when the precursor has reached the proper standoff from the target.) As the sled approaches the target, the four knife blades cut into the metal gauze screens of screen boxes, positioned to the left and right of the track. The screen boxes are connected to capacitive discharge units which fire first the precursor warhead and then the main warhead.
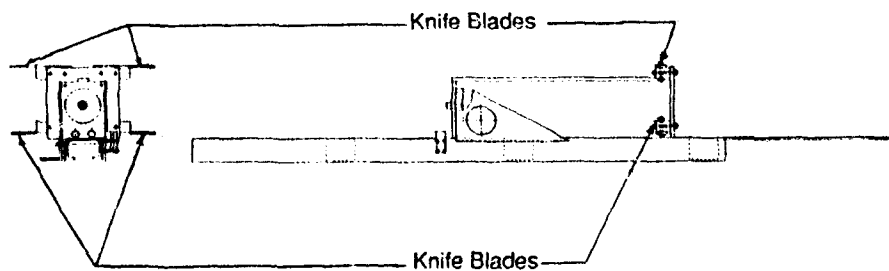

Figure 9.1 Rocket sled assembly, using knife blades (two per warhead charge) to transfer power to the sled [5]

Various alternative ways of firing warheads are conceivable, which dispense with direct electrical contacts. Among these are induction coupling and pulsed microwave radiation.

Yet another approach would consist of using a direct contact to fire the first detonator, while at the same time shock charging a capacitor aboard the launch vehicle. A time delay circuit aboard the vehicle could then discharge this capacitor across the second detonator at the correct time [30].

No matter how elegant, all of these methods have their disadvantages. Partly these have a practical background, partly they are based on safety considerations, and partly they centre on the perceived necessity of an extensive (and costly) development program.

For reasons like these, which will not be discussed in detail, the choice has ultimately fallen on a variant of the straightforward method of Figure 9.1.

9.2   Brush electrical contacts

The preferred electrical contact method takes the form of flexible brushes engaging solid contactors, with multiple charges of course requiring multiple brush sets.

The brush (having metallic bristles and of course a metallic handle as well) is mounted with its body out of the contactors path but with the tips of the metallic bristles extending a short distance inwards. The contactor would intercept the tips of dozens-to-hundreds of individual bristles, completing the electrical circuit which allows the charge to be fired.

Brushes appear to offer several advantages over solid, sliding contacts. Among these is a smaller likelihood of bounce-back effects, especially when contact is first established, but also at later times. In addition, brushes are less sensitive to small deviations from the planned projectile path; that is to say, they allow larger tolerances.

Contact options

The question is whether the brushes should be mounted stationary in the laboratory with the solid contactor mounted on the projectile or vice-versa. Also, whether extendible brushes should be considered, etc. Some of the available brush-contactor options are:

-   Projectile mounted contactors contacting stationary brushes whose bristles extend slightly inside the bore-diameter-size opening between the rails (Figure 9.2). This appears to be the most simple solution.
-   Extendible projectile mounted brushes contacting stationary contactors outside the bore diameter. The brushes must extend quickly (10 ms?) and reliably, and preferably lock into position to assure solid contact with the rigid contactors. (Figure 9.3 shows a system along these lines using

sliding solid contacts.) Lack of simplicity and doubts about reliability make this seem a less-than-ideal set-up.

- Non-extendable projectile mounted brushes contacting stationary contactors inside the bore diameter. This offers less flexibility than the first option: the firing sequence must have been completed by the time that the pusher plate arrives at the location of the first contactor.
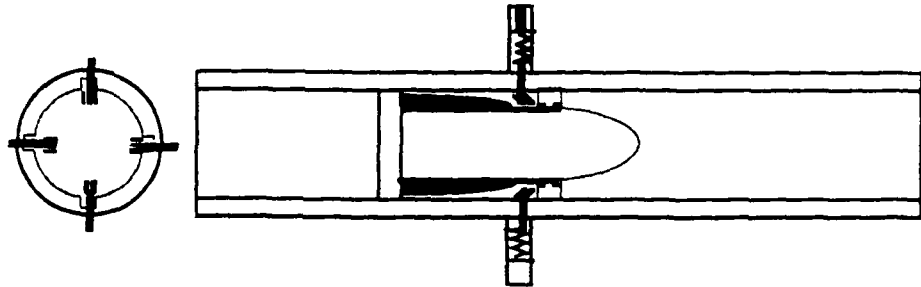

Figure 9.2   Stationary brushes contacting projectile mounted contactors. The springs providing contact pressure are probably an unnecessary embellishment.
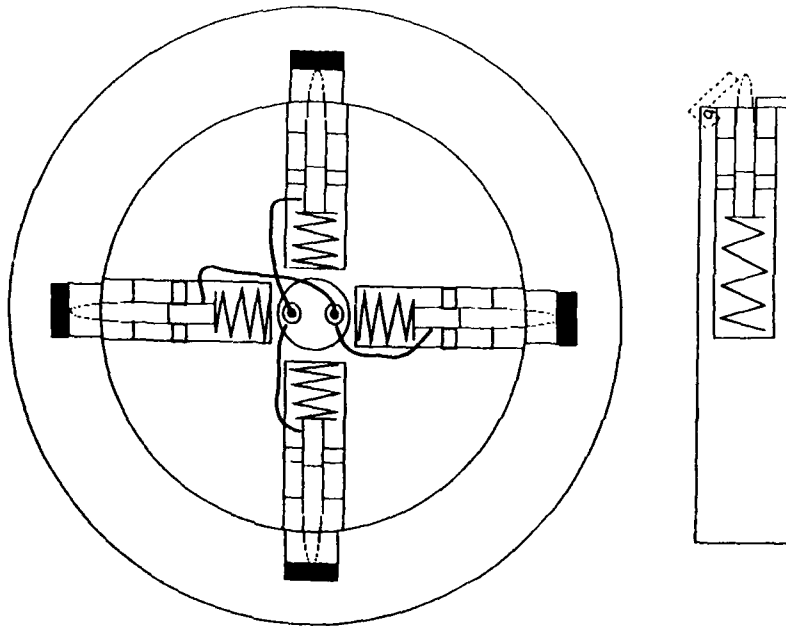

Figure 9.3   Projectile mounted, extendible solid contacts

An additional distinction can be made with respect to the duration of the contact between the brush and the rigid contactor, which can be either very brief or more prolongued:

- A simple brush and a small solid contactor offer a firing mode, where completion of the electric circuit automatically fires the detonator. Relatively simple firing equipment will suffice, but with a corresponding lack in flexibility. The timing of the charges is determined by the position of the contacts along their trajectory (Figure 9.4). In most cases, this would seem entirely appropriate for at least the precursor charge.

- An extended contact rail instead of a small contactor prolongs the contact with the brush, allowing controlled timing of the charges. The price for this increased flexibility is greater mechanical and electronic complexity. The contact rail may be either projectile mounted or stationary, with stationary rails offering more constructive freedom.

- In principle it is also possible to have a brush of extended length in combination with a small solid contactor. This would obviate any detrimental effects of prolonged mechanical contact on individual bristles. Also, the bristles actually involved in conducting the detonating current, would be mechanically supported by a great many surrounding bristles.
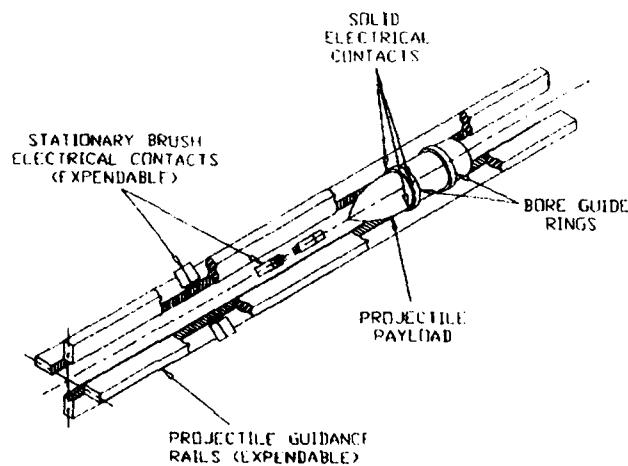

Figure 9.4   Triggering system where a charge is fired when a stationary brush contacts a contactor on the projectile package, thus completing the circuit [13]

Construction matters

Both the pusher plate and the sabot supporting the projectile in the bore offer a mounting surface for brushes or rigid contactors. While the sabot can be skeletonized to provide passage for either contactors or brushes, the pusher plate must at all times assure a good gas seal. In addition, any support construction for the front sabot can be configured to provide a ready-made set of contact rails.

As to the comparison between flexible brushes and solid sliding contacts, the latter need to be under spring pressure, complicating both design and construction. For the same reasons any kind of extendible contacts on the projectile package would be at a disadvantage. Figure 9.5 shows a possible design for a sliding brush contact, where contact pressure is assured by a spring.

In all cases the brushes and the corresponding solid contacts or contact rails would be mounted at separate predetermined angular locations around the projectile's circumference. For tandem charges requiring double ignition, the second set of brushes would be at a second position along the trajectory.

93269-9.5

contact rail
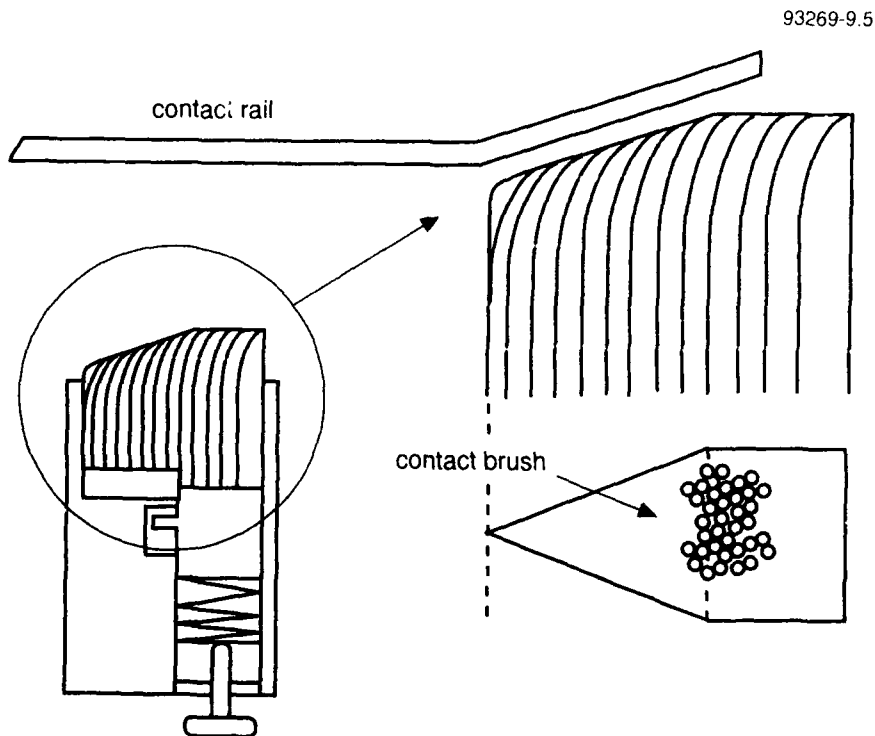
contact brush

Figure 9.5   Brush contact under spring pressure

Of course, the extent of the development program required for a given contact configuration depends
on its complexity. This is why, in general, the simplest option would obviously be best. In this
connection, it is fortunate that the Pulse Physics group has considerable expertise in the area of high
speed electrical contacts.

Lastly, a specific missile would probably impose various constraints on the available contact op-
tions. However, from the above discussion it would seem that there are no insurmountable difficul-
ties to be expected. Figure 9.6 gives an example of what a launch vehicle with contact rails doubling
as sabot supports might look like.

93269-9.6

Figure 9.6   Launch vehicle with contact rails between pusher plate and forward sabot

9.3 Firing circuit

From the point of view of the firing circuitry, we will explore the firing mode where a contact rail or brush of some length provides maximum flexibility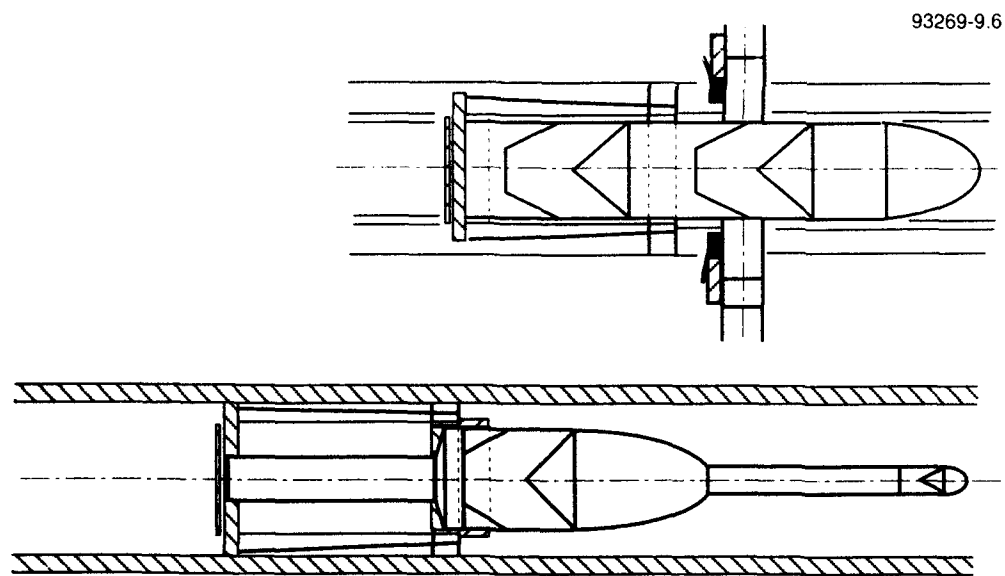 in the timing of the charges. In this connection it hardly matters whether the contact rail is stationary or projectile mounted, although extremely long stationary rails would affect the characteristics of the firing circuit. The alternative simple firing mode where completion of the circuit automatically discharges the firing capacitors, makes far fewer demands on both circuitry design and electronics. The following is a summary of an internal report [25] of the Pulse Physics group.

Circuitry options

Two firing circuits have been considered. They have numerous elements in common and differ only in the flexibility provided in the firing of the two charges. The second proposal constitutes a cost-saving alternative to the first.

A diagram of the first, more intelligent, circuit is given in Figure 9.7. Two transducers measure the projectile velocity. Based on the result, a smart trigger unit (STU) determines the firing time and, hence, the firing location of the first, precursor charge. A delay generator allows setting the delay between the precursor charge and the main charge to any desired value. The output signals of the STU and the delay generator, respectively, trigger two pulse forming networks (PFN's) providing the pulse to fire the detonators.

At present, there appears to be no reason, why velocity dependent triggering should offer any advantages over the more direct method employed in the second circuit (other, perhaps, than keeping the transducer(s) out of harm's way).
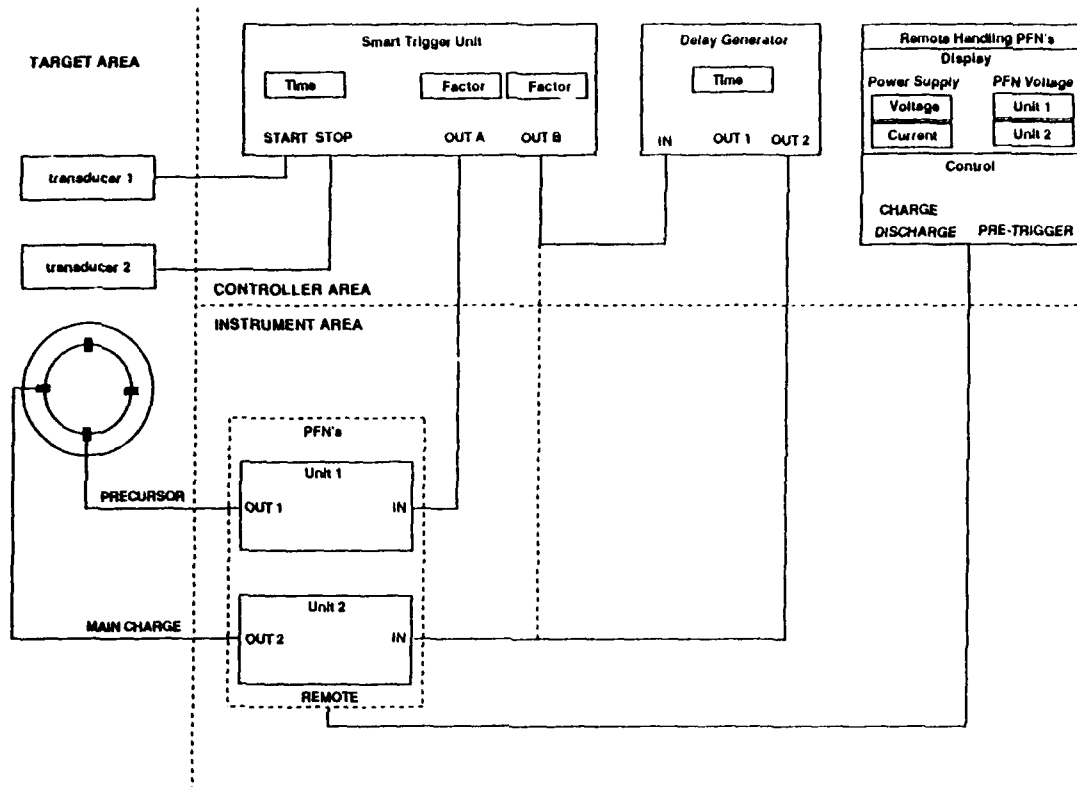
Figure 9.7   Block diagram of the firing circuit with Smart Trigger Unit; see the text for details

The second circuit, in Figure 9.8, differs from the first only in the absence of the STU. The precursor charge is triggered directly (or possible after a fixed delay provided by an additional delay generator) by the single remaining transducer. The main charge is again triggered by its delay generator.
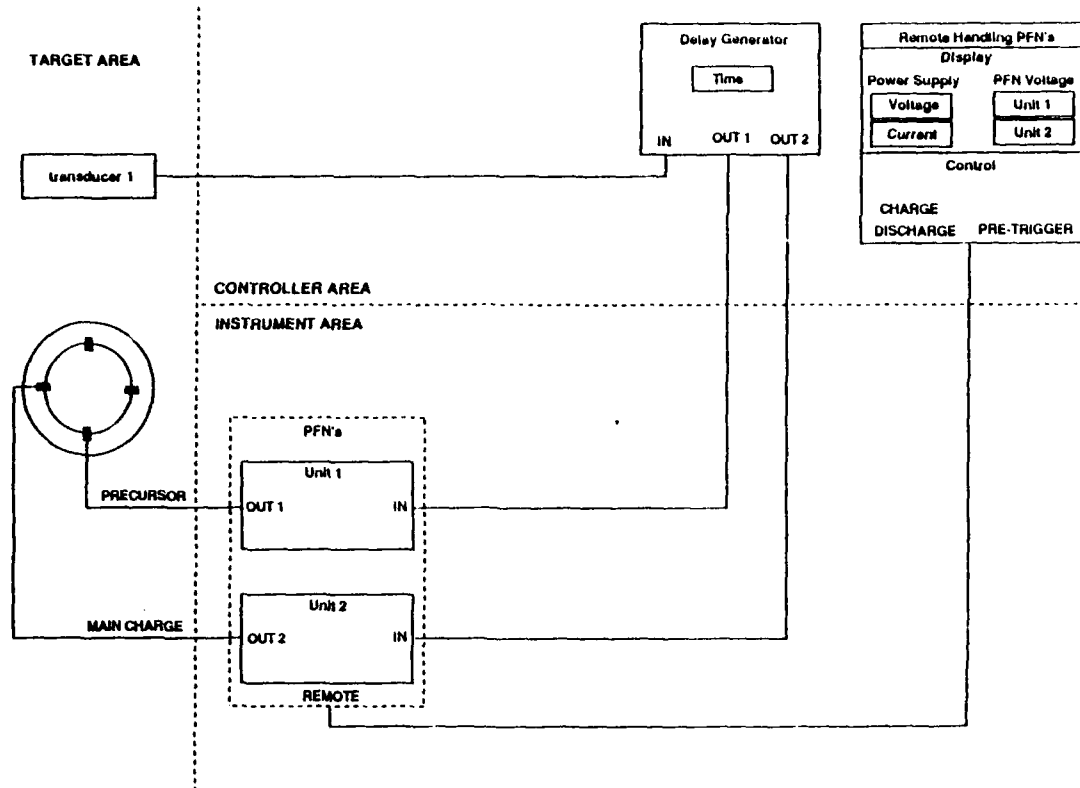
Figure 9.8   Block diagram of the firing circuit without Smart Trigger Unit; see the text for details

As has been indicated before, the precursor charge in particular might also be fired automatically upon completion of the firing circuit, doing away with the need for a transducer.

Emergency circuit

There is always a possibility of the main charge failing to detonate. In this case, the presence of an additional, emergency circuit to fire the main charge, would prevent it from crashing intact into the backstop, with all that this implies.

In its simplest form, such a safety circuit could consist of two extra brushes at 20 kV, firing the main charge directly on contact.

Trigger system

The trigger system serves two functions: detecting the presence of the projectile package when it passes a fixed position, and generating the trigger pulses for the pulse forming networks (PFN's).

The second function may be performed by the STU and the delay generator. The STU employs an internal clock to determine the time interval between the start/stop pulses generated by two transducers, which are a known distance L apart. Subsequently the STU determines the moment that the projectile package will be at a position k * L from the stop-transducer (with k a preset multiplication factor). At precisely that moment a trigger pulse is produced.

At projectile velocities around 400 m/s, the accuracy of the STU system (with e.g. L = 0.2 m and a 10 MHz clock) is such that over a distance of up to 4 m the triggering position is accurate to within 1 mm. Of course this assumes that the projectile velocity remains constant. On general principle it would be best to place the transducers as close to the firing position as possible.

Detecting the passage of the projectile is done by transducers. Two options are available, employing either a light-gate system or so-called B-dot sensors.

Both the Pulse Physics group and the Ballistics section have an operational fibre-optics light-gate system. For use in the direct vicinity of the exploding charges, the use of cheaper plastic fibres should be investigated. Otherwise, a non-expendable light gate system could be situated some distance away.

B-dot sensors, which react to a magnetic field change, are not only generally faster but also much cheaper. They can therefore be integrated into the firing section. All they require is a magnet attached to the projectile package. Figure 9.9 shows the response of a B-dot sensor to the rapid passage of a magnet.

In this connection it should be noted that some sort of velocity-measuring system will always be needed, irrespective of velocity-dependent triggering. Conceivably, transducers could also play a part in checking the roll orientation of top attack charges.
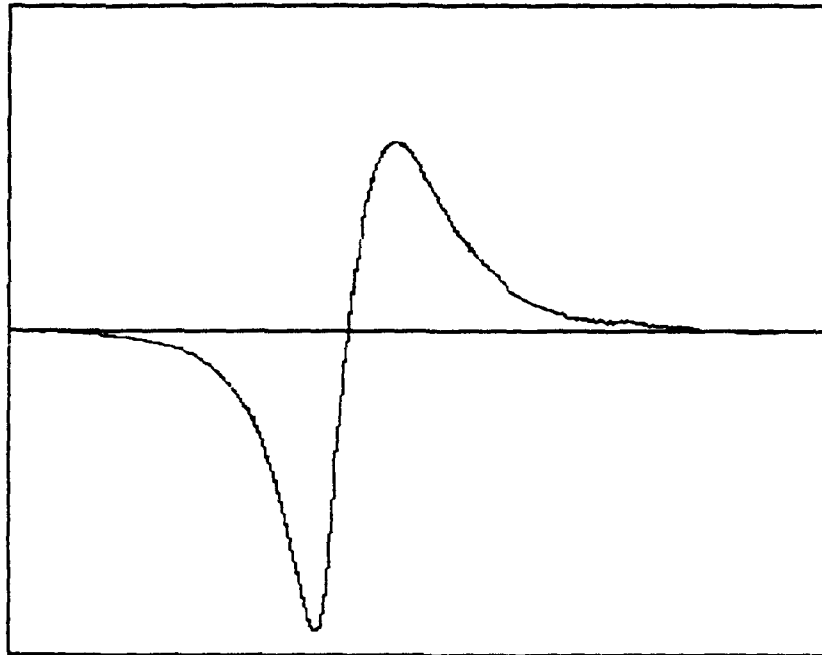
Figure 9.9   B-dot sensor response to passage of a magnet

Pulse forming network

Once the pulse forming network (PFN) has been triggered, the moment of initiation of the detonator is determined by the characteristic properties of the detonator and of the electric circuit, of which the detonator is a part.

The detonators must be of the high-voltage exploding bridgewire (EBW) type. These alone offer a sufficiently fast and reproducible response (on the order of μs), as opposed to low voltage detonators using a heating wire (ms).

Measurements have been performed with a Cordin 640R High Energy Pulser and the commonly used PL438 EBW-detonators. The initiation delay has been determined (6 ± 1 μs for the given network), as well as the voltage and current pulse shapes. The latter have yielded an estimate for the detonator's inductance and resistance.

93269-9.10

puls forming
network

rail system

L

R₁

R_r

L_r

C

L_d

ontsteker

R_d
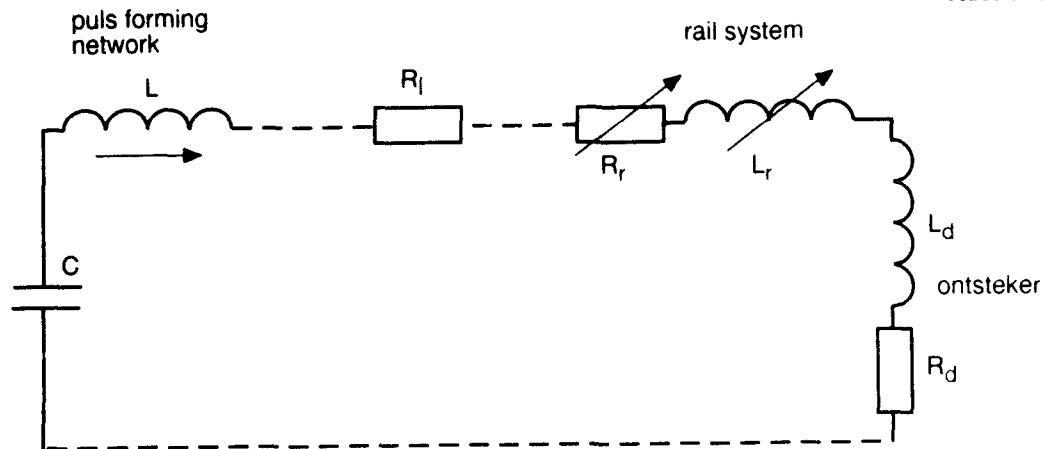
Figure 9.10   Electrical circuit of the pulse forming network

Subsequently, the pulse forming network required for the dynamic warhead tests has been analysed. Figure 9.10 shows the pertinent electrical circuit. It comprises the pulsed energy source, symbolised by the capacitor C and the inductance L; the rail system, modelled by the variable resistance R_r and the variable inductance L_r, and the detonator characterised by R_d and L_d. All remaining cable and transition resistance's have been summed up in the general loss-term R_l.

A detailed analysis (taking into account a.o. the skindepth of the rail current) indicates that an additional series-inductance $L'' \approx 10\mu H$ would result in the network's behaviour being largely independent of rail size and projectile position. For a capacitor $C = 5\mu F$ charged to $V_C = 10$ kV, the simulation program then shows the current pulse to have the shape of Figure 9.11. A pulse like this will reliably initiate the detonator.

93269-9 11
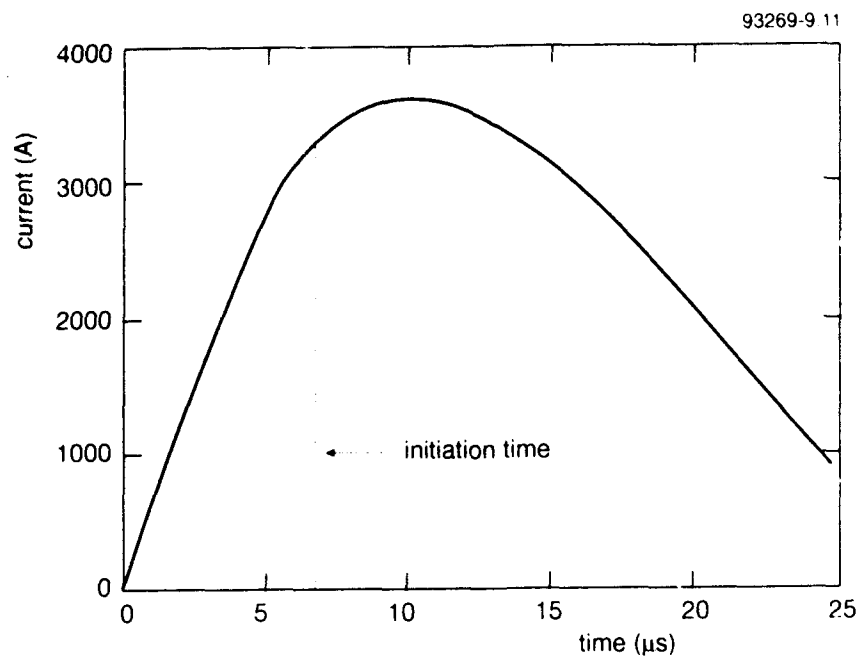
Figure 9.11   Calculated shape of a suitable firing pulse

9.4   Implementation

Contact pressure

The contact pressure between the brushes and the rails decreases when the current begins to flow. The initial contact pressure must be sufficiently large to compensate for this.

Assuming a rounded rigid contact of appropriate dimensions, and taking into account the hardness of the rail material and the strength of the current, preliminary calculations indicate that an initial force of 50 N provides an abundant safety margin. While this effect is considerably harder to evaluate for a flexible brush, no undue surprises are likely.

The two current-conducting rails will also experience the outwardly directed Lorentz force. This is on the order of 20 N, and should therefore be well within the capability of almost any rail construction to handle.

Remote control

Figures 9.7 and 9.8 show how the system components have been divided over the target area, the instrumentation area, and the control room. This has been dictated by both practical and safety considerations. For obvious reasons most of the components have been placed outside the target bunker.

The large capacitors of the pulse shaping networks represent a potential hazard, and have therefore been relegated to the instrumentation area adjoining the target bunker, where no personnel are allowed when a test is in progress. Charging and discharging of the capacitors is done by remote control from the control room. This is also where all electronic components are located, including both diagnostic equipment and the firing circuit's trigger unit and delay generator.

10   BACKSTOP

It has already been emphasised (in Chapter 2), that under no circumstances a shaped charge jet or explosively formed penetrator can be allowed to hit the wall of the target bunker. In case of a malfunction, the same holds for the undetonated charge. In both cases a fail-safe backstop system is required. Although somewhat outside the scope of this project, some requirements for such a backstop system are considered below.

Essentially, any backstop must meet two conditions. It must be correctly situated to intercept the projectile, and it must be capable of stopping it. These two conditions will be discussed in sequence.

Projectile intercept

Assuring that the backstop is in the correct position is easy, under the circumstances. It depends on knowing at all times where the projectile will be. As we have seen, the guiderail system leaves the projectile only a single degree of freedom, while the grooves in the launch tube fix its roll orientation (which is highly significant for a top attack charge).

The difference between the direct and top attack modes is that in the latter case the projectile produced by the charge, and the charge itself, must be stopped separately. (As indicated earlier, a top attack charge will typically be fired sidewards, i.e. horizontally, rather than downwards.)

Stopping requirements

The requirements for stopping a shaped charge jet are much more severe than those for stopping a explosively formed penetrator. The former may penetrate as much as 120 cm of armour steel. However, given an appropriate safety margin in the target's thickness, the only remaining problem is to make sure that the target is too big to be missed.

The undetonated charge with the launch vehicle still attached represents a weight of up to 30 kg, moving at up to 400 m/s (1300 km/u). On an outdoor firing range a soft deceleration method might be applied, e.g. by means of a large sandpile as has been used elsewhere. However, within the confined space of the target bunker the "braking distance" is limited to roughly 4 m. This means that only a very heavy backstop will do. The projectile's energy may be dissipated through friction of the backstop against the floor, or with the additional help of snubbers, or even an inclining ramp.

The backstop could perhaps even be allowed to abut directly against the rear wall of the target bunker, provided that some cushioning material like plywood were present to prevent point loading.

For a backstop composed of several parts which are assembled in the target bunker, even 15 t would not be too heavy. This is not unprecedented. At ISL, ramjet projectiles of even larger kinetic energy (but much smaller weight) are stopped in a catcher consisting of a 5 t cart moving along rails [28]. In the direct attack mode the target array, which may be very heavy in its own right, will generally be part of the backstop. This means that the undetonated charge may well impact on an oblique surface. While there is little chance of the charge of the ricochet-ing, it is bound to be deflected, and the target plates propelled in the opposite direction. A backstop with "closed" sides is therefore indispensable.

Additional aspect

There is yet an additional aspect to be considered. On impact the explosive charge is liable to be scattered. The clean-up procedure might be simplified if the backstop were completely enclosed. However, any interference with either the experiment or the diagnostics should be avoided at all costs. In addition the backstop will have to be capable of withstanding the explosive force of a successful experiment.

As an aside, we mention the potential problem of, e.g., the pusher plate being hurled against the wall of the target bunker by the force of the explosion. However, the target bunker's wall is protected by 2 cm steel plates and should be proof against this.

11   MUZZLE GATE VALVE

During operation of the warhead accelerator system, a number of violent phenomena will take place in the target bunker. Both the explosion of the warhead and the interaction with the target will produce fragments and blast.

To protect the gasgun from blast, it has been positioned outside the target bunker, with a guidance section bridging the gap to the target area. However, conceivably, the gasgun could also be in danger from fragments.

On the one hand, the probability of a fragment being propelled straight back along the projectile's trajectory would seem to be very low. Both the large distance between the gasgun and the explosion site, and the shielding effect of the launch vehicle behind the warhead, would mitigate against such an occurrence. On the other hand, if a mishap were to occur, the bore surface of the gasgun, in particular, would be decidedly vulnerable to fragment damage.

A detailed risk analysis of the problem was beyond the scope of the present project. However, even if the requirement for protective measures is not yet firmly established, it is possible to outline the form such measures might take. A fast closing valve in front of the gasgun's muzzle would seem to be the most appropriate way to address the problem.

Requirements

A fast-closing muzzle gate valve, positioned in front of the launch tube and activated by the passage of the projectile, would positively protect the gasgun from fragments.

Ideally, the valve must be fast enough to close before even the fastest fragments, and thick enough to stop even the most dangerous ones. Any compromise in these areas would imply less than complete protection. Given the probabilistic aspects of the problem, this might well be acceptable, however.

While a slight delay in the operation of the gate valve, or even a failure to operate, might have no serious consequences, premature closure would obviously be completely unacceptable. A warhead impacting on a closed gate valve not only will destroy the valve, but might well detonate. Even with the valve positioned inside the target bunker, damage to both the gasgun and the firing range cannot be ruled out.

Lastly, the valve mechanism itself will to some extent be exposed to fragments and blast. The labyrinth walls offer a degree of protection, but some additional protective measures are in order.

Gate valve construction

Depending on the thickness of the steel gate plate and the desired closing time, either an operating method based on explosive charges might be required, or a mechanism based on high-pressure gas cylinders might suffice. In the latter case, explosive bolts would probably still be the best means of releasing the gas pressure.

A shutter-like construction with two opposing gate segments has some advantages over a single gate. Among these are a faster closing time and/or less stringent acceleration requirements. Conversely, there is an additional need for nearly simultaneous operation of the gate halves.
In either case, some sort of buffer is needed to prevent bounce back of the gate.

Lastly, probably the best place to mount the gate valve would be on the set of doors closing off the target bunker. Not only do these appear to be of sufficiently heavy construction, but this would also ensure that the gate valve was out of the way once the doors were opened.

Gate valve initiation

To initiate gate operation, the passage of the projectile should be established beyond a shadow of a doubt. Equipment for this should incorporate at least two independent detectors, and preferably even two different detection methods. The associated electronic circuit must operate in an "and" mode only.

Prime candidates for a detection device would be the magnetic B-dot detector and the light gate detector, mentioned in connection with the firing of the warheads in Chapter 9. The fact that they will be located at some distance from the explosion site, offers considerable additional design leeway.
A variation on the light gate detector theme, geared to the circumstance that a completed passage of the projectile package is an absolute requirement, could use the reflection of a laser beam from a mirror aboard the launch vehicle.
These devices could even be combined with an additional make/break switch, operated by the projectile.

In all cases, the detectors should be proof against interference due to driver gas blow-by effects.

12   COST ESTIMATE

In the preceding chapters the desired gasgun accelerator system has slowly taken shape. On the basis of the "predesign" insights gained here, the cost of completing the design and constructing the gas-gun may now be estimated with some degree of confidence (i.e., within perhaps 20% or so).

Where possible, the remaining design effort has been separated from the anticipated con~   ·ion work, on the one hand, and hardware costs, on the other. In addition, we distinguish betwe   .r-nal costs (costs for labour performed in-house in the PML) and external costs (materials, hardware and services obtained from outside contractors or suppliers). Lastly, not only the once-only design and construction costs have been considered, but also the recurrent operating costs.

We have also obtained a cost estimate from an outside source for a gasgun based on regenerative valving technology, which we have not studied in detail. The valving question is of course closely related to the main unresolved design issue, the question of missile acceleration limits.

Please note that all costs are based on the situation as of December 1991!

12.1   Gasgun costs

The present gasgun cost estimate in Table 12.1 is based on a maximum work share by the PML Construction Department. It does not include any further modelling efforts. In the table, the system components have been roughly grouped in subsystems.

12.2   Firing equipment costs

The warhead firing equipment forms a separate but vital component of the gasgun accelerator sys-tem. The cost estimate in Table 12.2 is based on the assumption of the main work being done by the Pulse Physics group.

12.3   Total system costs

Adding the costs of the gasgun system and the warhead firing equipment yields the total costs pre-sented in Table 12.3. It is important to remember that the external costs have been minimised here, to the possible detriment of the overall costs.

Table 12.1   Estimated cost (December 1991) of the gasgun, excluding the warhead firing equipment and a muzzle gate valve, but including the backstop

COMPONENT	INTERNAL		EXTERNAL
	design & drawings	manufacture	
	(kf)	(kf)	(kf)
Gas reservoir	4	0	38
Gas reservoir support	6	2	11
Dual membrane	4	0	12
Safety catch [*]	7	0	12
Launch tube incl. couplers	18	6	77
Launch tube supports	7	0	12
Recoil suppression unit	4	0	10
Guiderails	9	7	1
Stationary contact brush frame [#]	5	2	0.2
Launch vehicle	7	2	0.2
Gas delivery system	9	0	12
Compressor plus buffer cylinders [*]	0	0	22
Launch tube evacuation system [*]	2	0	12
Backstop	12	0	21
Various equipment	4	0	11
Transport, assembly, tuning	1	9	0
Unforeseen	18	1	48.5
	120	30	300
TOTAL COST			450

[*]   Optional

[#]   Also part of firing circuit

Table 12.2   Estimated cost (December 1991) of the warhead firing equipment.

COMPONENT	INTERNAL (kf)	EXTERNAL (kf)
B-dot trigger transducers	12	1
Smart Trigger Unit	40	5
Delay generator	9	1
Pulse shaping networks (2)	30	20
Development brush contacts[#]	27	3
Supervision construction work[#]	20	0
Unforeseen	2	5
	140	35
TOTAL COST		175

[#]   Some overlap exists with section 11.1

Table 12.3   Estimated cost (December 1991) of the complete gasgun system for dynamic
warhead tests, including 25 kf for program management

	INTERNAL (kf)	EXTERNAL (kf)
	315	335
TOTAL COST		650

12.4   Operating costs

The cost of operating the gasgun accelerator are substantial. This stems mostly from the fact that in each experiment part of the set-up will be destroyed, including of course the launch vehicle. The extent of the damage to the guidance section will depend on the circumstances. For the moment it is assumed that half of the guidance section will be re-usable. The cost estimate cited in Table 12.4. is based on assumption that the repetitive manufacturing work will, for the main part, be contracted out.

Table 12.4   Estimated operating costs (December 1991) of the gasgun accelerator

COMPONENT	INTERNAL (kf)	EXTERNAL (kf)
Guiderails		4.3
Stationary contact brush frame		1.5
Launch vehicle	0.4	1.1
Helium reservoir charge		1.4[+)]
B-dot trigger transducers		0.4
	0.4	8.7
TOTAL COST		9.1

+)   Air reservoir charge 0.5 kf

It should be noted, that labour costs have not been included here. Given the elaborate nature of dynamic tests, these may easily run to 10 kf or more per experiment. On the other hand, any small series of elaborate terminal ballistics experiments, dynamic or otherwise, will carry a high price-tag. Finally, there will always be the additional cost of target and other materials.

12.5   Gasgun cost comparison

At our request, Physics Applications of Dayton, Ohio, have prepared a cost estimate for a gasgun of their own design, comprising a regenerative valving system, with a wrap-around gas reservoir.
In Table 12.5 the design costs have once again been split off. The breakdown in separate components is somewhat less detailed than in Table 12.1, but roughly analogous subsystems can still be identified.

Table 12.5 Gasgun cost estimate by Physics Applications (December 1991), with the US$ set at f 1,90. In a rough comparison, the approximate figures from Table 12.1 are given between parentheses

COMPONENT	DESIGN (kf)	FABRICATION (kf)
Gasgun	65	287
Gas reservoir		
Breech system		
Launch tube incl. couplers		
(Table 12.1 ≈ 46 / 193)		
Gasgun mount	38	113
Gas reservoir supports		
launch tube supports		
Recoil suppression unit		
Gas delivery system		
(Table 12.1 ≈ 36 / 84)		
Installation supervision	14	
(Table 12.1 ≈ 10)		
	117	400
(Table 12.1 ≈ 92 / 277		
TOTAL COST		517
(Table 12.1 ≈ 369)		

A comparison between the PML estimate and that of Physics Applications is far from straightforward. Generally speaking, the two estimates are not widely dissimilar. The scope of the present project did not allow a detailed study of regenerative valving technology. We are therefore in no position to judge the extent to which the cost difference stems from the increased complexity of the regenerative valve design.

No doubt, Physics Applications' experience in gasgun design has to a certain extent reduced the design costs, but the same can be said of the pre-design work described here.

Presumably the Physics Applications estimate contains both a profit and a safety margin. It is per-
haps relevant to add that Physics Applications routii.ely employ an outside construction shop to fab-
ricate their designs.

If previous experience is anything to go by, import duties on any shipment from Physics
Applications can probably be avoided, but this is not certain. Lastiy, shipping costs will also have to
be taken into account.

13   CONCLUDING REMARKS

13.1   Subconclusions

In the previous chapters many subjects have been discussed, sometimes in considerable detail. We now summarise some of the highlights, subdivided in three main categories.

Modelling
- The modelling efforts in particular have yielded considerable insight in the principles and operation of gasguns.
- Both a relatively simple zero-order model and a more elaborate model based on the characteristics method have been implemented in computer codes. (A hydrocode capability is present at the PML as well, but has not been applied to the problem at hand.)
- The zero-order gasgun model is well suited to establishing the general (un)feasibility of a gasgun solution to any set of requirements.
- The results obtained with the more elaborate computer code compare well with data from literature and from the ISL hydrocode calculations.
- The computer code needs some additional work, as far as a more thorough treatment of reflections in a gasgun with chambrage are concerned.
- The model calculations have established the feasibility of the proposed gasgun, with respect to the mass/velocity requirements on the one hand, and the limitations imposed by the present facility on the other.

Feasibility

- The general feasibility of a gasgun warhead accelerator has been established, on the basis of both model calculations and more specific design considerations. This includes the warhead firing circuit, and to a lesser extent the backstop.

- There are two major remaining areas of uncertainty; these concern the maximum allowable levels of jerk and acceleration, respectively.

- The jerk levels associated with in-launcher acceleration of a missile can be matched during launches from the contemplated gasgun if the captured-piston regenerative valving system is used. With dual-diaphragm valve technology, buffering may or may not provide sufficient protection for the payload.

- In a helium-driven gun, peak acceleration levels can possibly/probably be reduced to the point where the majority of missile-type payloads can (be made to) sustain them.

- It is unclear to what extent the demands made by advanced warhead initiation systems (e.g. proximity fuzes) can be met using external firing equipment.

- The need for protecting the gasgun by means of a fast-closing muzzle gate valve is still a matter for discussion

- Design and fabrication of the system is probably within the power of the PML, with the exception perhaps of the regenerative valve system. It may prove ultimately more efficient to obtain the latter from an outside agency (Physics Applications).

Design

- The predesign effort of the present project has resulted in an almost complete picture of the warhead accelerator system under contemplation. However regenerative valving has not yet been studied in any detail.

- Several critical components have been tested through scale experiments.

- Backstop predesign remains to be finalised.

- The Construction Department, while having no previous experience in gasgun design, is confident of its ability to complete the design along the present lines and execute/co-ordinate its execution.

- The same can be said of the Pulse Physics Group with respect to the warhead firing equipment.

Costs

- A cost estimate has been prepared, differentiating between internal and external costs.
- The estimate is based on maximum PML involvement, i.e. a large internal cost fraction.
- The cost estimate drawn up by Physics Applications is higher than the PML estimate, but the difference is not extreme.
- For some components, cost effectiveness considerations may favour engaging the services of outside consultants (Physics Applications).
- The PML estimate closely adheres to the original cost estimate, prepared for DMKL when the gasgun accelerator was first conceived.
- The operating costs of the accelerator will be substantial, as will be the cost of dynamic tests in general.

13.2 Overall conclusions

On an even higher level of abstraction than in the preceding section, the present report gives rise to the following general conclusions.

- The goals set for the project have been met, or in some areas exceeded. These goals are related to modelling, predesign, scale experiments, and cost evaluation.
- Considerable expertise has been gained in the field of gas dynamical modelling of a gasgun.
- The feasibility of a complete warhead accelerator system for dynamic tests has generally been established. Some questions remain, mainly related to the ability of the payload to withstand acceleration.
- Considerable progress has been made in the design of such a system. Design and construction of the system are largely within the capability of the PML.
- Even if some future warhead designs may prove unresponsive to the proposed warhead accelerator, other warheads will pose no such problems.
- There have been several signs of foreign interest in the future use of a PML dynamic warhead test capability [e.g. 15].

All in all, while it is still too early for any definitive pronouncements, the signs for this project are generally favourable.

14 RECOMMENDATIONS

When considering how to proceed next, one must take into account that possible funding, if any, will become available in 1993 at the earliest. When seen in this light, it is recommended that the intervening time be used as follows.

- An additional study of anti-tank missiles presently under development should ensure that the requirements drawn up for the warhead accelerator are kept up to date.
- Inquiries into the acceleration limits for typical antitank missiles must be continued.
- It is advisable to seek additional information on regenerative valving technology, to establish in more detail the design and cost consequences of opting for this type of gasgun.
- If at all possible, an effort should be made to properly document the computer codes developed in this project. It would be beneficial, if labour-intensive, to upgrade the codes slightly in both shape and substance.
- Reportedly, a gasgun is under development at BRL at the moment. This deserves looking into.
- The 1993 availability of PML personnel should be firmly established.

15 ACKNOWLEDGEMENTS

As mentioned earlier, a number of groups within the PML have co-operated in the gasgun accelerator project. These include the Ballistics section, the Gas & Dust Explosions section, the Electromagnetic Launching Research section, the Accidental Explosions section, the Detonation section, and the Land Systems section, in addition to the PML Construction department.

The ISL at St. Louis has been most helpful in providing information about ISL gasgun technology, both during a visit by the authors and afterwards.
Physics Applications' involvement with single stage gasguns became known only at a relatively late stage, but subsequent correspondence proved very useful. Swift of Physics Applications also visited the PML, while staying in the UK.
Lastly, throughout the project there have been numerous productive discussions with the Ammunition Division of DMKL (Directorate of Materiel Royal Netherlands Army).

16   AUTHENTICATION

M.P.I. Manders

(Author, Project Leader)

J.B.M.M. Eggen

(Author)

17   REFERENCES

1   Verheij Z.C. and Manders M.P.I., Planned Expansion of the TNO-PML Ballistics Facility, Proceedings 42nd ARA Meeting, Adelaide, Australia (1991)

2   Walters W.P. and Zukas J.A., Fundamentals of Shaped Charges, Wiley, New York (1989)

3   Schwartz W., Explosive Reactive Armour, MilTech 8/91 (1991) 57; Manders M.P.I. and Ehrlich M., Explosive Reactive Armour Research at TNO-PML, PML 1990-27 (Secret)

4   Ballistic Environment Simulation Facilities, Harry Diamond Laboratories (1983); Pollin I., On the Production of Controlled-Impact Pulse Shapes, 7th Intl. Congress on Instrumentation in Aerospace Simulation Facilities (1977) 150

5   Fradkin D.B., Flash Radiographic Analysis of Shaped-Charge Warhead Performance on a Dynamic Sled Track, 1989 Flash Radiography Topical (1989), 192

6   Woidneck C.-P., Brodbeck J.-M., Naz P., and Vermorel J., Gasgun for the study of Transverse Velocity Effects on Shaped Charge Performance, Proceedings ARA (1985) 1;

     Woidneck C.-P., Brodbeck J.-M., Carrière A., and Lacour A., Beschleunigung einer Hohllahdung mit einer 190 mm Druckluftkanone", ISL Report RT 503/84

7   Zuidgeest L.W.M. and Joosten R.P.F., personal communication, 20 August 1991

8   Test report TOW 2A flight tests Meppen 1991, to be published

9   Hogg I.V. (ed), Jane's Infantry Weapons 1989-90, Jane's Information Group, Coulsdon UK (1989),

10   Mayer E., Die Panzerabwehrlenkflugkörper der Sowjetarmee, Soldat und Technik 8/91 (1991) 540

11   Swift H.F., Physics Applications, personal communication, 11 November 1991

12   Beer J., MICOM, personal communication, 3 March 1992

13   Swift H.F., Physics Applications, personal communication, 6 December 1991

14   Chanteret P.-Y., ISL, personal communication, 21 November 1991

15   Braun et al., WTD 91 Meppen, personal communication, December 1992

16   Malcev A.A., Something New from the BMP-stable: The BMP-3, MilTech 11/91 (1991) 118

17   Soldat und Technik (1991)

18   Hewish M., Luria R., and Turbé G., Anti-tank Guided Weapons, Part 1: Non-US Systems, International Defense Rev. 12/89 (1989) 1631

19   Seigel A.E., "Performance Calcultaions and Optimization of Gasguns",U.S. Army Electronics Research and Development Command, HDL CR-81-723-1 (1981)

20   *Fowles G.R., Duvall G.E., Asay J., Bellamy P., Feistmann F., Grady D., Michaels T., and Mitchell R.,* Gasgun for Impact Studies, Rev. of Scientific Instruments 41 (1970) 984

21   Fauquignon C., ISL, personal communication, 9 December 1991

22   Swift H.F., Physics Applications, personal communication, 22 April 1993

23   Swift H.F., Physics Applications, personal communication, 13 December 1991

24   Hamlet T., MICOM, personal communication, 3 March 1992

25   Bourges, Physics Applications, personal communications, January 1993

26   Swift H.F., Physics Applications, personal communication, 24 February 1992

27   Swift H.F., Physics Applications, personal communication, 7 February 1992

28   Koops M. , "Ontwerp Afvuurinrichting", Internal report PML Pulse Physics MK_1 (1992), in Dutch

29   Giraud M., Legendre J.-F., and Simon G., "RAM Accelerator at ISL: First Experiments in 90mm Caliber", Proceedings 42nd ARA Meeting, Adelaide, Australia (1991)

30   Swift H.F., Physics Applications, personal communications, 2 November 1992

31   Heybey W. A solution of Lagrange's problem of interior Ballistics by means of its Characteristics lines NOLM 10819, March 1950

ANNEX A   VALIDATION OF CODE

A1   COMPARISON WITH RESULTS OF SEIGEL [19]

Figures A1.1 and A1.2 show two figures presented by Seigel [19] to quantify the performance of a constant diameter gasgun with air as driver gas in terms of non-dimensional variables. These results have been reproduced so accurately by the current program, that the curves essentially coincide.

Figures A1.3 and A1.4 are also reproduced from Seigel [19]. Figure A1.3 illustrates the effect of chambrage on the muzzle velocity, when air is used as driver gas and the total air mass is twice the projectile mass. Figure A1.4 is for helium, with the helium mass equal to the projectile mass. Here too, the present program's results are a very close match.
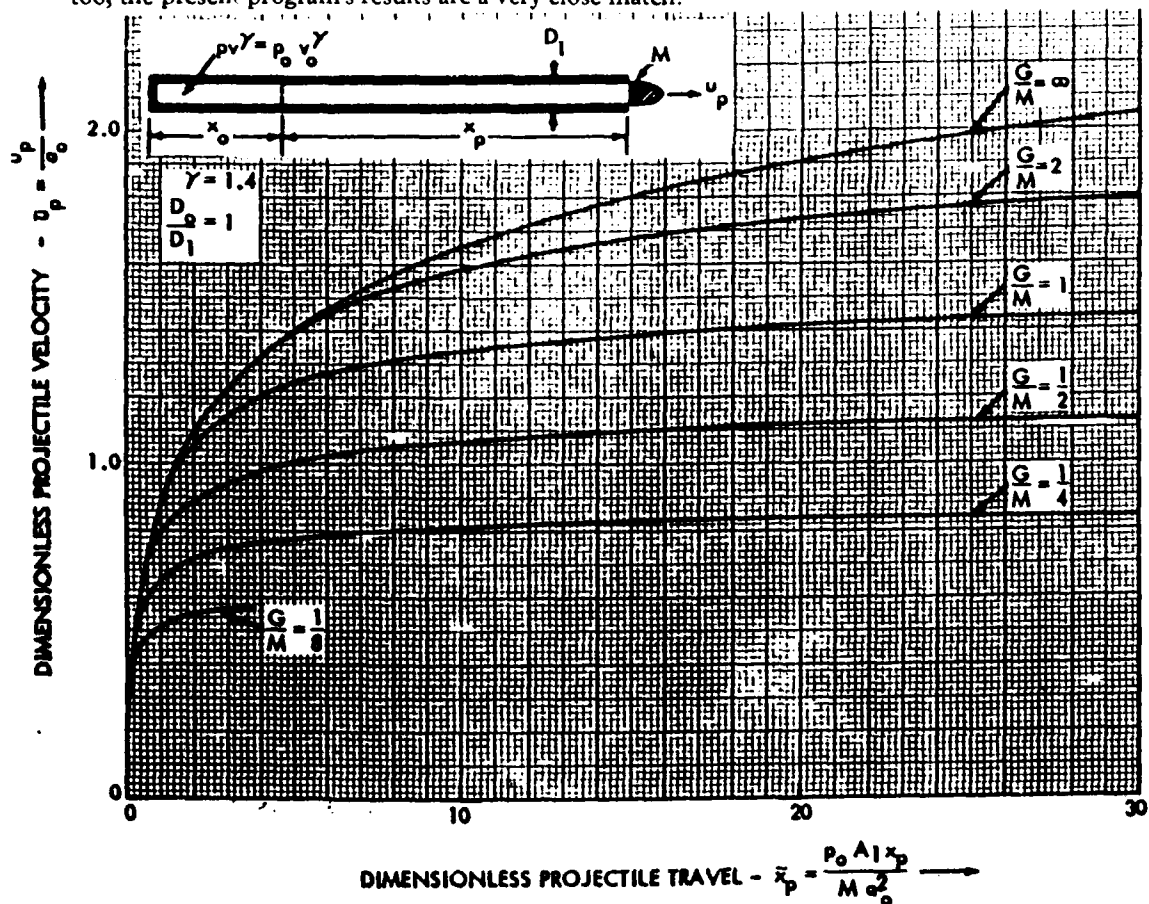
Figure A1.1   Projectile velocity as a function of position for several chamber diameters D_C and chamber lengths L_C, in non-dimensional form [19]
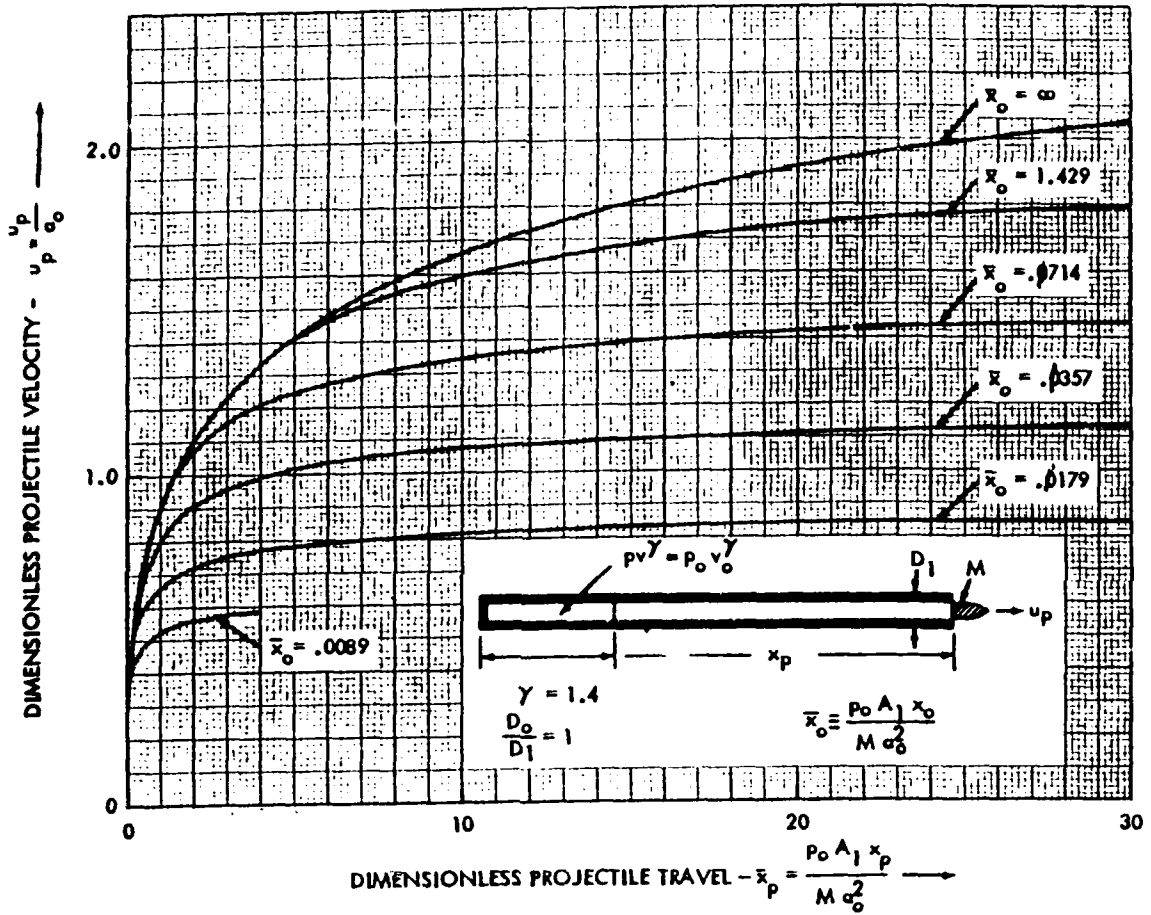
Figure A1.2 Projectile velocity as a function of position for several chamber diameters D_C and gas/projectile mass ratios, in non-dimensional form [19]
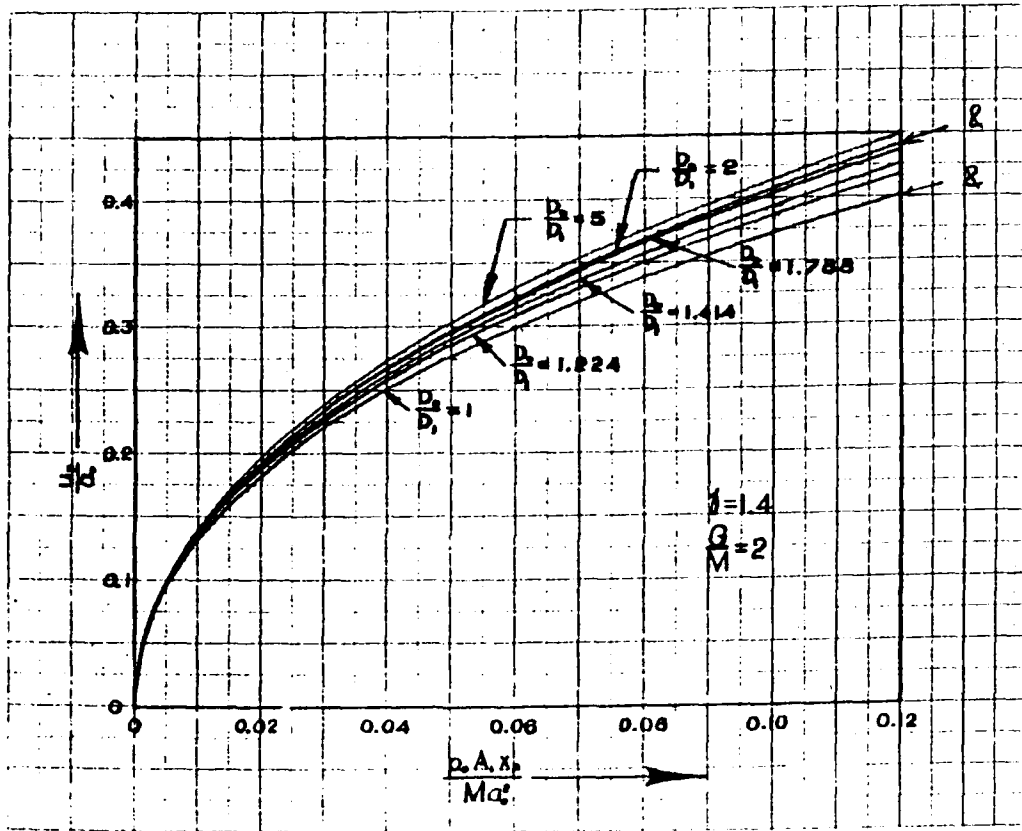
Figure A1.3   Projectile velocity as a function of position for several chamber diameters D_C for air, in non-dimensional form [19]
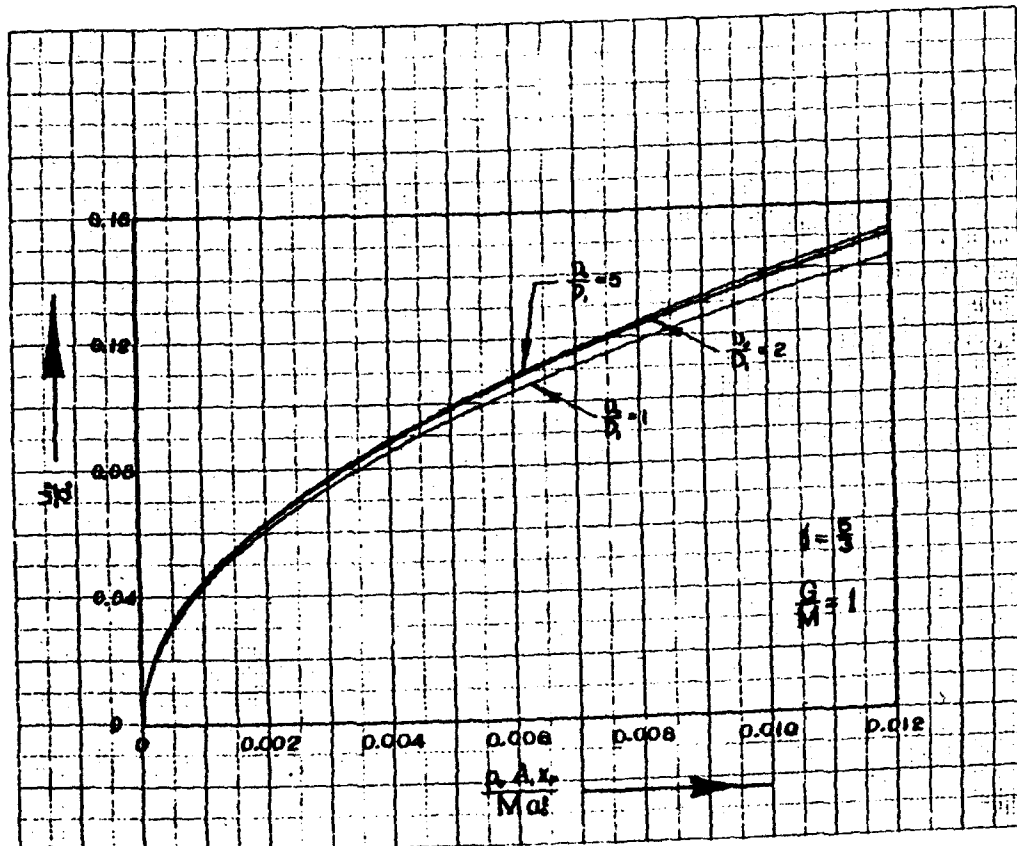
Figure A1.4 Projectile velocity as a function of position for several chamber diameters D_C for helium, in non-dimensional form [19]

A2   GASGUN SCALE EXPERIMENTS

At the Laboratory for Ballistic Research experiments were performed with a small one-stage gasgun, to provide some additional data for the validation of the developed computer code. The layout of the gasgun is shown in Figure A2.1. The relevant parameters of this small gasgun are: $V_c = 500$ ml, geometry approximated by $L_c = 470$ mm and $D_c = 37$ mm; $L_b = 200$ mm, $D_b = 5.39$ mm, $M_r = 1.1$ g.

In the experiments helium was used as driver gas and the initial chamber pressure varied from 30 to 150 bar. The installed diagnostics included an infrared velocity measurement system outside the barrel.

Figure A2.2 shows the velocities as measured and the velocities as calculated by the computer program. For the calculations the pressure in the barrel was ambient, so $P_b = 1$ bar; the friction was set to zero and the temperature to 288K.

Comparison of the experimental data with the calculated data shows a small discrepancy between the values of a few percent only; the calculated data over predict the observed velocities. This again validates the developed code and justifies application of the code as a prediction tool for the expected performance of a gasgun.
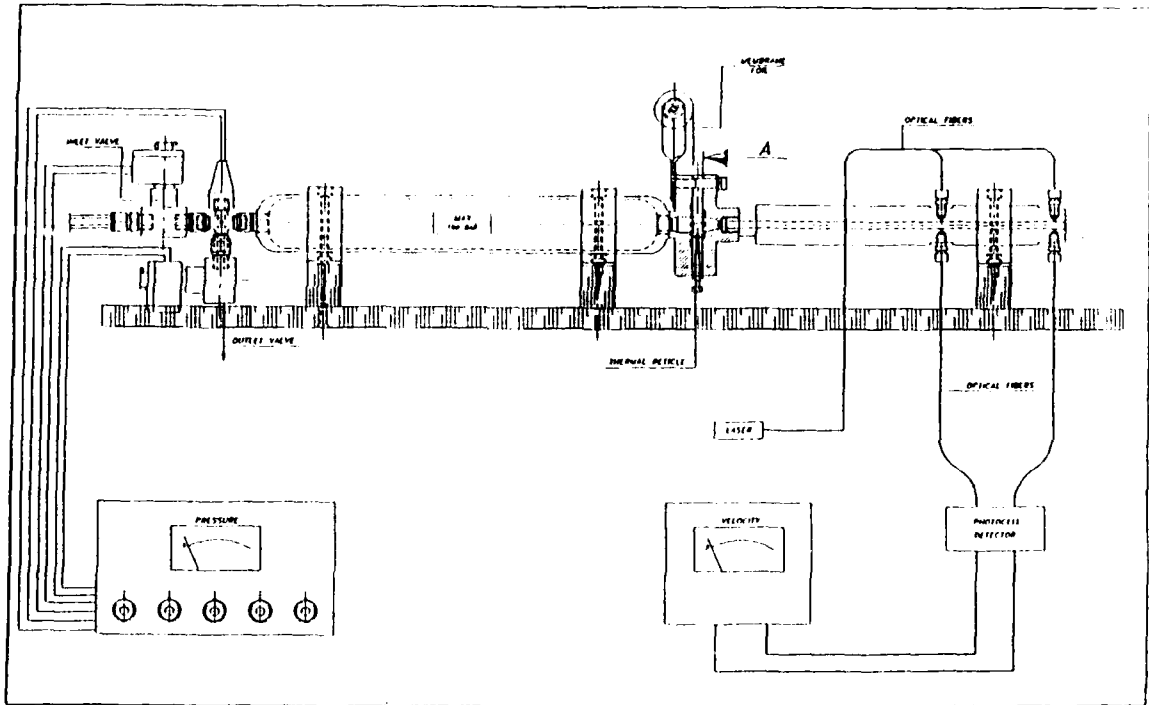
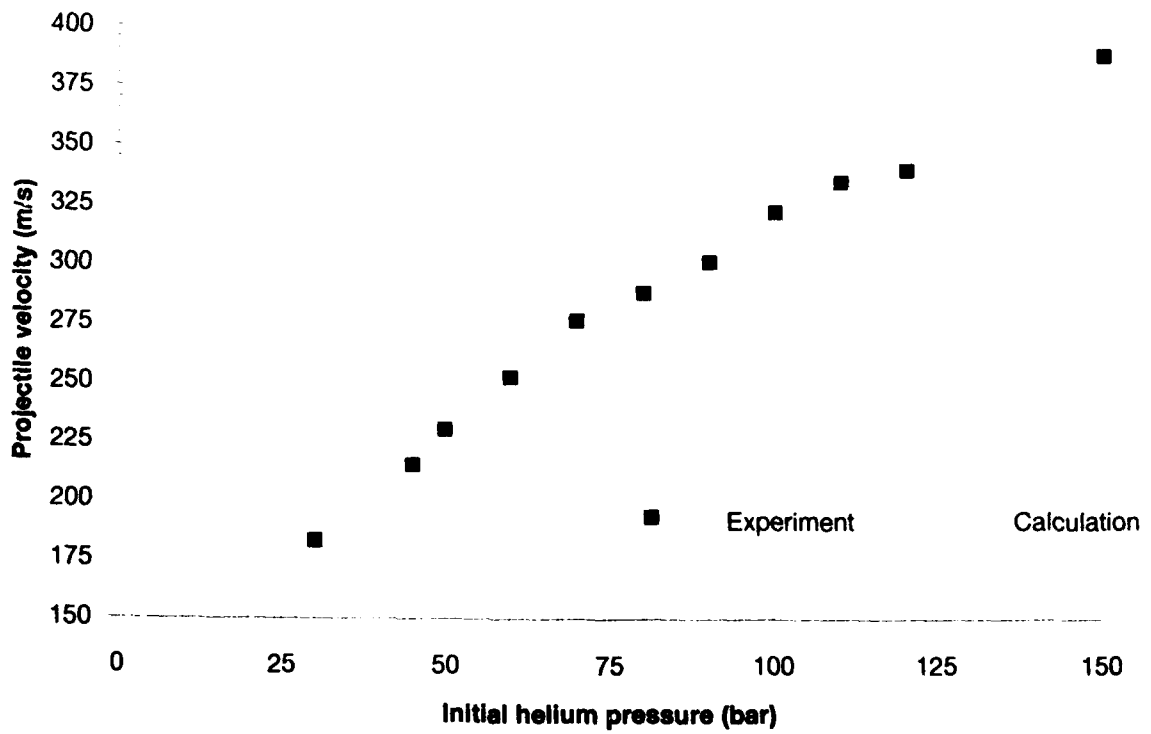Figure A2.1   Layout of gasgun configuration

Figure A2.2   Projectile velocity as a function of initial chamber pressure P_c, at muzzle. Driver gas is helium

ANNEX B   RUPTURE DIAPHRAGM EXPERIMENTS

The 19 cm gasgun at ISL uses a dual diaphragm construction, where each diaphragm comprises a large number of cellulose acetate foils (see section 6.2). The applicability of similar multi-foil diaphragms in the contemplated 30 cm PML gasgun has been investigated in a small series of experiments.

B.1   Experiment goals

The experiments aimed mainly to verify the reputed linear dependence of the rupture pressure on the number of foils, for foils of a different material and larger diameter than used at ISL. The effect of the thickness of the individual foils was another matter of interest. Other questions addressed by the experiments included the sensitivity of the rupture pressure to small foil defects; the reproducibility of the rupture pressure; and the ability of the foil package to stand up to pressures beneath the rupture threshold. Lastly, the foil rupture mechanism was unknown.

B.2   Theoretical analysis

Under the assumptions that the foil package will adopt a part-spherical shape, that rupture is caused by membrane, i.e. tensile, stress, and that all forces are distributed equally over all foils, it is possible to derive an analytical expression for the rupture pressure. This ignores the shear and bending forces which will occur at the edges, especially in thicker foils, but is otherwise entirely plausible.

In this case, the rupture pressure P of a foil package is given by

$$P / \hat{A} = (2 \, n \, t) / R \qquad (B.1)$$

where $\hat{A}$ is the strength of the foil material, n the number of foils, t the thickness of each foil, and R the radius of curvature of the foils.

In one of the experiments, the degree of curvature at the proposed holding pressure of 0.85 P has been determined to be 0.65 D, with D the internal opening of the clamping device. It is reasonable to attribute a more general validity to this finding. This yields a formula which may be used in scaling the measurements:

$$P / \hat{A} = (2 \, n \, t) / (0.65 \, D) \qquad (B.2)$$

B.3 Experimental set-up

The experiments were performed in the PML's 2m blast simulator, whose high pressure section has an internal diameter of 30 cm. The foils were hydraulically clamped between two smooth-surfaced flanges. Mylar foils were used, of 50, 125, 190 and 350 µm thickness, respectively. The pressure on the foils was raised slowly until rupture occurred. Some experiments had the nature of a duration test, where the pressure was maintained for some time at a given level

B.4 Experimental results

Rupture pressure

The results of the experiments are given in Figure B.1, which shows the rupture pressure to be indeed proportional to both the foil thickness and the number of foils, as predicted by Eq.(B.2). The 350 µm foils appears to be relatively weaker than the thinner foils. The spread in the single-foil results is largest for the 50µm foils, at 4%. This aspect has not been pursued for multiple foils.
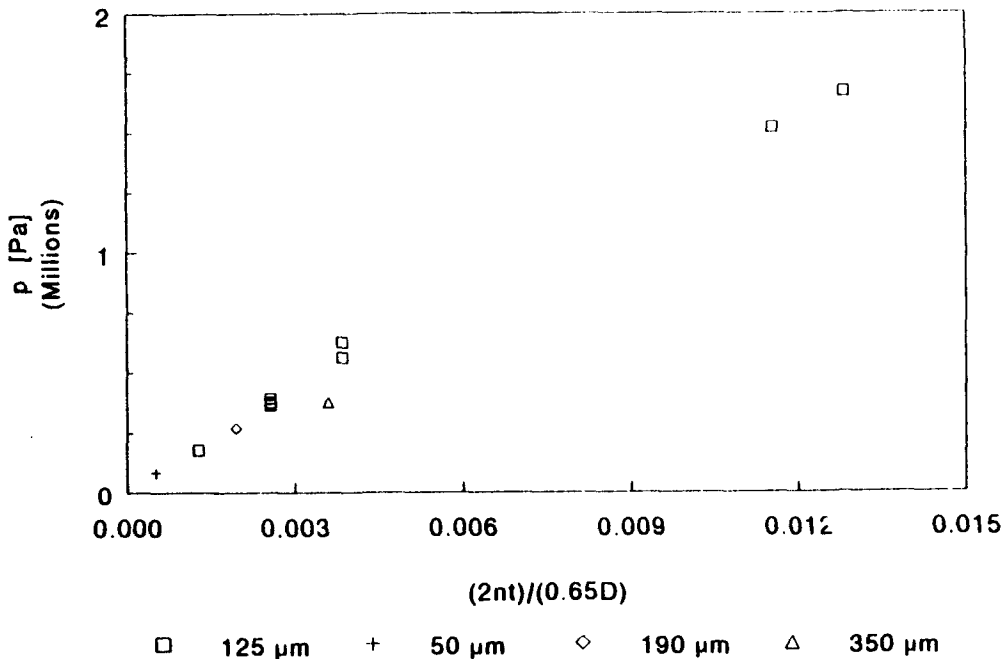

$(2nt)/(0.65D)$

| □ 125 µm | + 50 µm | ◇ 190 µm | △ 350 µm |

Figure B.1   Rupture pressure as a function of foil thickness and the number of foils: 1, 2, 3, 9, 10-foil tests for 125 µm foil; 1-foil tests for 50, 125, 190, 350 µm foils (7 measurements each). The abscissa $2nt/0.65D$ reflects Eq.(B.2)

Foil curvature

A package of three 125 µm foils at 0.5 MPa, i.e. 85% of the rupture pressure, acquired a curvature of radius R = 19.5 cm. This is 0.65 times the diameter of the opening. See Figure B.2.

Single...

Single... ... ...

quantity. ...

appeared ...

power ...

The num... ...

Two addition... ...

The resulting ...

into the full ...

Figure B.3   Ruptured 10-foil package

Long term effects and effect of foil damage

In three tests with 125 μm foils, packages of 1, 9, and 10 foils were subjected for 30 minutes to a pressure of approximately 85% of the rupture pressure. None failed.

Two tests have been performed with slightly damaged (creased, scratched) 350 μm foils. The rupture pressure was only slightly lower (less than 5%) than for undamaged foils.

B.5   Conclusions

The rupture pressure of a multi-foil diaphragm can be successfully predicted and is generally proportional to the number of foils. The rupture pressure reproduces well, even if inadvertently imperfect foils were to be used. The foil packages prove capable of withstanding substantial pressures over an extended period. The clamping arrangement merits special attention.

REPORT DOCUMENTATION PAGE
(MOD NL)

1. DEFENSE REPORT NUMBER (MOD-NL)	2. RECIPIENT'S ACCESSION NUMBER	3. PERFORMING ORGANIZATION REPORT NUMBER
TD92 1515		PML1992-64

4. PROJECT/TASK/WORKUNIT NO.	5. CONTRACT NUMBER	6. REPORT DATE
253291358	A91/K/429	October 1993

7. NUMBER OF PAGES	8. NUMBER OF REFERENCES	9. TYPE OF REPORT AND DATES COVERED
134 (2 Annexes)	31	Final

10. TITLE AND SUBTITLE

On the design of a gas gun accelerator for dynamic warhead tests.
(Het ontwerpen van een gasversneller voor dynamische warhead tests.)

11. AUTHOR(S)

M.P.I. Manders
J.B.M.M. Eggen

12. PERFORMING ORGANIZATION NAME(S) AND ADDRESS(ES)

TNO Prins Maurits Laboratory
P.O. Box 45, 2280AA Rijswijk, The Netherlands

13. SPONSORING AGENCY NAME(S) AND ADDRESS(ES)

DWOO
Postbus 20701, 2500 ES, Den Haag

14. SUPPLEMENTARY NOTES

The classification designation: ONGERUBRICEERD is equivalent to: UNCLASSIFIED

15. ABSTRACT (MAXIMUM 200 WORDS (1044 BYTE))

A study has been performed concerning the feasibility and general design of a gas gun accelerator for dynamic warhead tests in the Laboratory for Ballistic Research (LBO) of TNO-PML. The warhead accelerator system under consideration comprises the gas gun proper, a rail system to guide the warhead to the target, equipment to detonate the warhead, and a substantial backstop. The study included model calculations, scale experiments, design exercises, and cost evaluations.

The overall feasibility of the warhead accelerator system has been established and a number of design features formulated. Further design and construction of the system appear largely within the capability of the PML. Some questions remain, mainly related to the ability of anti-tank missile components to withstand acceleration. The attendant uncertainties may affect the present (December 1991) internal and external-cost estimates of 315 kf and 335 kf, respectively.

16. DESCRIPTORS	IDENTIFIERS
Design Warheads Experimental Calculations Feasibility Studies	Gas Guns Accelerators Dynamic Tests Cost Estimates

17A. SECURITY CLASSIFICATION (OF REPORT)	17B. SECURITY CLASSIFICATION (OF PAGE)	17C. SECURITY CLASSIFICATION (OF ABSTRACT)
ONGERUBRICEERD	ONGERUBRICEERD	ONGERUBRICEERD

18. DISTRIBUTION AVAILABILITY STATEMENT	17D. SECURITY CLASSIFICATION (OF TITLES)
Unlimited Distribution	ONGERUBRICEERD